M-PM-Min-A1UNIFORMITY OF ENZYME ACTIVITIES AMONG SINGLE DISSECTED FIBERS WITHIN DEFINED MOTOR UNITS. P. Nemeth, D. Pette and G. Vrbova`* Faculty of Biology, University of Konstanz. West Germany, and * Department of Anatomy and Embriology, University College, London, England.

Microchemical analyses of single dissected muscle fibers have shown that a rather continuous spectrum of enzyme activity levels exists within a fiber population, a variation that is not detected using histochemical techniques (Spamer and Pette, 1977; 1979; Lowry et al., 1978). It has been suggested that the variation is due to differences in the neural input to the muscle fibers. If so, it would be expected that metabolic characteristics of a motor unit be identical, as suggested by histochemistry (Edstrom and Edstrom, 1968). In the present study, malate dehydrogenase and fructose 1,6-bisphosphatase were measured in single dissected fibers of motor units identified by means of glycogen depletion. The malate dehydrogenase activity in single fibers of the general population of six extensor digitorum longus muscles of the rat showed up to tenfold differences in a single muscle. Enzyme levels of fibers of the same motor unit differed only slightly, 0.7 to 4.2 %. Fructose 1,6-biphosphatase activities measured in fibers of 1 motor unit showed 2.2 % variation. It is suggested by the unformity of malate dehydrogenase and fructose 1,6-bisphosphatase levels that the motor unit represents a metabolically pure population of fibers. The high resolution of microchemical techniques has revealed how precisely the metabolic enzyme properties of the muscle fibers are controlled by nerve.

M-PM-Min-A2MYOSIN TYPES AND FIBER TYPES IN STRIATED MUSCLE. Stefano Schiaffino, Institute of General Pathology, University of Padova, 35100 Padova, Italy.

Recent work from this and other laboratories has shown that myosin polymorphism in striated muscle is more extensive than previously supsected. We have used a variety of antimysoin antibodies to obtain a map of distribution of different isomyosins in skeletal and cardiac muscle fibers. Fractionation of antimyosin antisera by sequential cross-absorptions and correlated enzyme immunoassay tests indicate that the various isomyosins may have both common and unique antigenic determinants. Antibodies to specific determinants of myosin heavy chains permit to identify by immunofluorescence methods distinct isomyosins in slow-tonic, slow-twitch, fast-resistant and fast-fatiguable skeletal muscle fibers. Antimyosin immunofluorescence studies on cardiac muscle have revealed muscle cell heterogeneity in both atrial and ventricualr myocardium and also among cells of the conduction tissue. Regional variations inthe cellular distribution of ventricular isomyosins have been detected, in particular transmural gradients and differences between right and left ventricle. The pattern of antimyosin immunoreactivity varies in the course of postnatal development, under the influence of thyroid hormones and during cardiac hypertrophy induced by pressure overload. Shifts in isomyosin composition can be correlated with parallel changes in the contractile properties of cardiac muscle. Supported by MDA and by Dino Ferrari Foundation.

M-PM-Min-A3GENERATION OF FIBER DIVERSITY IN RAT MUSCLE. Alan M. Kelly and Neal A. Rubenstein. Departments of Pathobiology, School of Veterinary Medicine and of Anatomy, School of Medicine University of Pennsylvania, Phialdelphia, PA

The generation of distinct fiber types from a homogenous pool of embryonic muscle fibers was examined in the fast twitch Extensor Digitorum Longus (EDL) and slow twitch soleus muscles using affinity purified antibodies specific to adult fast (AF) and adult slow (AS) muscle. At 15 days gestation the EDL is composed of primary generations of myotubes which react definitively with AF, with AS the reaction is equivocal. At 18 days in utero these primary generation cells persist in their affinity for AF but now also react strongly with AS. By contrast, new, secondary generations of myotubes forming along the wall of primary myotubes react only with AF. In the EDL most of the primary generation fibers subsequently develope into slow, Type I fibers, whereas the numerous, secondary generation cells become fast, Type II cells. Primary myotubes are known to be innervated by 18 days gestation and this stage also coincides with the onset of fetal movements. We propose that primary myotubes of the 18 day fetus constitute the fundamental motor units of the muscles and generate these initial, slow movements. Secondary generation fast fibers are then added to the contractile machinery. As this occurs the rate of contraction increases and the initial slow response is eclipsed. In the soleus, the pattern of development is very similar. At 18 days gestation,primary generation cells react with both AF & AS. Secondary generation cells appear somewhat later, they initially only react with AF and appear to become Type II fibers. Their addition to the contractile pool may partially explain why this muscle transiently increases its speed of contraction after birth. Most secondary, Type II fibers then undergo a prolonged transformation to Type I cells and coincidently the twitch times of muscle increase. Supported by NL 14332 and HL 15835

M-PM-Min-A4REORGANIZATION OF SUBCELLULAR STRUCTURE IN MUSCLE UNDERGOING FAST-TO-SLOW TYPE TRANSFORMATION. B.R. Eisenberg and S. Salmons, Rush Medical School, Chicago, IL 60612 and University of Birmingham, England.

When a fast twitch mammalian skeletal muscle is subjected to chronic low-frequency stimulation, it gradually takes on the physiological, biochemical and histochemical character of a slow-twitch muscle. In the present study we have used stereological techniques to analyze the nature and time course of morphological changes in fast tibialis anterior muscles from rabbits stimulated via the nerve by continuous impulse activity at 10 Hz. After stimulation for 6 hr to 24 weeks, fiber bundles were removed from stimulated and unstimulated TA and soleus muscles. These were processed conventionally for electron microscopic examination, randomly selected fields being photographed for stereological analysis. During stimulation for 2 days to 2 weeks the amount of T-system declined to levels found normally in slow muscle. The amount of sarcoplasmic reticulum was similarly reduced. Between 11 days and 3 weeks after the onset of stimulation, the Z band thickness increased to values characteristic of slow muscle. The Z band width within a transitional fiber was more variable than normal. The mitochondrial volume fraction in stimulated muscles increased rapidly after about 11 days, and became significantly higher than that of of control muscles, either fast or slow. After 7 weeks of stimulation, the level declined but still remained above that of slow muscle. The membrane systems and mitochondria change in a continuous orderly manner, but in some fibers the myofibrils appear to be dismantled and rebuilt. In other fibers, the Z band appears to be rebuilt on the existing scaffold, without dismantling. These morphological changes occur during the same time period as an increase in the activity of oxidative enzymes and a change in calcium transport characteristics.

M-PM-Min-A5MYOSIN ISOENZYMES AND MUSCLE FUNCTION. Susan Lowey, Brandeis University, Rosenstiel Center, Waltham, Massachusetts 02254

Skeletal muscle fibers can be distinguished according to their physiological, metabolic and structural properties. Individual fibers also vary in their contractile protein composition as evidenced by electrophoretic and cytochemical techniques. I will limit my discussion to myosin isoenzymes, although polymorphs of tropomyosin and troponin have been described (Dhoot & Perry, 1979). Myosin isoenzymes can be demonstrated by (1) the reaction of frozen sections of muscle with antibodies specific for myosin, its subfragments and subunits (Gauthier & Lowey, 1977; 1979) and (2) the direct isolation of myosin molecules using immunoadsorbents specific for a particular type of myosin (Holt & Lowey, 1977; Silberstein & Lowey, 1981). The first approach was used to identify two major classes of myosin in fast-twitch mammalian muscles: a "slow" myosin in the slow red (type I) fiber, and a "fast" myosin in the fast red (type IIA) and white (type IIB) fibers. The observation that the fast red fiber differed from the white fiber in its reactivity towards certain antibodies suggested the existence of a distinctive myosin in that fiber. The second approach was used to prove the existence of three light chain isoenzymes in chicken pectoralis muscle: two homodimeric species (myosin containing A1 or A2 light chains) and a heterodimer (myosin with A1 and A2; Lowey et al., 1979). These myosins appear to be identical in their kinetic properties, and ability to assemble into filaments (Pastra-Landis et al., 1981). Immunoadsorbents have also permitted a partial fractionation of pectoralis myosin from 11-12 day chick embryos. We find that embryonic myosin is distinct from the adult form, and that there are a minimum of two heavy chain species (Benfield et al., 1981). Although the functional significance of these many myosin isoenzymes remains unclear, it is most likely related to the great variety of responses required of adult and developing muscles.

M-PM-Min-A6FAST FIBER TRANSFORMS TO SLOW TYPE ON LONG-TERM STIMULATION
F.A. Sreter, K. Mabuchi and K. Pinter, Dept. of Muscle Research, Boston Biomedical Research Institute, Boston, MA. 02114.

Phasic stimuli were applied (60 Hz, 2.5 sec duration) to rabbit fast-twitch extensor muscles (e.g. tibialis anterior) every 10 sec for a period of 5 weeks via an implanted electrode secured near, but not in contact with the common peroneal nerve. The weight of the stimulated tib. ant. was comparable to that of the contralateral tib. ant. and no visible atrophy was present. Transformation of muscle fibers was assessed by changes in myosin ATPase activities, by electrophoresis on SDS-polyacrylamide slab-gels and - under non-dissociating conditions - on pyrophosphate gels, and by histochemistry. Ca^{2+}-activated myosin ATPase activity (measured in 0.025M KCl, 10 mM $CaCl_2$, 2.5 mM ATP and 50 mM Tris, pH 7.6,25°) decreased from 0.6μmole/mg/min in the contralateral muscle to 0.3 in the stimulated tib. ant. SDS-slab gels showed the presence of both fast and slow type light chains and SDS-gels of single fibers from the stimulated muscle showed that both types of light chains were present within the same fiber. PP_i-gels showed both slow and fast myosin isozymes. Histochemical examination (diaphorase and ATPase staining after acid or alkali preincubation) also indicated a massive fast-slow and glycolytic-oxidative transformation. Histological examination of the stimulated muscle shows no signs of regeneration (de novo fiber formation), supporting the view drawn from the above results that transformation produced by phasic stimulation of a fast muscle leads to reprogramming of existing fibers.
(Supported by grants from NIH (AG-02103 and HL-23967) and the Muscular Dystrophy Assoc.)

M-PM-Min-A7SINGLE SKINNED SKELETAL FIBER Ca^{2+} AND H^{+} SENSITIVITIES: COMPARISON OF THE VARIOUS HISTOCHEMICAL TYPES. Sue K. Donaldson, Rush University, Chicago, Illinois 60612

Single fibers from rabbit soleus and adductor muscles were skinned by peeling off the sarcolemma. Each skinned fiber was cut transversely into five segments. The isometric force generating characteristics of one segment of each fiber was studied at several Ca^{2+} levels (activating submaximum and maximum force generation) at pH 7 and 6.5. The other four segments were stained for myofibrillar ATPase at pH 9.4 (following pre-incubation at pH 10.4, 4.6, and 4.4) and NADH. The histochemical type of each fiber was identified according to the pattern of staining of its segments. Type I and IIB fibers have distinct force generating properties. Type I fibers have high Ca^{2+} sensitivity that is not greatly altered by changing pH; the opposite is characteristic of IIB fibers. In contrast IIA and IIC fibers have variable and intermediate force generating properties. IIA fibers behave most similarly to the predominant fiber type of their muscle of origin. Supported by USPHS NIH grant HL23128.

M-PM-Min-A8SUBTYPING OF SINGLE MUSCLE FIBERS. K. Mabuchi and K. Pinter (Intr. by Mario Rosemblatt), Department of Muscle Research, Boston Biomedical Research Institute, Boston, MA., 02114.

Single fibers isolated from rabbit and human muscles have been stained for diaphorase activity and analyzed for myosin light chains and isozymes by gel electrophoresis under dissociating (SDS) and non-dissociating (PP_1) conditions, respectively. Single fibers were divided into two or three portions for these studies. Slow and fast fibers can be identified by their light chain complement on SDS gels. Slow fibers contain a single-band isozyme identified on PP_1 gels. Fast fibers can be sub-typed on the basis of their diaphorase activity. Other subdivisions are based on the LC_1/LC_3 ratio and on the isozyme pattern observed on PP_1 gels. In the latter respect, fibers not only differ in intensity of sub-bands, but a distinction can be made on the basis of the migration velocity of the isozyme multiplet. Some correspondence exists between homologous human and rabbit isozymes and light chains. Work is in progress to establish the correlation among the various bases of classification.

(Supported by grants from NIH(AG-02103 and HL-23967) and the Muscular Dystrophy Assoc.)

M-PM-Min-B1 BIOPHYSICS OF HYDROGEN AND OXYGEN EVOLUTION BY PHOTOSYNTHESIS.* E. Greenbaum, Chemical Technology Division, Oak Ridge National Laboratory.

The photoevolution of hydrogen and oxygen by photosynthesis is a biophysical approach to the problem of solar energy conversion. This presentation is concerned with the roles of Photosystem II and the electron transport chain of photosynthesis in providing reducing equivalents which are eventually evolved as molecular hydrogen. Experimental data will be presented on two systems which are capable of simultaneous photoproduction of molecular hydrogen and oxygen. The first is a green algal system. The second is a non-living cell-free system comprised of isolated chloroplasts, ferredoxin, and hydrogenase. Experiments have been performed which suggest that both the reducing side of Photosystem II as well as endogenous reductants R (interacting directly with the electron transport chain) can provide electrons which are evolved as molecular hydrogen. These data suggest that the photochemical machinery of photosynthesis can be used to perform true photosynthetic water splitting, i.e., $2H_2O \rightarrow 2H_2+O_2$. We have also performed the first experiments on the CFH system using the technique of single turnover saturating flashes of light. This is a powerful method for studying the kinetic and mechanistic aspects of photoreactions. Our preliminary results with this technique suggest that the turnover kinetics of the CFH system are relatively fast and comparable to that of normal photosynthesis. However, it appears that the number of functional photosynthetic units is relatively low as determined by the standard Emerson and Arnold Unit for normal photosynthesis.

*Research sponsored by the Office of Basic Energy Sciences, U.S. Department of Energy, under contract W-7405-eng-26 with the Union Carbide Corporation and the Solar Energy Research Institute under contract DK-9-8361-1.

M-PM-Min-B2 ENERGY TRANSDUCTION IN GREEN PLANTS: PRIMARY ELECTRON ACCEPTORS. J. Fajer, M.S. Davis, A. Forman, Brookhaven National Laboratory, Upton, NY 11973, and V. V. Klimov, E. Dolan and B. Ke, C. F. Kettering Research Laboratory, Yellow Springs, Ohio 45387.

A combination of redox, optical and magnetic data indicates that the first reduced products generated by light in green plants are the anions of chlorophyll (Chl) in Photosystem (PS) I (A_1^-) and of pheophytin (Pheo) in PS II (I^-). Comparison of the electron-nuclear double resonance spectra of A_1^- trapped in subchloroplast fragments enriched in PS I (TSF I), Fig. 1, with those of Chl^- in vitro suggests that A_1^- is a monomeric Chl^-. Similar results for TSF IIa and $Pheo^-$ support a monomeric $Pheo^-$ as I^-. Magnetic interactions between I^- and FeQ^-, the subsequent electron acceptor, yield a doublet ESR signal centered at g=2 with a 50G separation at low temperatures. Comparison of the integrated signal intensities of I^- and of the doublet at several temperatures indicates that the two signals are not interconvertible but reflect the influence of I^- on FeQ^-. Electron-electron double resonance establishes that microwave saturation can be transferred from the doublet to I^- and that the two species lie within the same reaction center. The above results suggest that chlorophyll-like acceptors may be obligatory to effect the rapid primary charge separations because they allow favorable orbital overlap between the chlorophyll donors and the acceptors; in PS I: $P700 + Chl \rightarrow P700^+ + Chl^-$ and in PS II: $P680 + Pheo \rightarrow P680^+ + Pheo^-$.

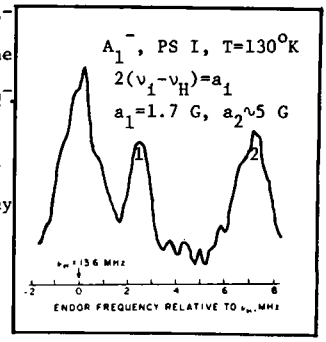

This work was supported by the Div. of Chemical Sciences, U.S. DOE under contract #DE-AC02-76CH00016.

M-PM-Min-B3 LIPID BILAYER-WATER INTERFACIAL PHOTOREDOX REACTIONS WITH MEMBRANES SOLUBLE AND INSOLUBLE ACCEPTORS. D. Mauzerall and A. Ilani The Rockefeller University, New York, NY

Charge transfer across the lipid bilayer-water interface of magnesium octaethyl porphyrin (MgOEP) or chlorophyll (Chl) containing membranes excited by a dye laser pulse (0.3 μs FWHM) was measured electrically. The maximum charge transferred at saturating concentrations of charged lipid insoluble acceptors added to one side of the membrane was independent of their chemical nature and redox potential up to a cut off level of -0.6V (vs SHE) for MgOEP and -0.5V for Chl. The acceptors were complex inorganic ions, sulfonated quinones and viologens. The reversible redox potential of MgOEP in the lipid bilayer is +0.8V. Thus 1.4 eV of reversible redox potential (a free energy) can be obtained from ∿1.9eV of excited state energy (an internal energy) of MgOEP. The constant characterizing of hyperbolic saturation depends on the chemical properties of the acceptor and its magnitude ($\sim 10^{-4}$M) showed that accumulation at the interface occurred. By contrast, lipid soluble acceptors (quinones) not only showed no photoresponse, they inhibited that of good hydrophilic acceptors. By crossing the membranes they equalized vectorial photoelectron transfer at each interface. Proof consisted of adding a hydrophilic donor to one side, whereupon full response was obtained. The increased rate of back reaction at the oxidizing interface by quinone mediated reduction of acceptor is evidence for a redox shuttle. It is concluded that hydrophobic quinones have a maximum concentration at the polar side of the interface relative to the pigment, with minima in the lipid core and in the aqueous phase. The isoprenoid side chain of coenzyme Q does not appear to prevent its motion or protonation in the interfacial region. The combination of hydrophobic and hydrophilic properties of the assymetric anthraquinone-2-sulfonate make it the most efficient acceptor.

This research was supported by NIH grant #GM-15693-02

M-PM-Min-B4 REACTION CENTERS FROM PHOTOSYNTHETIC BACTERIA: MODIFICATIONS, CONSTRUCTIONS, AND ELECTRICAL PROPERTIES OF MONO- AND MULTI-LAYER FILMS. P.L. Dutton, D.M. Tiede, N.K. Packham, M.R. Gunner, R.C. Prince, K. Matsuura and P. Mueller. U. of Pennsylvania, Phila., PA 19104.

The reaction center (RC) converts light energy into two forms of free energy: an electrical potential across a membrane ($\Delta\psi$) and a redox potential difference (ΔE) between a reduced quinone and oxidized cytochrome *c*. The ΔE drives another protein complex, the ubiquinone-cytochrome c_2 oxidoreductase (Q-c_2 O/R), which together with the RC forms a cyclic electron transfer system. The Q-c_2 O/R converts the ΔE into further $\Delta\psi$ and ΔpH. We are endeavouring to develop this biological system into a flexible experimental vehicle that will provide useful views of the factors that are important to the operation of submicron devices capable of converting solar energy into electrochemical gradients. Current progress: (a) developed techniques for incorporating RCs into a planar phospholipid bilayer separating aqueous phases; (b) developed techniques to form oriented RC mono- and multi-layers on glass or between electrode films; (c) analyzed, in these systems, laser and steady state light activated electric currents under voltage clamped conditions and *vice versa*; (d) obtained optical spectra and linear dichroic information of RCs in monolayers, and EPR information in multilayers; (e) modified the RC by replacing the native quinone with other quinones of known electrochemistry; (f) combined *in vitro* the RC with the Q-*c* O/R from mitochondria to form a functional light activated cycle. The results reveal novel views of electron transfer steps within the highly organized RC, and that the energy levels of the RC modified by Q-replacement (altered ΔE) dictate kinetics and pathways of electron flow. The *in vitro* RC-Q-*c* O/R construction offers the opportunity to study a light activated cyclic electron transfer system in the form of films on electrodes.

[Supported by grants from DOE (ER 10590), NSF (PCM 79-09042), and NIH (GM 27309)].

M-PM-Min-B5 THE PHOTOSYNTHETIC APPARATUS: A MODEL BIOLOGICAL SOLAR CELL. Michael Seibert, Solar Energy Research Institute*, Golden, CO 80401

The development of solid-state photovoltaic devices for direct conversion of solar energy into electricity has led to a highly visible and a potentially practical technology. However, photovoltaics is not the only quantum conversion process that might be harnessed for the production of useful energy. Photoelectrochemical cells that employ photoactive, biological components and generate electrical currents have been reported in several laboratories. Our studies include the adsorption of isolated bacterial reaction centers (the simplest molecular complex that carries out primary photosynthetic charge transfer) and chromatophores (the photosynthetic vesicles of photosynthetic bacteria) onto tin oxide electrodes. Photoelectrochemical cells utilizing these electrodes are driven by red light absorbed by the biological material (tin oxide is transparent and does not absorb in the red spectral region). Consequently, these systems act as primitive solar cells and may serve as useful models for future organic photovoltaic devices. Although the conversion efficiencies and stability of biological photoconversion devices are not comparable to solid-state semiconductor devices at the present time, the promise of cheap materials costs and theoretical maximum conversion efficiencies as high as silicon solar cells encourage further research on biological systems.

*A division of the Midwest Research Institute and operated for the U.S. Department of Energy under Contract EG-77-C-01-4042. This work was supported in part by the Division of Biological Energy Research, Office of Basic Energy Sciences.

M-PM-Min-B6 A PHOTOSYNTHETIC PHOTOELECTROCHEMICAL CELL. R. L. Pan, R. Bhardwaj and E. L. Gross, Department of Biochemistry, The Ohio State University, Columbus, Ohio 43210

We have been developing a photosynthetic photoelectrochemical cell using the photo - system I (PSI) subchloroplast particles or isolated chloroplasts (Chlp). The photosynthetic photoelectrochemical cell has two compartments separated by a PSI or Chlp-impregnated matrical filter. One compartment which was illuminated contained electron acceptor while the other compartment contained electron donor of PSI. The electron acceptors, such as flavin mononucleotide (FMN) and phenosafranine (SAF), could also be reduced photochemically by tricine and EDTA. The electron donor was $Fe(CN)_6^{-3}/Fe(CN)_6^{-4}$ couple. A maximum power of 2 mW across a 60 Ω resistance and 0.75 mW across 200 Ω resistance was obtained when FMN and SAF were electron acceptors respectively. The front surface power conversion efficiency was 1% for the FMN system and 0.1% for the SAF system respectively. The photoresponse is the sum of photochemistry of the electron acceptor and photosynthetic reaction. The reactions operate in a synergistic manner.

M-PM-Min-B7 BACTERIORHODOPSIN AND HALORHODOPSIN RELATED ELECTROCHEMICAL POTENTIALS. Lester Packer, Naoki Kamo, Toinette Racanelli, and Rolf J. Mehlhorn. Membrane Bioenergetics Group, Lawrence Berkeley Laboratory and the Department of Physiology/Anatomy, University of California, Berkeley, CA 94720.

Membranes of Halobacterium halobium contain two retinoproteins, bacteriorhodopsin (BR_{568nm}) and halorhodopsin (HR_{588nm}). We have investigated the light- and sodium-dependent activities in vesicles from the HR containing R1mR strain, and the BR + HR containing Sg strain to study energy conversion and ion flow mechanisms. Simultaneous ΔpH and $\Delta\Psi$ measurements have been made with electrodes. Also ΔpH, $\Delta\Psi$, surface potential ($\Delta\Psi_s$), boundary potential ($\Delta\Psi_b$), and volume (ΔV) have been measured with spin probes. In R1mR vesicles $-\Delta\Psi$ and H^+ uptake occurs in NaCl, but not in KCl medium. In Sg vesicles net H^+ extrusion is reduced at high light intensity in NaCl but not KCl medium. Such results indicate Na^+/H^+ exchange in vesicles from both strains. As Sg contains BR + HR, it is unclear whether the Na^+ extrusion is due to a Na^+/H^+ antiporter and/or HR which has been proposed by Lindley and MacDonald (BBRC 88: 491-499, 1979) to be a light driven Na^+ pump. To evaluate these concepts for Na^+ transport, the light intensity dependence and action of several membrane transport active agents have been compared. Digitoxin, electroneutral exchangers (triphenyltin, monensin), and phloretin yielded similar results for HR (R1mR) or HR + BR (Sg) vesicles. Moreover, treatment of vesicles with carboxyl reacting reagents inhibited Na^+ dependent activity in both types of vesicles. Thus, common mechanisms of Na^+ transport are indicated in Sg and R1mR vesicles.

Research supported by the Department of Energy.

M-PM-A1 RATE-LIMITING COMPONENTS OF TRK-MEDIATED POTASSIUM UPTAKE IN *ESCHERICHIA COLI* K-12
Georgia Helmer and Wolfgang Epstein, Department of Biochemistry, University of Chicago, Chicago, IL 60637

The rate of potassium uptake by the high rate, modest affinity constitutive Trk transport system of *E. coli* K-12 is affected by mutations in four unlinked genes: *trkA*, *trkD*, *trkE* and *trkG*. Three of the *trk* genes have been cloned into the multicopy plasmid pBR322; the effect of gene dosage on the Trk system has been studied using these plasmids and F-episomes. Increasing the gene dosage of the combination *trkA*, *trkE*, and *trkG* significantly increases the Vmax of uptake, whereas increasing dosage of only one or two of these genes does not alter Vmax. We conclude that these three genes code for rate-limiting components of the Trk transport system.

These recombinant plasmids are being used to identify products of the *trk* genes. We have studied expression of cloned genes in cells whose chromosomal DNA has been degraded due to ultraviolet damage and in which the recombinant plasmid has been amplified. Using plasmids with either the wild-type or amber *trkA* allele, we have identified the product of the *trkA* gene as a 57,000 dalton integral membrane protein.

M-PM-A2 EFFECT OF NA_o-DEPENDENT CALCIUM EFFLUX ON THE MEMBRANE POTENTIAL OF INTERNALLY PERFUSED BARNACLE MUSCLE FIBERS. M.T. Nelson and M.P. Blaustein, Dept. of Physiology, U. of Maryland, Baltimore, MD.

The intracellular solute composition of giant barnacle muscle cells was controlled by internal perfusion. Intracellular Ca sequestration by mitochondria and sarcoplasmic reticulum was minimized by FCCP and caffeine, and by ATP_i - depletion. Membrane potential (V_m) and ^{45}Ca efflux were measured. Ca efflux into Na seawater from fibers with high $[Ca^{2+}]$ (~ 10 μM) was about 10 pmol/cm^{2}s. The replacement of external Na (Na_o) by Li caused an ~ 80% reduction in Ca efflux and ~ 2 mV hyperpolarization. Ca efflux was activated and V_m depolarized by Na_o in an identical, sigmoid fashion, with half-maxima at $[Na]_o$ ~ 60 mM (see Fig.). The 'Hill coefficients' for Na_o activation curves of Ca efflux and ΔV_m was ~ 2.6. In fibers perfused with low $[Ca^{2+}]$ (0.1 μM), Ca efflux was 0.2 pmol/cm^{2}s, the replacement of Na_o by Li has no effect on Ca efflux and caused a slight depolarization (~ 0.5 mV). Thus, Na_o-dependent Ca efflux can contribute about 2 millivolts to V_m of barnacle muscle fibers. These data are consistent with an electrogenic Na-Ca exchange mechanism that exchanges more than 2 Na^+ ions for each Ca^{2+} ion. (Supported by NSF, MDA, and an AHA fellowship to MTN)

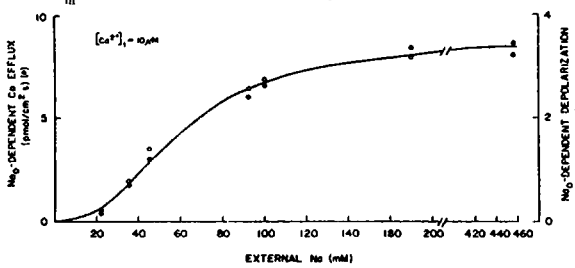

M-PM-A3 THE MEASUREMENT OF INTERNAL H^+ IN SQUID AXONS DURING STIMULATION. T. Tiffert, L. J. Mullins, J. Whittembury and F. J. Brinley, Jr. University of Maryland School of Medicine, Baltimore, Maryland, 21201.

The pH of squid axoplasm has been measured *in situ* by two techniques: spectrophotometric measurement of absorption changes of microinjected phenol red, and axial insertion of a pH sensitive microelectrode. The dye measures an average pH throughout the axon whereas the microelectrode measures pH only at a center point. Repetitive stimulation of the nerve fibre in 100 mM Ca seawater leads to a decrease in internal pH that is abolished if Ca is omitted from the seawater. A similar but larger response is observed if Ca entry is produced by the application of 100 mM K seawater. Recovery from the acidification produced by stimulation in Ca-containing seawater is slow compared to the rate of onset of decrease of pH upon Ca entry. The observations made are consistent with the idea that the buffering of Ca in axoplasm occurs by the displacement of H^+ upon the binding of Ca^{++}. They complement the measurements of Mullins and Requena (J. Gen. Physiol. 74,393-413, 1979), who showed that alkalinizing axoplasm with external NH_4^+ decreased the internal Ca^{++} concentration. Supported by NIH Grant NS 14800.

M-PM-A4 EFFECT OF DEPOLARIZATION ON BEHAVIOR OF INTRACELLULAR pH (pH_i) IN FROG MUSCLE. R.F. Abercrombie and A. Roos, Dept. of Physiology & Biophysics, Washington University, St. Louis, MO. 63110.

The pH_i, measured with Thomas-style microelectrodes, of frog semitendinosus muscle in Ringer buffered with HEPES (pH_o 7.34), was 7.13 ± .06 (n=4). We confirmed the findings of others that the pH_i, when depressed by exposure to 5% CO_2 (pH_o 7.34), did not recover, in contrast to its behavior in other cell types. However, recovery did occur in any one of 3 depolarizing solutions (V_m = -20 to -30 mV), applied 40 min before electrode introduction: (a) 50 mM K^+, normal Cl^-, (b) 50 mM K^+, normal $[K^+]\cdot[Cl^-]$, (c) 0.5 mM Ba^{2+}, 2.5 mM K^+, 5.9 mM Cl^-. There was also recovery in normal Ringer after 1 hr in 50 mM K^+, normal Cl^-; V_m after this high K^+ exposure remained -20 to -30 mV. Recovery even occurred, though at a reduced rate, when the H^+ electrochemical gradient was inward ($[HCO_3^-]_o$ = 12 mM, pH_o 7.03). Either 0.5 mM amiloride or Na^+-free Ringer greatly reduced recovery. In other studies, contracture was prevented by either hypertonic medium containing 250 mM mannitol, or by 2 mM tetracaine, so as to observe the pH_i course from the start of depolarization produced by 50 mM K^+, normal Cl^-. Upon depolarization in hypertonic solution, there was a prompt fall in pH_i of about 0.5; pH_i returned within 20-30 min, overshooting the control value. Amiloride abolished this overshoot. With tetracaine (which blocks Ca^{2+} release from the sarcoplasmic reticulum) there was no acidification on depolarization. The drug also reduced the pH_i recovery from CO_2-induced acidification. Thus, depolarization can profoundly affect pH_i behavior even if contracture if blocked; this behavior might be related to the initial Ca^{2+} release. (Supported by NIH Grant HL00082.)

M-PM-A5 ALAMETHICIN REVEALS INTERNAL SURFACE CHARGES AT FROG NODE OF RANVIER. J.E. Hall and M.D. Cahalan, Dept. of Physiology and Biophysics, Univ. of Calif., Irvine, CA 92717.

Alamethicin, a voltage-dependent channel-forming polypeptide, partitions into frog node of Ranvier from the external solution, inducing a conductance activated by hyperpolarizing or depolarizing the membrane. The endogenous Na and K conductance mechanisms were blocked by bathing the fiber in isotonic CsCl + Ca + TTX external solution and cutting the fiber in end pools containing Cs. With low alamethicin concentrations (1-2 μg/ml) discrete changes in current are observed from -80 to -100 mV with three conductance levels of about 200, 500 and 800 pS. With higher doses of alamethicin, conductance can be activated by voltage pulses delivered from a holding potential of -20 to 0 mV. If the fiber interior is exposed to isotonic CsCl, the current for hyperpolarizing pulses turns on exponentially and then undergoes partial inactivation over a time course of a few seconds. Inactivation is completely abolished by internal EGTA, or by lowering external Ca. Raising external Ca decreases the slope of the conductance-voltage curve, but does not alter the potential required to turn on a very small number of alamethicin channels. A methylester derivative of alamethicin that forms nearly symmetrical I-V curves for both positive and negative voltages in symmetrical lipid bilayer membranes results in an asymmetric I-V curve in the node; more depolarization than hyperpolarization is required to activate conductance. We can account for these results by postulating an internal negative surface potential of about -50 mV, with little or no external surface charge. Inactivation is produced by the influx of calcium through conducting alamethicin pores, resulting in a decrease in the internal surface potential, decreasing the field across the membrane, thus turning off conductance. (Supported by NIH Grants HL23183 and NS14609.)

M-PM-A6 LASER LIGHT-BEATING AND RAMAN SPECTROSCOPIC STUDIES OF NEURONS. B. Simic-Glavaski and G. J. Mpitsos, Department of Chemistry, CLES, Case Western Reserve University, Cleveland, Ohio 44106.

We have analyzed light scattered from nerves, at resting and at different levels of steady state polarizations by means of laser autocorrelation and Raman spectroscopies. Observations were made on the walking leg nerves of the lobster, *Homarus americanus*, and the connectives between cerebropleural and buccal ganglia of a slug, *Pleurobranchaea californica*.

In laser autocorrelation spectroscopic studies, one measures the time dependent fluctuations of the intensity of scattered light from which diffusion and size of molecules can be obtained. The molecular diffusion constants $D \approx 10^{-9}$ cm^2/s were calculated and were greatly affected by applied electric fields and optical probe molecules such as fluorescent dyes. The diffusion constants indicate a change of about 60 Å in the scattering diameter for a change of 60 mV in polarization. Dyes that are often used in studies of neurons have reversible but pronounced effect on the diffusion properties of the nerves examined.

Raman light scattering from lobster nerves was recorded at room temperature. A comparative analysis of spectra leads us to an interesting similarity between our spectra and that obtained from an aqueous solution of RNA and C-H and C-O stretches. A resonant Raman spectrum was observed from methyl orange and the methyl orange nerve system. The spectrum from the dye-nerve system shows a drastic change in intensity and position of bands, indicating N=N symmetrical stretch, S=O bonds and skeletal π electrons interactions.

The work encourages us to use molecular properties of membranes that might be used as naturally existing probes for photoic monitoring of the steady state and dynamic properties of neurons.

Supported by NSF BNS78-08536.

M-PM-A7 POTASSIUM CHLORIDE CO-TRANSPORT IN STEADY STATE ASCITES TUMOR CELLS: DOES BUMETANIDE INHIBIT? Felice Aull. Dept. of Physiol. and Biophys., NYU Sch. Med., New York, NY 10016.

The steady state exchange of K and Cl was investigated in Ehrlich ascites tumor cells treated with bumetanide. Bumetanide did not alter the cellular content of K or Cl but the self exchange of both ions was depressed. K self exchange was inhibited by 55% at bumetanide concentrations as low as 10^{-6}M. Cl^- self exchange was less sensitive to this drug but at low concentrations (between 10^{-6} and 10^{-3}M) bumetanide was a more effective inhibitor of Cl transfer than furosemide. The steady state K flux of cells equilibrated in NO_3 media was compared with the K flux in cells treated with 10^{-4}M or 10^{-3}M bumetanide; the Cl^- sensitive K exchange was equivalent to the bumetanide sensitive K exchange. Since the results suggested that a bumetanide sensitive (Cl + K) co-transport could be operative in steady state cells, the stoichiometry of the bumetanide sensitive fluxes was determined by measuring Cl and K fluxes simultaneously in the same cell suspension. At 5 x 10^{-4}M and 10^{-3}M bumetanide concentrations, the ratio of these fluxes was 0.98 $\pm$ 0.07 (S.E.) and 1.04 $\pm$ 0.06, respectively, consistent with the postulated co-transport mechanism. At 10^{-4}M and 10^{-3}M, however, the ratio of the bumetanide sensitive Cl/K flux was significantly less than 1.0. Since the magnitude of the bumetanide sensitive K flux at 10^{-4}M was close to that of the Cl^- sensitive flux, a ratio of less than 1.0 at this drug level indicates that Cl^- sensitivity and drug sensitivity may not reflect inhibition of the same process under all circumstances. Supported by Grant No. 10625 from the National Cancer Institute, DHEW.

M-PM-A8 SINGLE-CHANNEL STUDIES ON GRAMICIDIN A ANALOGS. E.W. Barrett*, L.B. Weiss*, O.S. Andersen, and L. Stryer.(SPON: D. Gardner). Dept. Physiology and Biophysics, Cornell University Medical College, New York, N.Y. and Dept. Structural Biology, Stanford University School of Medicine, Stanford, Ca.

Single channel conductance characteristics of selected gramicidin A (gram A) analogs, with substitions at positions #1 or #11, have been studied in an effort to correlate structural modifications with permeability changes. Substitutions at #1 were made using the procedure of Morrow et al.(J.Mol.Biol,132:733(1979)). Effects of changes in chain length and in polarity were analyzed. Measurements were made in diphytanoylphosphatidylcholine/n-decane bilayers, at 0.1 and 1.0 M NaCl. This enables us to determine if changes in channel conductance reflect changes in the maximal conductance (G) or changes in the dissociation constant (K) between Na^+ and the channel. Sequential increases in the length of the (linear) carbon chain at position #1 (α-NH_2-butyric acid through norleucine) increases G slightly, but has no significant effect on K. Increasing the polarity of the chains (by replacing the terminal methylene with the more polar sulfur) decreases the channel conductance. This results from a decrease in G (about 2-fold), and an associated decrease in K. Even more dramatic effects are seen when substituting hexafluorovaline for valine. G decreases by more than one order of magnitude, this is again associated with a decrease in K. The natural gram A analogs, gram B and gram C, were used to probe at position #11. We confirm the results of Bamberg et al.(BBA,419:223(1976)), that the conductance of gram B channels is less than of gram A or gram C channels. We can additionally show that the decreased conductance is due to a decrease in G. The permeability of gram A channels varies with both the bulk and the polarity of the amino acid side-chains.

M-PM-A9 ON THE POSITION OF THE ALKALI METAL CATION BINDING SITES IN GRAMICIDIN CHANNELS. O.S. Andersen, E.W. Barrett*, Dept. Physiology and Biophysics, Cornell University Medical College, New York, N.Y., and L.B. Weiss*, Dept. Structural Biology, Stanford University School of Medicine, Stanford, Ca.

There is considerable X-ray crystallographic information about the possible structure of gramicidin A (gram A) channels, including information about possible locations of the cation binding sites in the channel (Koeppe et al., Nature,279:723(1979)). But the precise relation of the crystal structure to the structure of the channel in a membrane is uncertain. The present studies were designed to adress this question. Gram A single-channel current-voltage characteristics were obtained in diphytanoylphosphatidylcholine/n-decane bilayers at high salt concentrations (3.5-5.0 M), where the currents become essentially concentration-independent. The measurements were extended up to very high potentials (300-500 mV). At these high potentials the voltage-dependence of the currents should reflect the properties of the least voltage-dependent of the steps involved in ion translocation through the channel. The single-channel currents are indeed exponential functions of the applied potential in this potential range, and the voltage-dependence of the currents is remarkably similar for all of the alkali metal cations: 8.3-9.6 % of the applied potential is expressed in the currents. This suggests that we indeed have visualized the ion movement from an energy well (binding site) across an adjacent energy barrier, whose peak is about 2.5 A from the well (the gram A channel is about 26 A long). Experiments with gram A analogs (using substitutions in position #1 or #11) show that the wells and the barriers are located close to the C-terminal ends of the channel - that is, close to the channel entrances. This conclusion, as well as the separation between wells and barriers, is consistent with the data of Koeppe et al.

M-PM-A10 INITIATION OF MONAZOMYCIN SINGLE-CHANNEL ACTIVITY. R. Muller* and O.S. Andersen. (SPON: E.E. Windhager). Dept. Physiology, Downstate Medical Center, Brooklyn, N.Y. and Dept. Physiology and Biophysics, Cornell University Medical College, New York, N.Y.

Although the voltage-dependent monazomycin (Mon)-induced conductance presumably rests on the existence of oligomeric channels, no rigorous proof has yet been acheived; it is not yet possible to account for the voltage-dependence of the macroscopic conductance by the statistics of single-channel events. We now believe we understand why this connection has been so hard to establish. Kinetic studies of the macroscopic conductance show that the rate constant for the slow step in channel formation is proportional to the amount of Mon already in the film. In a virgin bilayer, the rate constant for this autocatalyzed path is identically zero. Therefore, there must be some non-autocatalytic, very slow, process which allows the first Mon molecules to enter the film. We have devised a technique to demonstrate this complexity directly. We simultaneously record the conductance of a large ($1mm^2$) film, and of a very small ($10^{-4}mm^2$) film isolated by pushing a micropipet through the large film. The voltage of each film can be independently set. If the small film is taken when the large film is at very low conductances, it is quiescent and shows no channel activity until very large (~500mV) potentials are applied. By contrast, if the small film is taken when the large film is at high conductance, it immediately shows channel activity at applied potentials in the range of 100-150mV. We conclude that the initiation of channel activity requires a very infrequent event to occur. Also, the ability to dissociate the conductance of the two films rests in the 10^{-4}-fold probability ratio of having such an event in the small film. That very high potentials can promote channel activity indicates that the non-autocatalytic process is either voltage-dependent or requires the disruption of the bilayer matrix by high voltage.

M-PM-A11 INTERNAL GATING OF ION CONDUCTANCE IN A GRAMICIDIN CHANNEL. Gabor Szabo, Department of Physiology and Biophysics, U.T.M.B., Galveston, Texas 77550

Gramicidin A forms ion conductive channels in lipid bilayer membranes. Once formed, these channels show no detectable conductance fluctuations. Replacement of the N-terminal -H residue of gramicidin A by a $-CH_3$ residue (N-acetyl gramicidin) results in channels that rapidly fluctuate between two well defined states, one conductive (high) and the other practically non-conductive (low). Transitions between these two states are described by first order kinetics. Thus, the channel lifetimes in the "high" and "low" state are distributed exponentially with time constants τ_1 and τ_2 equal to the mean lifetime of the "high" and "low" states respectively. Furthermore, the power spectrum of the conductance fluctuations is Lorentzian, with a corner frequency $fo = (1/\tau_1 + 1/\tau_2)/2\pi$ expected for the simple two-state model. The rate constants of high to low ($\alpha = 1/\tau_2$, typically 250 sec^{-1}) and low to high ($\beta = 1/\tau_1$, typically 1500 sec^{-1}) transitions have been determined for a variety of experimental conditions. Both α and β are found to be practically independent of membrane potential and membrane lipid composition. Temperature, in contrast, alters both α and β. Arrhenius plots of α and β are linear over the 10°C to 35°C temperature range. The activation energies are found to be large, 14.5 KCal/mole and 19.8 KCal/mole for α's and β's respectively. All of these results are predicted by a model in which the rather bulky $-CH_3$ residue in N-acetyl gramicidin rotates into the lumen of the channel and thereby blocks ion movement through it. Consideration of molecular models show this process to be feasible through the rotation of only a few residues at the N-terminus. The proposed steric mechanism of channel gating may prove to be a useful model for the gating of conductive channels in excitable membranes as well. (Supported by N.I.H. Grant GM-26897).

M-PM-A12 MOLECULAR MECHANISMS OF ALAMETHICIN CHANNEL GATING AND FORMATION. R. Latorre and S. Quay; Department of Physiology, Harvard Medical School, Boston, MA 02115, and Department of Pathology, School of Medicine, Stanford University, Palo Alto, CA 94304

In order to obtain more information about the molecular processes involved in the formation of the alamethicin channel, and also to test the different models for channel formation, we have synthesized an alamethicin analog consisting of an alamethicin molecule covalently bound to a phospholipid molecule. This conjugate was made by incorporating alamethicin into phospholipid vesicles made of phospholipids containing photoactivable carbene precursors. The carbene precursor was localized at the center of the bilayer. The alamethicin conjugate was prepared by photolysis of the vesicle sample. Preliminary experiments indicate that the phospholipid is preferentially bound to amino acid residues 2-13. This alamethicin conjugate induces a voltage-dependent conductance very similar to that of natural alamethicin. The conjugate was made with two purposes in mind: first, to make alamethicin more soluble in the bilayer, and second, to orient the alamethicin molecule perpendicular to the plane of the membrane. In view of the fact that the alamethicin conjugate induces a voltage-dependent conductance, it is tempting to suggest that alamethicin gating is a configurational change of the alamethicin molecule itself and not, as current models propose, insertion of monomers into the membrane.

M-PM-A13 Ca CHANGES THE I-V CHARACTERISTIC OF THE GRAMICIDIN CHANNEL TO THAT SEEN IN THE LIMIT OF LOW PERMEANT ION CONCENTRATION. G. Eisenman, Dept. Physiol., UCLA, L.A., Ca. 90024.

A many-channel method was used to study the influence of Ca on the I-V shape of single gramicidin channels, first described by Bamberg and Läuger (J. Memb. Biol., 35:351 (1977)). For all permeant ions studied (Cs, Na, Li and CH_3NH_3) Ca was found to change the shape at any conc. to one characteristic of that species at low conc., as illustrated for Cs below (G^C/G^O = normalized chord conductance = G(V)/G(0)). This limiting shape (middle and right) implies that the barrier for leaving the channel is slightly lower than that for crossing it (Eisenman et al., Uppsala, J. Med. Sci., in press) and that the ratio of these barriers is unaltered by Ca, in contrast to the selective raising of the entrance barrier suggested by Bamberg and Läuger. It appears that the Ca binding site is not only external to the 1st barrier but that Ca raises the energy uniformly across the channel as if it reduced the concentration of permeant ion at the mouth of the channel by a simple electrostatic repulsion.

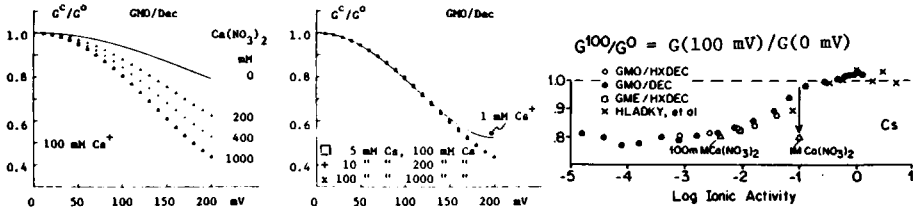

Supported by Grants from NSF (PCM 7620605) and USPHS (GM 24749).

M-PM-B1 MECHANISMS OF PROTON RELAXATION IN DNA, D.R. Kearns, T.A. Early, J. Feigon, and R. Behling, Department of Chemistry, University of California-San Diego, La Jolla, CA.

The relaxation behavior of the exchangeable and non-exchangeable protons in DNA have been monitored by pulsed NMR techniques. The effect of partial deuteration on the relaxation behavior of the imino protons has been used to test various aspects of relaxation theory. The ratios of spin-spin and spin-lattice relaxation times are accurately predicted for AT and GC base pairs and in short DNA the relaxation behavior can be accounted for in terms of a rigid rotor model using a single rotational correlation time. For the larger DNA the rotational correlation times deduced from the NMR experiments are substantially shorter than those expected from hydrodynamic calculations assuming a rigid cylinder model for the DNA. A comparison of selective and nonselective spin-lattice relaxation measurements clearly indicates that there is extensive spin diffusion in DNA molecules which are shorter than 40 base pairs. Another manifestation of spin diffusion is the observation of transient nuclear Overhauser effects in the spectrum. It appears that measurements of selective spin-lattice relaxation rates, transient NOEs and spin-spin relaxation rates will provide detailed structural and dynamic information on DNAs in solution.

M-PM-B2 DNA INTERNAL MOTIONS IN SOLUTION. M. Hogan, J. Wang, R. Austin

We have studied fast DNA internal motions by measuring triplet anisotropy decay of dye labels intercalated into the helix. We have measured the rate of decay of triplet absorbance and phosphorescence (triplet emission) for two dyes (methylene blue, and an eosin analogue). Together, these measurements allow us to monitor DNA motions over the whole time range from 10^{-8} to 10^{-4} seconds, using dye concentrations less than 1 μM. Preliminary measurements were made on fragments which were prepared by digesting calf thymus DNA with DNAase 1 and an excess of S1 nuclease, then fractionating the DNA by length over Sepharose 6B. The average length and length distribution of the resulting fractions was determined from their electrophoretic mobility relative to restriction fragments. In subsequent work, we have used individual, sequenced DNA fragments produced by the HAE III restriction enzyme digest of the E. Coli plasmid pBr322.

M-PM-B3 LONG RANGE FORCES IN DNA. E. W. Prohofsky, W. N. Mei*, M. Kohli*, and L. L. Van Zandt*, Dept. of Physics, Purdue University, W. Lafayette, Indiana 47907

The role of nonbonded forces in double helical polymer DNA has been analyzed by fitting theoretical calculations of the acoustic velocity to experimental observations (G. Maret et. al., Colloid and Polymer Science, 257, 339-340 (1979)) of this velocity. The fits were attempted with both short and long range interaction models. The results indicate that long range "electrostatic like" interactions are necessary to explain the observations for A conformation. Long range forces are also likely necessary to explain the B conformation results. The results indicate significant base pair interaction over a range of 40 base pairs in A conformation and 30 base pairs in B conformation. The fitted nonbonded results indicate that a change in effective dielectric constant by a factor of eleven is likely between fairly dry samples in A conformation and wet fibres in B conformation. The results lead to an estimate of twenty for the effective dielectric constant for long range electrostatic interactions between base pairs in wet samples. The calculated acoustic modes have been used to estimate the microwave absorption of double helical DNA. Finite segment acoustic resonant absorption has been examined and long segments of DNA are found to have orders of magnitude more absorption than an equivalent mass of water over a range of frequencies. The detailed arrangement of DNA in chromatin can determine the probable hazard due to microwave absorption by the DNA.

M-PM-B4 X-RAY SCATTERING FROM RANDOMLY ORIENTED SUPERHELICAL DNA. G.W. Brady, S.J. Irving*, D.B. Fein and V. Grassian. N.Y. State Dept. of Health and SUNY, Albany, NY 12201. *Rensselaer Polytechnic Institute, Troy, NY 12181.

The x-ray scattering from a circular DNA, the plasmid COP608, a deletion from PT181, and containing 4221 base pairs has been measured over a range of temperatures at various concentrations of intercalated Platinum (PtTS). The measurements are an extension of those presented by Brady, Brumberger and Fein on PM2 (Nature 264, 231-234, 1976) to a much shorter molecule, and improvements in equipment have allowed continuous measurements in the correlation range from 300 to 10,000 A. The concentration of DNA was kept below 15 mg/ml to minimize association effects. The results in their present form show that the behavior of COP608 is similar to that of PM2, indicating that the supercoiling is not primarily dependent on the molecular length. Two orders of supercoiling are observed. The results have been interpreted in terms of electron pair correlation functions (Benham, Brady and Fein, Biophys. J. 29, 351-366, 1979). The scattering is shown to be consistent with a coiled coil DNA geometry. (Supported by NSF grant PCM 79 13078).

M-PM-B5 ELECTROSTATIC CONSIDERATIONS IN BRANCH POINT MIGRATION. Nadrian C. Seeman, Center for Biological Macromolecules, SUNY/Albany, Albany, NY 12222 and Bruce H. Robinson, Dept. of Chemistry, University of Washington, Seattle, Wash. 98195.

Branch point migration is a central event in the process of genetic recombination. We have generated a model for the structure of the branch point formed when two DNA double helices exchange strands. This model maintains the twofold symmetry inherent in the covalent structure, yet has three degrees of freedom parameterized by virtual bonds. We have calculated the electrostatic energy and torque about the helix axes associated with each of the sterically allowed conformations of the branch point. The most favored conformation with respect to electrostatic criteria involves a pseudo-4-fold symmetric structure. The productive torque, which is the net torque in the direction favoring migration, is an antisymmetric function which passes through zero at the minimum energy conformation. The torque becomes appreciable, however, at accessible displacements from the minimum energy conformation. The structure of the electrostatic energy-torque profile of our model thus indicates that there is an equal probability of migration in either direction, as has been assumed in earlier treatments. However, it also indicates that the unit migrational event may not be a single transition, but rather a series of concerted transitions, driven by the productive torques, which exist when the structure makes highly probable deflections from the minimum energy conformation. This conclusion reflects on the problem of strand exchange between DNA molecules which are homologous, but are not identical: occasional mismatches will not generate kinetic barriers which seriously inhibit strand exchange.

This research has been supported by grant GM26467 from the National Institutes of Health, and a Basil O'Connor Starter Grant from the March of Dimes Birth Defects Foundation.

M-PM-B6 STUDY OF THE B-TO-Z CONFORMATION CHANGE OF POLY(dG-dC) INDUCED BY MODERATE CONCENTRATIONS OF $Mg(ClO_4)_2$. Eugene Hamori and Thomas M. Jovin, Department of Biochemistry, Tulane Medical School, New Orleans, La. and Max-Planck Institut für Biophysikalische Chemie, Göttingen, West Germany.

Poly(dG-dC) has been known to undergo a cooperative B-to-Z conformational transition involving a change in the chirality of the double helix from a left to right handed form. It was believed that this conversion takes place only at rather unphysiological high salt or organic solvent concentrations. We have found, however, that $Mg(ClO_4)_2$ can cause the same transition at the moderate concentration of 0.26 M. The comparison with the effects of NaCl, $MgCl_2$ and $NaClO_4$ indicates that $Mg(ClO_4)_2$ is more effective that it would be anticipated from the combined presence of its ions. These results suggest the importance of some ion-specific interactions. The transition can be followed spectroscopically through a large hyperchromic change at 295 nm wave length. The reaction is fully reversible and can be described by a single exponential function with half time values between 5 and 150 minutes. The average relaxation times observed are strongly salt-concentration dependent with a distinct maximum at the salt concentration of the transition point. Following the completion of the conformation change the polymer slowly precipitates. The natural DNA from M. Lysodeicticus which has a GC content of 72% is also precipitated by $Mg(ClO_4)_2$ but not Calf Thymus DNA (41% GC) or Poly-(dA-dT). We could find no spectroscopic signs, however, for any B-to-Z conformational transition in M.-Lysodeicticus DNA solutions prior to or after the precipitation point.

Supported by a fellowship from the Max-Planck Institut für Biophysikalische Chemie and an NIH Grant (GM 20008-06A1).

M-PM-B7 CIRCULAR DICHROISM OF DNA MICROCRYSTALS MEASURED BY A CD MICROSPECTROPHOTOMETER. Kenneth H. Downing and Marcos F. Maestre, Biology and Medicine Division, Lawrence Berkeley Laboratory, Berkeley, CA 94720.

Calf thymus DNA and poly d(A-T) poly d(A-T) crystals have been obtained from ethanolic solutions. These crystals are in the form of thin hexasonal platelets, up to 50 μm across and apparently several tens of nm thick. Electron diffraction patterns from these crystals (1), obtained with the beam normal to the broad faces, show a sixfold symmetry indicative of the packing of the DNA strands. Using a CD microspectrophotometer (2), the CD spectrum of the crystals has been measured in the 350-200 nm wavelength region, in a direction perpendicular to the crystal faces. The crystals have a conservative CD spectrum, commonly associated with DNA in the B form. There is no birefrinsence contribution or perturbation of the CD signal, when measured normal to the crystal faces. The values of the CD spectrum agree well with those reported for the CD of flow oriented DNA when measured along the direction of flow (3). These results indicate that the DNA strands are parallel to each other and oriented perpendicular to the crystal faces to within one degree.

This work is supported by NIH grants GM27291 and A108247, and DOE contract W-7405-ENG-48.

(1) K.H. Downing and R.M. Glaeser, Biophys. J., in press.
(2) M.F. Maestre, work in progress.
(3) S.-Y. Chung and G. Holzwarth, J. Mol. Biol. 92: 449 (1975).

M-PM-B8 THERMAL ANALYSIS OF REPEATED DNA SEQUENCE HETEROGENEITY. Douglas L. Vizard, Allen T. Ansevin and J.-Numa Lapeyre, Departments of Physics and Experimental Pathology, The University of Texas System Cancer Center, Houston, Texas 77030.

Selected repeated sequences of the mouse, rat and other eukaryotic genomes were subjected to thermal denaturation, reassociation and re-denaturation analyses. In many cases, heterogeneity within a given repeated sequence class was apparent in all three types of thermal analyses; however, the re-denaturation analysis was particularly revealing in assessing the degree and kind of sequence heterogeneity, manifested by the altered thermal stability of mismatched complementary DNA strands. Even in the case of the most homogeneous repeated sequence selected for this study, the re-denaturation analysis implied either the existence of sequence subclasses or a highly non-random mutation distribution among DNA molecules, which are indistinguishable alternatives. Only in the case of marked sequence heterogeneity is the primary thermal denaturation experiment informative as to the state of heterogeneity. We have also found that the kinetic reassociation experiment, which has been widely used to assess the degree of mismatching among otherwise complementary DNA strands, cannot be unambiguously interpreted in terms of sequence heterogeneity, since both the DNA sequence itself and its length influence the rate of reassociation.

Supported by NIH Grant GM-23067.

M-PM-B9 THEORY OF HELIX-COIL TRANSITION FOR DNA WITH MONOMER BINDING INCLUDING INTERCALATION UNDER FIXED TOTAL MONOMER CONCENTRATION. Takashi Tsuchiya (Intr. by Terrell L. Hill) LMB, NIAMDD, NIH, Bethesda, Md 20205.

Utilizing the matrix method, we formulate the problem in as general a way as possible so that we can treat all the different schemes of binding of monomers, including nearest-neighbor interactions, to two complementary chains in helical or melted states. The treatment can be said to be exact as long as the Ising model description of the system is valid. We calculate the helical fraction θ and the ratio p of the number of bound bases to the total number of base pairs under the condition of constant total monomer concentration, as is the case in experiments. We compare our results for helix stabilizers and destabilizers with those of McGhee's approximate treatment (Biopolymers 15, 1345 (1976)). We find, as well as quantitative differences, a qualitative one, namely, biphasicity appears in our case for sets of parameters for which his calculation gives a monophasic curve. The ratio p definitely takes a maximum value during the biphasic transition, which means that released monomers increase the concentration of free monomers in the solution. Hence further binding is encouraged to favorable regions of DNA. If we interpret that the double helix of DNA consists of two grooves, major and minor, instead of two complementary chains, our general matrix can also describe all the possible modes of intercalation of drug molecules into the DNA. We can produce either monophasic or biphasic transition profiles with reasonable values of parameters. By fitting our results to Noji's UV-absorption data obtained with three different acridine dyes added to DNA (J. Sci. Hiroshima Univ. Ser. A 44, 119 (1980)), we estimate differences in binding constants.

M-PM-B10 INTERACTION OF PROFLAVINE AND ETHIDIUM BROMIDE WITH DNA AND MONONUCLEOSOMES, Kenneth S. Schmitz, Jennifer Gauntt Gayle Grunke, and Brinda Ramanathan, Department of Chemistry, University of Missouri-Kansas City, Kansas City, Mo. 64141.

Binding data involving small ligands with nucleic acids are generally represented as Scatchard plots, i.e. r/m vs. r where r is the ligand/site and m is the free ligand concentration. The McGhee-von Hippel model(J.Mol.Biol. 86,1974(469)) has in recent years been the theoretical basis for interpretation of these Scatchard plots. This theory, although generally applicable to random and cooperative binding systems, has limited applicability to anti-cooperative systems in that negative values of r/m are obtained if the number of excluded sites is an odd number. We have developed a model which finds general applicability over all ranges of neighbor interactions (Biopolymers 17,1978(2171)), viz.,

$$r/m = (B/\sigma)\,\frac{r^2}{(r-\phi)}\left\{\frac{1-qr-\phi}{1-qr}\right\}^q \qquad (1)$$

where

$$\phi = \frac{-\{(r+1-qr)\sigma\} + \sqrt{\{(r+1-qr)\sigma\}^2 + 4r(1-qr)(1-\sigma)\sigma}}{2(1-\sigma)} \qquad (2)$$

σ is the neighbor interaction parameter, q is the number of excluded sites, and B is the intrinsic binding constant. Optical absorbance methods were employed to determine Scatchard plots for proflavine and ethidium bromide binding by DNA and chicken erythrocyte mononucleosomes with the preliminary results that a small number of binding sites in the mononucleosome more strongly bind these ligands than naked DNA and that both electrostatic effects and strain on the DNA helix upon intercalation influence the stability of the mononucleosome. (Partial support for this project was provided by the American Cancer Society(NP-332)

M-PM-B11 LASER LIGHT SCATTERING STUDIES OF THE BINDING OF INTERCALATING DRUGS TO SUPERCOILED DNA. K.-L. W. Wun and R.H. Shafer, University of California, San Francisco, CA 94143.

We present results of quasi-elastic laser light scattering (QELS) experiments on the binding of various drugs to supercoiled DNA. Intercalation of increasing amounts of ligand molecules in supercoiled DNA will first lead to a loss of negative supercoils, followed by a gain of positive supercoils. This behavior produces a minimum (maximum) in a plot of sedimentation coefficient (intrinsic viscosity) as a function of added drug. Analogously, a minimum is expected in a titration measuring the translational diffusion coefficient, D_T. We have determined the variation of D_T with added ligand using QELS for several drugs, including ethidium and daunomycin. A D_T minimum was found for each intercalator consistent with previous sedimentation studies. Results are also presented for N-acetyl bleomycin, an analog of bleomycin that binds to DNA but shows no nicking activity. Here also a minimum in the D_T plot was found, supporting the notion that bleomycin binds to DNA by intercalation. QELS is fast, requires little material and also has the potential of measuring ligand effects on internal motions. Supported by grant # GM27492 awarded by NIH, DHEW.

M-PM-B12 SALT PERTURBATIONS ON THE FLUORESCENCE OF TRANSFER RNA. Barbara D. Wells, Chemistry Department, University of Wisconsin-Milwaukee, Milwaukee, WI 53201.

Transfer RNA conformation is recognized to be quite sensitive to salt concentration as is any polyelectrolyte. The fluorescence of wyebutine (Y) at position 37 in yeast $tRNA^{Phe}$ is quite sensitive to solvent composition. Various aspects of this sensitivity have been noted. A systematic study of the variation of the fluorescent parameters was undertaken in the hopes of using these parameters to describe the conformation of the anticodon loop. The emission and excitation spectra, polarization, and Stern-Volmer quenching of Y fluorescence were all measured. The tRNA was dissolved in a Tris buffer and titrated with magnesium or potassium salts. Iodide or acrylamide quenching was followed at selected salt concentrations. The quenching studies were evaluated by both intensity and polarization changes. As would be expected, magnesium concentration was the major perturbant; however, small spectral changes could still occur at saturating magnesium concentrations. The salt effects are interpreted to be a stabilization of the phosphodiester backbone resulting in a more rigid state for the Y base (high polarization). The Y base thus offers a probe for studying dynamic motions in transfer RNA.

M-PM-C1 PERMEANT CATIONS ALTER K CHANNEL KINETICS AND PERMEABILITY. G.S. Oxford and D.J. Adams. Department of Physiology, University of North Carolina, Chapel Hill, NC 27514 and the Marine Biological Laboratory, Woods Hole, Mass. 02543

The kinetic behavior and instantaneous current-voltage relations of delayed rectifier K channels were examined in perfused squid axons under voltage clamp. Various monovalent cations were substituted for potassium on either side of the membrane and their relative permeability determined from reversal potential measurements. The sequence of relative permeabilities for several ions was similar to previous reports ($Tl > K > Rb > NH_4 > Li \geq Na$). Curiously, the absolute permeability ratios were consistently larger for changes in the external cations than for internal cations. The reversal potential and kinetics of K currents were measured in symmetrical internal and external solutions of varying potassium concentration between 50 and 600mM. An 'inert' cation substitute, N-methylglucamine (NMG), replaced K on an equimolar basis. The reversal potential remained within a few millivolts of 0 over this range and the activation kinetics of K channels were unchanged, thus verifying the inertness of NMG and reflecting the lack of effect of K concentration on these parameters. During outward NH_4 current through K channels the rate of activation of the conductance was significantly faster than observed normally when K ions carry the current. The characteristic delay in turn-on of the conductance was nearly absent in some cases. Similar observations were made with Tl currents. The shape of the instantaneous I-V for I_{NH4} suggests voltage-dependent interactions of NH_4 ions as they pass through the K channel. The reversal potential in symmetrical NH_4 solutions differed from that in symmetrical K solutions. These results may suggest an interaction of certain permeant cations with the gating machinery during their passage through the K channel. (Supported by NSF grant BNS79-21505 and the Grass Foundation).

M-PM-C2 INTERNAL ANIONS MODULATE POTASSIUM CHANNEL GATING IN SQUID AXONS. D.J. Adams and G.S. Oxford. Marine Biological Laboratory, Woods Hole, Mass. and Department of Physiology, University of North Carolina, Chapel Hill, NC 27514.

Kinetic and steady-state properties of the delayed rectifier K channel of perfused squid axons were examined under voltage clamp in the presence of a variety of internal anions. Changing the internal potassium salt from 320mM K-glutamate (Glu) to 320mM KF (F) resulted in a gradual (30-60 min) decline in outward I_K at all voltages to ~30% of control. The rate of opening of K channels was also dramatically slowed by ~3-10 times as determined from the rise of I_K upon depolarization or from g_K tail envelopes. The rate of closing, however, was unaffected as K tail current time courses in F^- were identical to those in Glu. Both the amplitude and activation rate of I_K were rapidly (30-60 sec) restored upon return to Glu as the internal anion. Significant recovery of K channel gating was seen with F:Glu ratios as low as 1:200. The effects of F were specific for K channels as Na currents remained unaltered during these procedures. The effects of prolonged exposure to internal F^- could also be partially reversed by the addition of small concentrations of cationic agents known to block K channels from the axoplasmic surface (e.g., TEA^+, 4-AP^+, and Cs^+). The reduction in g_K by F ions was not antagonized by elevating the external potassium concentration. Of 12 anions tested all inorganic species induced similar decreases and slowing of g_K, while K currents were maintained at control levels during extended perfusion (1-2 hrs) with several organic anions. More than half of the control g_K was observed even following a 1 hr exposure to K-free media and internal glutamate. Our observations suggest that inorganic anions may alter the gating properties of K channels by interaction with a site(s) on the internal channel surface identical with or related to sites of interaction with certain cationic channel blockers. (Supported by NSF grant BNS79-21505).

M-PM-C3 LOW EXTERNAL pH BLOCKS AND SHIFTS K CHANNEL OF FROG SKELETAL MUSCLE. Andrew L. Blatz (Intr. by B. Hille), Univ. of Washington, Seattle, WA 98195.

The Hille-Campbell vaseline-gap voltage clamp technique was used to examine the effects of low external pH on currents through the delayed rectifier K channel in single frog skeletal muscle fibers. Cut ends of the fibers were bathed in either 70 mM K_2EGTA or 70 mM $[N\text{-Methyl-Glucamine}]_2EGTA$. External solutions contained 0-120 mM KCH_3SO_4, 5-20 mM RbCl, 2 mM $CaCl_2$, 500 nM TTX and 5 mM each of the buffers N-Acetyl Glycine, MES and MOPS. The solutions were titrated to various pHs with N-Methyl-Glucamine. Between pH 7.1 and 4.0 conductance curves were shifted by 20 mV per unit drop of pH. When the pH was lowered to 4.0 outward currents were about 20% blocked for a depolarization to 100 mV. The block was partially relieved at larger depolarizations. Inward currents through delayed rectifier channels decreased below pH 6 and fell to 10% of normal at pH 5.2. These results suggest that hydrogen ions bind, not only to charged groups on the surface of the membrane, but also to sites within K channels. When the pH was lowered from 7.1 to 5.2 in 20 mM K^+ + 20 mM Rb^+ the reversal potential shifted in a positive direction by at least 5 mV, but the exact value was obscured by a strong block of inward currents. Assuming that the ionic selectivity of K channels is unchanged by pH, this shift indicates that P_H/P_K is at least 1000. (Supported by NIH Grants NS-08174 and GM-07270.)

M-PM-C4 SOLUTION MICROVISCOSITY MODULATES THE KINETICS OF K-CHANNEL BLOCK BY TETRAETHANOL AMMONIUM. R. J. French[1], J. J. Shoukimas[2], M. S. Brodwick[3], and D. C. Eaton[3]. [1]Department of Biophysics, University of Maryland School of Medicine, Baltimore, MD, 21201; [2]Laboratory of Biophysics, NINCDS, Marine Biological Laboratory, Woods Hole, MA, 02543; [3]Department of Physiology and Biophysics, University of Texas Medical Branch, Galveston, TX, 77550.

Internal tetrakis(2-hydroxyethyl)ammonium causes a voltage dependent block of the potassium conductance in voltage clamped, perfused squid giant axons. It is a less potent blocker than non-hydroxylated tetraalkylammonium ions of similar size. Preliminary analysis of the steady state block indicates that the tetrakis binds at a site 25-30% of the way through the transmembrane voltage with an apparent dissociation constant, at E=0, of about 20 mM. With the conductance fully activated, when a voltage step is applied, the current rapidly relaxes to a new level with a time constant, $\tau \approx 40$ μsec for 2 mM tetrakis, $40 \leq E$ (inside minus outside) ≤ 180 mV. The reciprocal of the time constant was linearly dependent on the tetrakis concentration. Time constants did not vary greatly (≤25%) over the voltage range studied. Sucrose (1 M) added to both internal and external solutions increased τ approximately 3-fold. A similar, but smaller, effect was produced by mannitol. Ficoll (MW ≈ 400,000) added to internal and external solutions to give the same macroscopic viscosity as the sucrose-containing solutions produced no detectable change in τ. These effects of the non-electrolytes parallel their abilities to modify the mobility of ions in free solution. Our data suggest that the access of tetrakis to its site of action is rate-limited in the aqueous phase. This rate-limiting step is influenced little, if at all, by the applied voltage.

M-PM-C5 PANDINUS SCORPION VENOM MODIFIES K CHANNEL GATING. M. Cahalan† and W. Culp††; Depts. of Physiology and Biophysics, †Univ. of Calif., Irvine, CA 92717 and†† Biochemistry, Dartmouth College, Hanover, NH 03755.

Pandinus scorpion venom prolongs the duration of action potentials in frog myelinated nerve or skeletal muscle fibers. Unlike Leiurus scorpion venom which produces a similar effect on the action potential by slowing sodium inactivation, Pandinus venom has virtually no effect on sodium channels, but specifically alters the kinetics and voltage dependence of potassium channels. The effects of crude Pandinus venom and a low molecular weight (2000) peptide fraction have been studied on single frog nodes of Ranvier under voltage clamp. Crude venom at 10-100 μg/ml results in a block of K current that is stronger at moderate depolarizations than at very positive potentials. At 50 μg/ml, crude venom blocks about 80% of K current at -30 mV, but only about 20% of K current at +50 mV. Both outward K current and inward K current with 115 mM extracellular K are blocked. The time course of K channel activation is slower than normal at moderate depolarizations, but inward tail currents at -90 mV are more rapid, upon exposure to the venom: The midpoint of the K channel activation-voltage curve, obtained by analyzing inward K tail currents, is shifted in the depolarizing direction by 25 mV in the presence of the venom. These effects, observed with crude venom and the partially purified peptide fraction, are only partially reversible upon washing. A working hypothesis for the action of this venom is that peptide toxin molecules bind to K channels and accelerate the closing rate constant, β_n. (Supported by NIH grants NS14609, NS12067, NS00058 and the Muscular Dystrophy Association.)

M-PM-C6 IONTOPHORETIC INJECTION OF QUATERNARY AMMONIUM COMPOUNDS BLOCKS OUTWARD CURRENTS IN CARDIAC PURKINJE FIBERS. R.S. Kass, K.J. Malloy, and T. Scheuer. Dept. of Physiology, Univ. of Rochester, Rochester, N.Y. 14642

Voltage clamp analysis of plateau currents in Purkinje fibers is complicated by the similar voltage-dependence of the activation of three currents: the transient outward current (I_{qr}), the delayed rectifier (I_x), and the slow inward (calcium) current (I_{si}). Attempts at pharmacological dissection of these currents using calcium channel blocking agents have been restricted since these agents have been shown to also reduce I_x and I_{qr}. We report an alternate approach to this problem: block of these outward currents by iontophoretic injection of the quaternary ammonium compounds TEA^+ (tetraethylammonium ion) and TBA^+ (tetrabutylammonium ion). We injected these compounds, determined their effects on I_{qr} and I_x, and found that both agents are effective in reducing these currents. Shortened segments of calf or dog cardiac Purkinje fibers were alternately voltage- or current-clamped using a conventional two microelectrode arrangement. The current micropipette was filled with 1.5 M TEA-Cl or 1.5 M TEA-Br and then bevelled to a tip resistance on the order of 40 M-Ohms. TEA^+ or TBA^+ ions were injected by passing trains of outward current pulses. Injection of 10-30 μCoul of either compound over periods of 15-30 min consistently reduced, but did not always abolish, the outward transient. Comparable injection of TEA or TBA blocked 70-90% of I_x, estimated by isochronal activation curves. TBA^+ appears more effective than TEA at reducing I_x. We conclude that iontophoretic injection of these compounds provides a useful technique for blocking these outward currents and should allow for a more detailed analysis of Purkinje fiber plateau currents.

Supported by AHA 78-993 and NIH HL21922.

M-PM-C7 THE EFFECT OF 4-AMINOPYRIDINE ON THE LATE OUTWARD PLATEAU CURRENTS IN CARDIAC PURKINJE FIBERS. J.M. Jaeger and W.R. Gibbons*, Dept. of Physiol. and Biophys., Univ. of Vermont, College of Med., Burlington, VT 05405.

The K+ channel blocking agent, 4-Aminopyridine (4-AP), abolishes the majority of the early outward current (I_{eo}) in sheep cardiac Purkinje fibers (PF) activated by voltage clamp pulses positive to -20mV. Using a standard two microelectrode voltage clamp on short segments of sheep PF, we studied the effects of 0.5mM 4-AP on the late outward plateau currents, I_{x1} and I_{x2}. PF, obtained from electrocuted sheep, were superfused with normal Tyrode's solution (pH 7.3-7.4) at 37±0.5°C. In some experiments, NaCl was replaced with Na methylsulfate. 4-AP had little or no effect on the steady-state net I/V relationship for membrane potentials positive to -60mV (holding potential (V_h)=-70mV). Since over this potential range a large fraction of the steady-state net current is attributed to I_{x1} and I_{x2}, we conclude that 4-AP does not alter the magnitude of I_x activation. We attempted to analyze the effect of 4-AP on I_x activation kinetics by applying a series of clamp pulses (range, -80 to +30mV; duration, 100 msec to 20 sec) from a V_h of -30mV, a procedure identical to that used by Noble and Tsien (J. Physiol. 200:205, 1969). 4-AP did not appreciably influence the time course of the current during clamps from -60 up to +30mV; below -60mV the data are less consistent. The decay of tail currents produced upon the break of clamps positive to -50mV were also unaffected. More negative clamps resulted in outward decaying tails which were reversed by 4-AP. Graphical separation of either the control or 4-AP data into I_{x1} and I_{x2} produced widely variable rate constants with a voltage-dependence unlike that previously published. From these results we conclude that 4-AP does not affect currents (aside from I_{eo}) activated in the plateau range of membrane potentials. Also the data raise questions concerning the nature or proper analysis of I_{x1} and I_{x2}. (Supported by NIH #HL-14614).

M-PM-C8 POTASSIUM CURRENTS IN MAMMALIAN MUSCLE. Kurt G. Beam, Dept. of Physiology & Biophysics, University of Iowa, Iowa City, IA 52242. The three microelectrode technique of Adrian, Chandler & Hodgkin (J. Physiol. 208:607-644) has been used to measure potassium currents in rat skeletal muscle at temperatures ranging from 1 to 37°C. Sucrose (350-400 mM) was used to block contraction; methylsulphate was used as an impermeant substitute for extracellular Cl; extracellular Ca was raised from 2 to 10 mM in order to improve electrode sealing. Depolarizing test pulses were superimposed on a holding potential of -90 mV. The resulting currents had reversal potentials ranging from -90 to -80 mV. The relationship between peak g_K and voltage was sigmoid in nature: at 20°C g_K vs V was half maximal at -20 mV, had maximal slope e-fold/25 mV, and saturated at 10 mV where its value was 14 mmho/cm^2. Cooling appears to cause a rightward shift in g_K vs V as well as a decrease in the maximum slope.

For $V \geq -40$ mV τ_n was obtained by fitting n^4 to the measured currents. n^4 provided a fair fit of the rising phase but at longer times the currents showed considerable inactivation, especially for larger depolarizations. In addition, at short times the actual currents showed a greater delay than could be accounted for by n^4. For $V \leq -40$ mV τ_n was measured from tail currents. τ_n vs V was bell shaped with a maximum at about -40 mV. At 20°C τ_n (+10 mV) was ∿2.1 msec, τ_n(-40 mV) was ∿14 msec, and τ_n(-70 mV) was ∿5.3 msec. A semilog plot of τ_n(+10 mV) vs 1/T shows no obvious break points but does become less steep at higher temperatures. Thus τ_n(+10 mV) decreases roughly five-fold from 0 to 10°C, but only about two-fold over the range 20 to 30°C. Taus measured at other potentials, including those derived from tail currents, showed similar behavior. This research was supported by MDA and NS 14901.

M-PM-C9 POTASSIUM CONDUCTANCE AND PERMEABILITY OF SQUID GIANT AXON MEMBRANES by Eric Jakobsson, Department of Physiology and Biophysics and Program in Bioengineering, University of Illinois, Urbana, Illinois 61801 and Stewart Jaslove*, Department of Physiology, Duke University Medical Center, Durham, North Carolina 27710 and Marine Biological Laboratory, Woods Hole, Mass. 02543.

We have found a method for integrating the Nernst-Planck electrodiffusion equation, given the boundary condition of an instantaneous I-V curve. The integrated equation for K^+ current is:

$$I_K = \frac{F^2}{RT} \cdot P_K \cdot \frac{(K_i - K_o)}{\ln(K_i/K_o)} \cdot (V - V_K) \qquad (1)$$

For comparison, the well-known integrated equation using the constant field boundary condition is:

$$I_K = \frac{F^2}{RT} \cdot P_K \cdot V \cdot \frac{-K_i \exp(FV/RT) + K_o}{1 - \exp(FV/RT)} \qquad (2)$$

Equation (1) has the advantage over the ordinary conductance formalism in that it accounts separately for permeability and concentration of K^+ ions within the membrane, whereas these two quantities are ordinarily lumped together in g_K. We have applied eq'n (1) to analysis of K^+ current during long depolarizations of squid axon which cause K^+ accumulation in the periaxonal space. Our analysis suggests that during a long step the following events all happen simultaneously: i) I_K falls, ii) g_K rises, iii) P_K falls, iv) The density of K^+ in the membrane rises, v) The number of open K^+ channels goes to a constant. Support was received from National Institutes of Health and from the Bioengineering Program of the University of Illinois.

* Present address is: Einstein College of Medicine, Department of Neuroscience, Kennedy Center, Bronx, New York 10461.

M-PM-C10 ANALYSIS OF INTERNAL CATION EFFECTS ON NODAL MEMBRANE STEADY-STATE POTASSIUM I-V RELATIONSHIPS - A 3-STATE APPROACH. E.Levitan, and Y.Palti, Department of Physiology and Biophysics, Technion-Medical School, Haifa/Israel.

In the presence of internal cations, such as Cs^+, steady-state potassium I-V curves show a peak at about 30mV. In the node at very strong depolarizations they also have an additional maximum at about 180 mV. Nodal steady-state potassium currents were analysed in terms of gating units having three states where the two transition dipole moments are of different signs. The internal cation (Cs^+) is assumed to be taken up by the gating unit from the internal solution according to a Langmuir adsorption isotherm. Once the cation is adsorbed it is assumed that the parameters of the gating unit are modified.

All the parameters of the model have been determined by fitting the equations of the model to the experimental I-V curves at various Cs^+ concentrations. The model allows for a physical(thermodynamic)interpretation of the characteristics of the current-voltage relationships of ionic current gating in the frog nodal membrane.

M-PM-D1 MOLECULAR MOTION OF INDIVIDUAL LDL MOLECULES ON CELL MEMBRANES. L. S. Barak and W. W. Webb, Cornell University, Ithaca, NY 14853.

The low density lipoprotein molecule (LDL), a complex of protein, phospholipid, cholesterol. and cholesterol esters about 250 Å in diameter binds to a specific receptor on human fibroblasts. We have stained LDL so bright that single molecules of LDL are visible in fluorescence microscopy. With the fluorophore dioctadecylindocarbocyanine iodide (diI) incorporated into the LDL structure, individual molecules bound to their receptors were visible on cell surfaces. Using fluorescence photobleaching recovery the diffusion coefficient of an LDL-receptor complex between 10-27 C was determined to be no greater than 2-3 x 10^{-11} cm^2/sec, At low temperatures LDL often moves primarily in localized Brownian motion as if locally tethered on the membrane. In regions where the plasma membrane had been decoupled from the cytoskeleton by bleb formation the diffusion coefficient increases to approximately D ≈ $10^{-9}cm^2$/sec. The diffusion of individual molecules confined to the two dimensional membrane manifold was observed to differ qualitatively from occasional molecules seen tumbling in solution. These results suggest new models for the relationship between the LDL receptor, the cell membrane and internalization phenomena. The large fluorescent intensity of individual molecules of LDL offers a unique opportunity to study molecular motion on cells.

M-PM-D2 LATERAL DIFFUSION OF CONCANCAVALIN A RECEPTORS AND LIPID ANALOG IN NORMAL AND BULBOUS LYMPHOCYTES. E. S. Wu[+§*], D. Tank[+] and W. W. Webb[+] (Intr. by R. F. Steiner). [+]Cornell University, Ithaca, NY 14853, and [§]University of Maryland Baltimore County, Baltimore, MD 21228.

Following treatment with concanavalin A (con A), a small fraction of mouse lymphocytes and RDM_4 (mouse T lymphoblasts) develop a large blebbing hemispherical protrusion of the membrane. The hyaline interiors of such blebs are phase bright and staining with NBD-phallacidin indicates that all filamentous actin is excluded. As the blebbed region grows, the cell becomes a spherical bulb, with nucleus and filamentous actin segregated to one edge where most of the con A patches have aggregated on the overlying membrane. A low concentration of con A receptors remains distributed over the bulbous membrane. Lateral diffusion coefficients (D) of con A receptors, labeled with rhodamine conjugated con A, and the lipid analog diI-C_{16}(3) were measured in both normal and bulbous membranes of mouse lymphocytes and RDM_4 by the methods of Fluorescence Photobleaching Recovery (FPR). In bulbous membranes of RDM_4, D=$7.10^{-9}cm^2$/sec for con A receptors, with a percentage fluorescence recovery (R≥97%); for diI C_{16}(3), D=$4.10^{-8}cm^2$/sec (R≥96%). In normal membranes, D<$10^{-11}cm^2$/sec for con A receptors with small fluorescence recovery and D=$1.2.10^{-8}cm^2$/sec (R≥92%) for diI-C_{16}(3). These results suggest that con A receptors are immobilized, in normal membrane, by their association with microfilament structure and are released with ~1000 fold mobility increase when the membrane is detached from the underlying cytoskeleton. The 3 fold increase of diI-C_{16}(3) diffusibility in bulbous membrane may result from changes of cell surface topology and/or reduction of protein-lipid interactions by a decrease in protein density. Similar results were obtained for mouse lymphocytes, except diI-C_{16}(3) diffusibility increased only 2 fold in bulbous membranes.

M-PM-D3 ENHANCED MOBILITY OF ACETYLCHOLINE RECEPTOR AND MEMBRANE PROBES IN MUSCLE MEMBRANE BLEBS. D. W. Tank[+*], E. S. Wu[+§] and W. W. Webb[+], (Intr. by G. P. Hess) [+]Cornell University, Ithaca, NY 14853, [§]University of Maryland Baltimore County, Baltimore, MD 21228.

Crosslinking agents, anoxia, physical injury, and prolonged protease treatment are known to induce blebbing of cell membrane. Lipid and integral membrane protein compositions are similar in normal and blebbed regions; however, protein densities may be lower. Bleb interiors are phase bright; the expected absence of cortical actin cytoskeleton was confirmed by lack of staining with NBD-phallacidin. Fluorescence Photobleaching Recovery (FPR) was used to measure the lateral diffusion coefficient (D) of acetylcholine receptor (AChR), labeled with rhodamine α-bungarotoxin, and the fluorescence-labeled lipid NBD-PC in both normal and blebbed membrane of enzymatically dissociated single muscle fibers of adult mouse flexor digitorum brevis. In normal cells, the AChR is immobilized at the endplate and D≤$10^{-12}cm^2$/sec with percentage fluorescence recovery (R) negligible; for NBD-PC, D=$1\cdot10^{-9}cm^2$/sec (R=100%). AChR, found in blebs forming at the endplate region, has ~1000 fold increased mobility: D=$2.0\cdot10^{-9}cm^2$/sec (R=100%). NBD-PC, found in all blebs, has D=$1.5\cdot10^{-8}cm^2$/sec (R=100%). D was also measured for rhodamine conjugated stearoyldextran (AcRSD) and NBD-PC on normal and blebbed membranes of L_6 muscle cells in culture. In normal L_6 membrane, D for AcRSD is $4.5\cdot10^{-10}cm^2$/sec (R=72%), while for NBD-PC D=$4.4\cdot10^{-9}cm^2$/sec (R=100%). In blebbed membrane, AcRSD diffuses 7 fold faster with complete recovery: D=$3\cdot10^{-9}cm^2$/sec (R=100%), identical to its diffusibility in large unilamellar vesicles. NBD-PC diffuses slightly faster, D=$1.2\cdot10^{-8}cm^2$/sec (R=100%). These results suggest that molecular interactions for membrane components differ in blebbed and normal membrane. Cytoskeletal interactions capable of inhibiting diffusibility are excluded in blebs, perhaps allowing unrestrained diffusion in accord with the Saffman-Delbruck hydrodynamic theory.

M-PM-D4 MEASUREMENT OF ROTATIONAL DIFFUSION OF MEMBRANE COMPONENTS BY FLUORESCENCE PHOTOBLEACHING. Lloyd M. Smith, Robert M. Weis and Harden M. McConnell, Department of Chemistry, Stanford University, Stanford, CA 94305.

Previous measurements of the rotational diffusion of membrane components have employed the observation of time-dependent dichroism following partial (or transient) photobleaching, spin label paramagnetic resonance spectra, or depolarization of fluorescence emission. Unfortunately none of these techniques has the sensitivity or appropriate time scale to measure the rotational correlation times of many membrane components in single cells. We have found that fluorescence photobleaching can be used to measure rotational diffusion of membrane components with high sensitivity, and in a time range that should be appropriate to many membrane proteins.

The lipid probe diI was incorporated at a concentration of 0.01 mole % in multilamellar liposomes composed of various phospholipids. Measurements were made at temperatures below the chain melting transition temperatures. Individual liposomes were partially bleached with a short intense burst of polarized laser radiation and the remaining fluorescence intensity was recorded as a function of time. The time dependence of the fluorescence intensity is attributed to rotational diffusion of the diI molecules. The observed dependence of the magnitude and sign of the fluorescence intensity change (increasing or decreasing) is in accord with theoretical expectations: When the polarization of the bleach and probe beams are parallel (perpendicular) the fluorescence intensity increases (decreases) with time. The rotational correlation times are remarkably long (50 msec-1 sec) and depend strong on the host lipid composition and on temperature. The applicability of this measurement to the study of the interactions of membrane components will be discussed. [This work has been supported by the National Science Foundation Grant No. PCM 77-23586.]

M-PM-D5 INFLUENCE OF MEMBRANE DYNAMICS ON ANTIBODY-INDEPENDENT ACTIVATION OF COMPLEMENT. Chang-Lin Wey and Alfred F. Esser, Department of Molecular Immunology, Scripps Clinic and Research Foundation, La Jolla, California 92037.

Activation of the first component of complement (C1) requires the binding of the C1q subcomponent to at least two adjacent IgG molecules. Therefore, IgG-antigen complexes that are situated on a membrane and freely diffusible are expected to activate C1 better or less depending on their lateral mobility. Indeed, previous studies demonstrated that at 32°C IgG-antigen complexes on fluid lipid bilayers - prepared from dimyristoyl lecithin (DML)-activated better than those on solid bilayers (dipalmitoyl lecithin, DPL) (H.M. McConnell (1978) Harvey Lect. 72,231). We have now compared the activation of C1 on fluid and solid bilayers by bacterial lipopolysaccharide (LPS), an activator that does not require specific antibody (Ab). LPS from S.minnesota mutant Re595 which contains only the Lipid A moiety and three KDO groups is known to activate C1 when free in solution but apparently not when bound to liposomes. However, we have prepared liposomes from DML or DPL each containing 3 mole% LPS (Re-595) and have observed that such liposomes deplete complement activity in whole human serum, activate partially purified native C1 directly, as well as C1 reconstituted from purified subcomponents C1q, C1r and C1s. The latter result indicates the Ab-independent nature of this process. The temperature profile of C1 activation shows a marked discontinuity at about 41°C for DPL-LPS (Re595) liposomes but no change for DML-LPS (Re595) liposomes and DPL-LPS (Re595) liposomes that also contain 25 mole% cholesterol. In contrast, C1q binds equally to DPL-LPS (Re595) liposomes above or below the phase transition temperature (41°C) for DPL. These results are similar to those obtained earlier on Ab-dependent systems and we are investigating whether the differences in C1 activation are caused by lateral mobility of LPS (Re595) or other mobility parameters.

M-PM-D6 DISAPPEARANCE OF MACROPHAGE SURFACE FOLDS FOLLOWING SPECIFIC ANTIBODY-DEPENDENT PHAGOCYTOSIS OF PHOSPHOLIPID VESICLES. Howard R. Petty, Dean G. Hafeman and Harden M. McConnell, Department of Chemistry, Stanford University, Stanford, CA 94305.

Phospholipid vesicles formed by the ether injection technique were composed of 98-99 mol% dimyristoylphosphatidylcholine and 1 mol% of a fluorescent phospholipid and/or lipid hapten containing phospholipid. Lipid-hapten containing phospholipid vesicles were taken up by resident guinea pig peritoneal macrophages in a time- and temperature-dependent fashion. Vesicles which contained ferritin trapped in the internal aqueous volume were identified within macrophages by transmission electron microscopy. Scanning electron microscopy (ScEM) has shown that macrophage surface folds decrease dramatically following phagocytosis. The method of Burwen and Satir (J. Cell Biol. 74:690) has been employed to measure the disappearance of surface folds from macrophages following antibody-dependent phagocytosis. The surface fold length (μm) per unit smooth sphere surface area (μm^2) decreases from 1.3±0.03 μm^{-1} to 0.53±0.04 μm^{-1} (mean±SEM) when cells are incubated in the presence of specific antibody and vesicles at 37°C. No significant effect was observed in the presence of antibody only or vesicles only. Macrophage radius as measured by ScEM and volume as measured by ^3H_2O tracer experiments increased slightly after phagocytosis. However, this increase could not account for the decrease in surface folds. Our studies show that phagocytosis is associated with a loss of cell surface folds and a loss of cell surface area, which is consonant with current views of the endocytic process. Based upon our uptake data, we estimate that approximately 400 μm^2 of vesicle surface membrane is internalized. The macrophage plasma membrane has a total area (including folds) of about 400 μm^2 in control studies whereas the cells have roughly 300 μm^2 following phagocytosis. We suggest that during antibody-dependent phagocytosis a membrane reservoir is made available to the cell surface.

M-PM-D7 TWO-DIMENSIONAL GEL ELECTROPHORESIS OF MACROPHAGE MEMBRANE PROTEINS: EVIDENCE SUPPORTING ENRICHMENT AND DEPLETION OF CERTAIN MEMBRANE COMPONENTS DURING ANTIBODY-DEPENDENT PHAGOCYTOSIS. Frank D. Howard, Howard R. Petty and Harden M. McConnell, Department of Chemistry, Stanford University, Stanford, CA 94305.

Macrophage membrane proteins were analysed by two-dimensional polyacrylamide gel electrophoresis before and after antibody-dependent phagocytosis. Cell surface proteins were labeled by lactoperoxidase-catalyzed radioiodination of intact cells. After detergent solubilization, membrane proteins were analysed by isoelectric focusing (IEF) or nonequilibrium pH gradient electrophoresis (NEPHGE) followed by sodium dodecyl sulfate-polyacrylamide gel electrophoresis in the second dimension (O'Farrell et al., Cell 12:1133). The resulting pattern of protein spots (approx. 30) was calibrated against several protein standards of known pI and mol. wt. Phospholipid vesicles containing 99 mol% dimyristoylphosphatidylcholine and 1 mol% phospholipid hapten were formed by the ether injection technique. In the presence of hapten-specific antibody at 37°C these vesicles are phagocytosed by RAW264 macrophages in a time-dependent fashion. Following phagocytic uptake of phospholipid vesicles we have noted the appearance of a ≃30K membrane component utilizing NEPHGE in the first dimension. Control experiments show that this spot is not surface-bound antibody. We have also noted the disappearance of two higher molecular weight spots (≃70K and ≃140K). The latter proteins are not observed in gels run under reducing conditions. The functional attributes of these phagocytosis-associated membrane proteins are presently under investigation. Our results support the concept of topographical separation or directed motions of membrane molecules during antibody-dependent phagocytosis.

[This work was supported by the National Institutes of Health Grant no. 5 R01 AI13587.]

M-PM-D8 RED CELL-MEMBRANE BIOPHYSICAL RESPONSES BEFORE, DURING AND AFTER HEMOLYSIS H. C. Mel and G. V. Richieri, Department of Biophysics and Medical Physics, and Donner Laboratory, Lawrence Berkeley Laboratory, University of California, Berkeley, California 94720.

The act of abrupt osmotic hemolysis, as viewed microscopically and by resistive pulse spectroscopy is an explosive, local membrane event (Biorheol. 15, 321-339, 1978). Following such hemolysis the membrane has been shown to recover its osmotic and mechanical integrity over different time courses. Post hemolytic electrical (membrane-resistivity) properties follow their own particular dynamic course (Akeson-Mel, Abstract). Recent attention has been focussed on a different phase of the hemolytic process, namely, events occuring in the short times just prior to the hemolysis itself, and the later consequences of this pre-hemolytic stress. Red cells subjected to 5 sec exposure to 120 mOsm phosphate buffered saline (PBS), then "rescued" by immediate transfer to isotonic PBS, are studied at successive 0, 30, and 60-minute time intervals. Initially, no hemolysis occurs, and the cells differ in only minor ways from control cells, with respect to mean and modal size, size heterogeneity and deformability. With increasing time following restoration, however, the cell condition deteriorates in all of these respects, including the onset of hemolysis. The cell-membrane alterations observed are considerably greater than those seen for abruptly hemolyzed cells that have been allowed to recover for a few minutes. Other, different patterns of responses are observed when the protocols of exposure stress-rescue-recovery are followed. These results are discussed together in the context of the membrane-related ionic processes that are known or likely to be occuring.

M-PM-D9 VOLTAGE-DEPENDENT MEMBRANE CONDUCTANCE IN RED BLOOD CELLS AND RESEALED GHOSTS, AS MEASURED BY RESISTIVE PULSE SPECTROSCOPY. S.P. Akeson and H.C. Mel, Dept of Biophysics and Med Physics and Donner Lab., LBL, Univ. of Calif., Berkeley, CA 94720.

Resistive pulse spectroscopy (RPS), an extension of Coulter-type electronic particle sizing, normally assumes infinite resistance for the particles being sized. The application of modern interactive computers for data collection and analysis, plus careful control and monitoring of the voltage drop across the sensing orifice, reveals however some quite distinctive voltage-dependent conductance phenomena. In normal discocytes, osmotically swollen spherocytes, and newly resealed hypotonic ghosts there is a distinct threshold in applied electric field strength, above which the induced membrane potential produces a transmembrane (ionic) current. While these three types of particles have approximately the same threshold, they do not have equivalent voltage-dependent conductances at higher fields.

Regarding resealed ghosts, many researchers have reported a transient drop in ghost "volume" with a minimum occuring about 25 seconds post-lysis, and have speculated that this may reflect a transient drop in membrane resistivity. When normal cells are injected into hypotonic PBS and the kinetics of "volume" changes are followed using a graduated series of sensing voltages, it is shown that the initial drop in ghost "volume" is not electrical in nature. However, there is a previously unreported long term reduction in the threshold for induced current in resealed ghosts ($t_{\frac{1}{2}}$ about 120 seconds), possibly due to long term effects of high (1 mM) Ca^{+2} concentrations inside these cells. In contrast, osmotically swollen but unlysed spherocytes show no time-dependent behavior in membrane resistivity. Thus, by RPS we find clear differences between ghost and intact cell membranes at later times following hemolysis. In the context of repair of the lesion created by explosive hemolysis, there is an initial rapid recovery of membrane resistivity, which subsequently deteriorates.

M-PM-D10 METALLOPORPHYRIN-LIPOSOME SYSTEMS AS MODELS FOR ELECTRON TRANSFER IN MEMBRANES. Jennifer A. Runquist, Thomas J. Dannhauser and Paul A. Loach. Departments of Biochemistry and Molecular Biology and Chemistry, Northwestern University, Evanston, IL 60201.

We have previously shown that iron porphyrins such as hemin dimethyl ester and iron or manganese tetraphenylporphyrin catalyze high rates of electron transport across phospholipid bilayers prepared from egg yolk phosphatidylcholine (1,2). The aqueous redox materials used in these studies were $K_3Fe(CN)_6$ inside the vesicles and reduced indigotetrasulfonic acid outside the vesicles. We have further characterized these systems by specifically assaying for anion transport which accompanies electron transport. In a phosphate buffer system neither phosphate nor cyanide were found to be transported,but pH change measurements indicate that a hydroxide coordinated to the ferric porphyrin is likely the anion transported as the oxidized iron porphyrin diffuses from the inner surface to the outer surface. This may also be viewed as transport of a H^+ along with the electron because a water molecule is very likely coordinated to the ferrous iron as the reduced iron porphyrin diffuses from the outer surface to the inner surface. Consistent with an electrically neutral electron transport mechanism were the findings: (1) that electron transfer goes to completion (reduction of all ferricyanide present) without breakage of the vesicles; (2) valinomycin plus potassium was without effect on the system; and (3) FCCP was without effect. Electrochemical properties of several metalloporphyrins incorporated into liposomes are being measured by direct potentiometric titration and compared with their properties in water and organic solvents. The relevance of these results to *in vivo* electron transport will be discussed.

(1) Runquist, J.A. and Loach, P.A. (1979) Biophys. J. 273a, 25.
(2) Runquist, J.A., Dannhauser, T.J. and Loach, P.A. (1980) Fed. Proc. 39, 2147.

This research was supported by the U.S. Public Health Service (NIH Grant No. GM-26098).

M-PM-D11 TRIFLUOPERAZINE INHIBITS THE SECRETORY RESPONSE IN PARAMECIUM. Robert S. Garofalo and Birgit H. Satir, Department of Anatomy, Albert Einstein College of Medicine, Bronx, N.Y.

Wild type Paramecium tetraurelia exhibit exocytic release of hundreds of secretory organelles, called trichocysts, in response to picric acid (PA), the routine stimulus for secretion. Release involves a transition from a 3μm long membrane bound condensed form to a 20-40μm long needle-like structure, which can be monitored at the light microscope level. When cells are fixed for electron microscopy (TEM), a partial expansion of the trichocysts often occurs, leading to loss of electron density and increase in volume. Late log phase cells are washed and suspended in 1mM Hepes, 20μM Na-citrate, 20μM $CaCl_2$, and 0.5-1.0mM Tris buffer and exposed to 14μM trifluoperazine (TFP) for varying times (1-10 min) before PA addition and assay for release. TFP interacts with calmodulin (CaM) in a calcium dependent manner, and blocks the CaM activation of certain enzymes. The percentage of cells releasing >50 trichocysts/cell decreases with increasing exposure to TFP. Cells are examined in TEM after varying times in TFP, and analysis shows that trichocysts remain in the cells after 10 minutes in 14μM TFP, thus the decreased response to PA is not due to a TFP induced depletion of trichocysts. In addition, incubation in TFP blocks expansion of the trichocyst content usually seen after fixation. The number of condensed trichocysts increases from 1% in untreated control cells to 99% in cells exposed to TFP for 10 minutes. This increase follows a time course parallel to that observed for the decrease in secretory response to PA. These results suggest that TFP inhibits secretion in Paramecium at a step prior to the actual fusion event, possibly by affecting components of the cytoplasm, trichocyst membrane or the content of this organelle. The ability of TFP to affect the secretory process in these cells may indicate a role for CaM in the secretory process.

This work was supported by USPHS Grants GMS 27298, 24724, and 5T32 GM07128

M-PM-D12 BIOPHYSICAL STUDIES OF MAMMALIAN LENS JUNCTIONS

J. David Robertson, Guido Zampighi and Sidney A. Simon.
Departments of Anatomy and Physiology, Duke University Medical Center, Durham, N.C. 27710 and Department of Anatomy, UCLA, Los Angeles, CA.

We have developed a method for isolating pure junctional membranes, in milligram quantities from bovine lens without detergent solubilization. SDS-PAGE shows two bands, a major one at 27,000 d and a minor one at 21,000 d. Thin section electron microscopy of this fraction has revealed junctions comprised of two closely apposed membranes having the following characteristics: 1) lengths greater than 10 um with a wavy contour, 2) pentalaminar structure with an overall thickness of 150 A.

The junctions have also been studied by negative stain and freeze fracture electron microscopy and by x-ray diffraction. All four techniques were in agreement regarding the structural organization of the junction. The junctions consisted primarily of extensive domains of subunits arranged in a square lattice with a lattice constant of 65 A.

Freeze fracture studies of unfixed, unglycerinated mouse lens fragments have revealed extensive areas of square arrays with dimensions and characteristics similar to that of the isolated fraction. In addition, we have observed extensive loose aggregates of particles that occasionally were hexagonally arranged. Our studies have suggested that the dominant organization of the lens fiber cell junctions is a tetragonal array of subunits.

Supported by NIH Grant # 1-R01-GM/AM 28224-01 and Membrane Training Grant.

M-PM-E1 RADICALS OF Fe(II) ISOBACTERIOCHLORINS: MODELS OF SIROHEME AND OF NITRITE AND SULFITE REDUCTASES. L. K. Hanson and J. Fajer, Brookhaven National Laboratory, Upton, New York 11973 and C. K. Chang, Michigan State University, East Lansing, Michigan 48824 (Intr. by S. W. Feldberg).

Sulfite and nitrite reductases catalyze the six-electron reductions of sulfite to hydrogen sulfide and of nitrite to ammonia, respectively. Siroheme, the prosthetic group of the enzymes, is an iron isobacteriochlorin, a porphyrin in which two adjacent pyrrole rings are reduced. A salient feature of the isobacteriochlorin skeleton is its ease of oxidation and difficulty of reduction when compared to porphyrins or chlorins. This facile oxidation suggests that the siroheme macrocycle itself may undergo redox reactions in the enzymatic cycles.

Charge iterative extended Hückel molecular orbital calculations 1) provide a rationale for the redox properties of isobacteriochlorins compared to porphyrins and chlorins, 2) predict that Fe(II) pyridine carbonyl (py-CO) complexes of isobacteriochlorins, unlike porphyrins and chlorins, should undergo oxidation from the macrocycle rather than the metal to yield π cation radicals, 3) suggest that the site of oxidation of a hexacoordinate Fe(II) isobacteriochlorin complex, i.e. metal or macrocycle, will depend on the ligand field induced by the axial ligands, and 4) indicate that the unpaired spin density profiles of metal-free and Fe(II)py-CO isobacteriochlorin radicals should be similar. Experimental redox, optical and electron spin resonance data for three isomeric models of siroheme and sirohydrochlorin (its demetallated form) support the theoretical calculations and unambiguously establish the existence of Fe(II) isobacteriochlorin π cations.

This work was supported by the Division of Chemical Sciences, U.S. Department of Energy, Washington, D.C., under Contract No. DE-AC02-76CH00016.

M-PM-E2 CYTOCHROME c: THE REDUCTION SITE AND POSSIBLE ELECTRON-TRANSFER PATH. Yash P. Myer, A. Pande, J. Pande, K. K. Thallam, A. F. Saturno, and B. C. Verma, Institute of Hemo-Proteins, State University of New York at Albany, Albany, NY 12222.

The ascorbate reduction of native and urea-perturbed cytochrome c follows a three-step mechanism: a urea-dependent equilibrium step between a reducible and an irreducible form with $[Urea]_{\frac{1}{2}}$ of 7.5 M, a binding step with a constant of 5.9 M^{-1} and a reduction step with a urea-independent rate constant of 2.9 ± 0.3 sec^{-1}. Equilibrium studies of the urea denaturation process show a three-step mechanism, N == X_1 == X_2 == D, where N, D and the Xs are the native, the 9-M-urea and the intermediate forms, and the steps are the loosening of the heme crevice, the solvent exposure of the polypeptide backbone, and the disruption of the tryptophan-porphyrin interactions, respectively. Studies of the oxidizability of protein-ascorbate-urea systems show that the intermediate forms, X_1 and X_2, are directly reduced by ascorbate, and the X_2 == D step generates the irreducible form. The reaction of the arginines with 2,3-butanedione, a group-specific reagent, is inhibited by ascorbate, but only one of the two arginines is inhibited. Ascorbate reduction is thus shown to be independent of the state of the heme crevice opening and of the polypeptide organized structures, but it is determined by the integrity of the tryptophan indole-porphyrin interactions. The selective inhibition of one of the two arginine side chains by ascorbate establishes the binding site of ascorbate. From the three-dimensional structure of the protein, and taking into consideration the variability of the protein sequence, it is apparent that Arg-38 is the ascorbate binding site, and that the electronic interaction between the indole of Trp-59 and the porphyrin moiety must constitute, at least in part, the electron-transfer path to heme iron. (Supported by National Institute of Health grant GM 24854.)

M-PM-E3 A PICOSECOND INTERMEDIATE IN THE MbCO AND MbO_2 DISSOCIATION PROCESS. A. H. Reynolds, S. D. Rand and P. M. Rentzepis, Bell Laboratories, Murray Hill, New Jersey 07974.

Picosecond time resolved kinetics of MbCO and MbO have been measured after excitation in the β and δ bands. Optical density changes were monitored between 400 nm and 460 nm and thus determined the optical density changes for the 420 nm liganded and 440 nm ligand detached species. We find that the rates for MbCO and MbO_2 dissociation do not reflect the 30X difference in the dissociation quantum yield of these species. To reconcile these results we propose the existence of an intermediate which is responsible for the difference in quantum yield and apparent rates for the dissociation of MbCO and MbO_2. Picosecond time resolved spectra between 300 K and 4 K provide further supporting evidence for the existence of such intermediates.

M-PM-E4 STUDY OF HYPERFINE INTERACTIONS IN DEOXY- AND OXY-COBALTGLOBIN.
Shantilata Mishra, Jane C. Chang* and T.P. Das Physics Dept., SUNYA, Albany, New York 12222.

We have investigated the electronic energy levels and wave functions in deoxy- and oxy-cobaltglobin using the self-consistent charge extended Huckel procedure, with the aim to understand the ^{59}Co and ^{14}N hyperfine interactions observed[1] in these compounds by the EPR technique. Our investigations show that the unpaired spin electron in the deoxy compound is in a cobalt d_{z^2}-type molecular orbital. In the oxy compound on the other hand, the unpaired spin electron is primarily in a π-type molecular orbital corresponding to d_{xz} type symmetry on cobalt, the major atomic orbital components of this molecule belonging to the two atoms of the oxygen molecule. This result is in keeping with a model of nearly complete transfer of the unpaired spin electron to the oxygen molecule and is supported by satisfactory agreement between our calculated ^{59}Co and ^{14}N hyperfine constants and experiment. Our results also provide an explanation of the observed[2] inequivalent hyperfine interactions for the two ^{17}O nuclei of the oxygen molecule, the major contribution being dipolar in origin, with a small but significant contribution arising from the isotropic hyperfine interaction produced by the exchange polarization mechanism. (supported by NIH grant HL 15196)

1. B. Hoffman et. al., Proc. Nat. Acad. Sci. 67, 637 (1970); J.C.W. Chien et. al., Proc. Nat. Acad. Sci. 69, 2783 (1972); T. Yonetani et. al. J. Biol. Chem. 249, 2168 (1974).
2. R.K. Gupta, A.S. Mildvan, T. Yonetani and T.S. Srivastava, Biochem. Biophys. Res. Commun. 67, 1005 (1975); J.C.W. Chien et. al. (to be published).

M-PM-E5 ELECTRONIC STRUCTURE AND ASSOCIATED HYPERFINE INTERACTIONS IN MANGANESEGLOBIN.
Shantilata Mishra*, Jane C. Chang* and T.P. Das Physics Dept., SUNYA, Albany, New York 12222.

We have investigated the electronic structure of a model compound involving imidazole as the fifth ligand of the manganese atom of manganese porphyrin, using the self-consistent charge extended Huckel procedure. This model system is expected to be representative of the immediate environment of manganese atom in manganeseglobin. The manganese atom was taken as lying 0.56Å above the porphyrin plane[1], in contrast to the smaller height of 0.27Å in the divalent porphyrin compound[2] with H_2O as fifth ligand. Using the calculated wave-functions and spin-distributions, we have obtained the ^{55}Mn hyperfine constants $A_{\parallel}$ and $A_{\perp}$, corresponding to the principal axes perpendicular to and in the plane of the porphyrin ring, as -240.8MHz and -235.0MHz respectively, in good agreement with the nearly isotropic constant of 207.2MHz found experimentally[3] in the analogus five-liganded compound, Mn(TPP)Py. Comparison will be made with the corresponding theoretical and experimental[4] results in divalent manganese porphyrin system with H_2O as fifth ligand and results for the ^{14}N and ^{1}H hyperfine constants will also be discussed.

1. B. Gonzalez, J. Kouba, S. Yee, C.A. Reed, J.F. Kirner and W.R. Scheidt, J. Amer. Chem. Soc. 97, 3247 (1975).
2. See S. Mishra, J.C. Chang and T.P. Das, J. Amer. Chem. Soc. 102, 2674 (1980).
3. C.J. Waschler, B.M. Hoffman and F. Basolo, J. Amer. Chem. Soc. 97, 5278 (1975).
4. T . Yonetani, H.R. Drott, J.S. Leigh, G.H. Reed, M.R. Waterman and T. Asakura, J. Biol. Chem. 245, 2998 (1970).

M-PM-E6 NANOSECOND TRANSIENT RAMAN STUDIES OF LIGATION INDUCED HEME-HEME POCKET INTERACTIONS IN HEMEPROTEINS.
J. M. Friedman and R.A. Stepnoski, Bell Telephone Laboratories, Murray Hill, N. J. 07974

By comparing the deligated heme resonance Raman spectrum of photodissociated liganded hemeproteins to the corresponding spectrum of the respective equilibrium deoxy species, we have been able to observe the effect of ligation upon the interaction between the porphyrin and the heme pocket in several hemeproteins. We have mapped out these interactions by focussing on Raman peaks that are sensitive to the electronic make up of the porphyrin, the porphyrin core size, and the frequency of the vinyl stretching mode. With respect to alterations that modify the electronic structure of the porphyrin, ligation affects the following proteins in the sequence: Hb > α chains > β chains > Mb. It has previously been shown[1] that the subsequent time evolution of this modified electronic structure is related to the events that trigger quaternary structure change in Hb. A discussion will be presented on the relationship between these ligand-induced changes and the trigger mechanism for the R → T transition.

[1]K. B. Lyons and J. M. Friedman, Interaction Between Iron and Proteins in Oxygen and Electron Transport (ed. Ho, C.) (Elsevier-North Holland, in press).

M-PM-E7 HEMOGLOBIN R-STATE IRON-IMIDAZOLE STRETCHING FREQUENCY OBSERVED BY TIME-RESOLVED RESONANCE RAMAN SPECTROSCOPY. Paul Stein, James Terner, and Thomas G. Spiro, Department of Chemistry, Princeton University, Princeton, NJ 08544.

Low frequency resonance Raman spectra of R-state hemoglobin were obtained by rapidly flowing carbonmonoxy-hemoglobin through a focused argon ion laser beam (4579Å). The laser interaction time was 0.3μsec. The iron-imidazole stretching bands at 207 and 220 cm^{-1}, assigned by Nagai and Kitagawa [Proc. Natl. Acad. Sci. USA, 77, 2033 (1980)] to the α and β chains of deoxyhemoglobin, both shift to approximately 223 cm^{-1} in the R-state phototransient. The experiment also showed band I of the phototransient at 1355 cm^{-1}; it appears at 1356.5 cm^{-1} for deoxyhemoglobin. This study, along with the work of Nagai and Kitagawa on chemically modified hemoglobins, shows that there is a substantial shift in the iron-imidazole stretching frequencies between the R- and T-quaternary structures. These shifts can be interpreted in terms of molecular tension in the T-state or alternatively, changes in proximal imidazole hydrogen bonding.

M-PM-E8 KINETICS OF MACROMOLECULES REACTING WITH LIGAND-A SIMPLE ANALYTIC MODEL FOR HEMOGLOBIN. Paul E. Phillipson, Dept. of Physics, Univ. of Colorado, Boulder, Colorado 80309 (Intr. by Mircea Fotino).

It is proposed that the saturation function descriptive of the kinetics of ligand binding by hemoglobin can be represented by,

$$Y(t) = Y(\infty)\{[1 + \varepsilon][1 - \exp - (\sigma t)]\}/\{[1 + \varepsilon] - \varepsilon \exp - (\sigma t)\}$$

where Y(t) is the fraction of sites bound as a function of time, $Y(\infty)$ the fraction at equilibrium and σ,ε are parameters fixed by experiment. This expression would be exact if the sites bound independently, in which case there are fixed functional relations between the three parameters. Cooperativity characteristic of hemoglobin appears in that these quantities are treated as independent and so can assume values forbidden for independent sites. Application to experiment shows favorable agreement with more rigourous but non-analytic treatments, and comparison with the latter shows that the present formulation represents a contraction to the limit that the multiplicity of chemical relaxation processes are dominated by a single one. Refinement of the scheme is outlined which lifts this restriction for more accurate and extensive applications.

M-PM-E9 SELF-ASSOCIATION KINETICS OF HEMOGLOBIN βO_2 SUBUNITS. J. S. Philo, M. Potschka, and T. M. Schuster, Biochemistry and Biophysics Section, Biological Sciences Group, University of Connecticut, Storrs, CT 06268.

The kinetics of the monomer-tetramer association reaction of oxy-β^{SH} subunits of human Hb A have been investigated over a wide concentration range using both mixing and temperature-jump techniques. The association was detected using the previously-reported tetramer-monomer absorption difference spectrum (1). Small perturbation analysis of the data using a monomer-dimer-tetramer pathway has enabled us to deduce rate constants for each elementary step. The observed relaxation times are very sensitive to the concentration of dimer present at equilibrium, and thus these data serve to provide a better estimate of the dimer association constant than was obtained by gel permeation studies (2). The data also show that the spectral change probably occurs at the monomer-dimer step.

Supported by NIH HL24644 and NSF PCM-79-03964

(1) M. L. Adams, J. S. Philo, and T. M. Schuster (1979) Biophys. J. 25, 38a.

(2) Valdes, R. L. and Ackers, G. K. (1977) J. Biol. Chem. 252, 74-81.

M-PM-E10 OXIDATION OF HUMAN OXYHEMOGLOBIN BY NITROFURANTOIN
Mark Dershwitz and Raymond F. Novak, Department of Pharmacology, Northwestern University Medical and Dental Schools, Chicago, IL 60611

We have previously investigated the effects of the red cell hemolytic agent nitrofurantoin (NF) on normal human erythrocytes *in vitro* and found it to produce depletion of red cell ATP and reduced glutathione levels and increases in hydrogen peroxide levels [*The Pharmacologist*, 21, 170 (1979)]. In the present study, we evaluated NF in terms of its ability to oxidize oxyhemoglobin to methemoglobin in intact cells and in solution. After a 20 hour incubation in the presence of 840 μM NF, more than 20% of the red cell's oxyhemoglobin had been oxidized while less than 1% had been converted to methemoglobin in the controls. In order to investigate the molecular interaction of NF with oxyhemoglobin, the oxidation of oxyhemoglobin by NF was studied by utilizing UV-visible difference spectroscopy. Purified human oxyhemoglobin (0.5 μM in 20 mM KPi, pH 7.5) and NF (10-400 μM in 20 mM KPi, pH 7.5) were mixed. A hypsochromic shift in the Soret band occurred along with a decrease in the absorbances at 542 and 576 nm indicating the oxidation of oxyhemoglobin to methemoglobin. The interaction constant for NF, K, was approximately 0.5 mM. NF was also found to interact with purified human methemoglobin using difference spectroscopy. Using the oxidation of epinephrine to adrenochrome as an indicator of superoxide anion generation, the interaction of NF with oxyhemoglobin was found to form superoxide. Superoxide dismutase (100 units/ml) was found to partially inhibit the oxidation of oxyhemoglobin by NF. These data are consistent with a model in which NF decreases the affinity of hemoglobin for oxygen resulting in methemoglobin formation and the concomitant release of oxygen as superoxide anion which subsequently causes further oxidation of oxyhemoglobin to methemoglobin. [Supported in part by NIH Training Grant GM 07263 to the Department of Pharmacology and by Chicago Heart Grant C80-13 to RFN].

M-PM-E11 ANTI-SICKLING ACTIVITIES OF MEMBRANE-INTERACTING COMPOUNDS. Koji Hashimoto, Mark Singer and S. Tsuyoshi Ohnishi, Biophysics Laboratory, Dept. of Anesthesiology, Hahnemann Medical College, Philadelphia, PA 19102

The sickling of sickle cell anemia is caused by the formation of polymers of sickle hemoglobin (Hb S) upon deoxygenation. Studying the anti-sickling effect of cetiedil, Asakura et al. found that this drug inhibits sickling without directly interacting with Hb S, and have proposed a new concept of "membrane-linked" anti-sickling mechanisms (PNAS (1980) 27, 2955). We have screened various membrane-interacting drugs and have found the following: (1) Many anti-psychotic drugs have an anti-sickling effect and that the mechanism may be related to the ability of these drugs to bind to calmodulin, a ubiquitous cellular-calcium binding protein. (2) Propranolol, a β-adrenergic blocker has some anti-sickling effect. Propranolol is believed not to bind to calmodulin (personal communication from R. M. Levin). (3) Zinc has been known to have an anti-sickling effect. We have observed that the effect appears to be mainly caused by an increase of red cell volume (and decrease of cellular hemoglobin concentration). Zinc was shown to have no specific calmodulin binding activity (Vincenzi, F.F., personal communication). (4) Local anethetics such as procaine did not show significant *in vitro* anti-sickling effects at pharmacologically-used concentrations. These results suggest that the mechanisms of membrane-linked anti-sickling drugs are not simple, but may involve different interactions at different sites.

Supported in part by NIH grant HL 23200.

M-PM-E12 ANTI-SICKLING EFFECT OF PROSTAGLANDIN B_1 DERIVATIVES. Mark T. Devlin, Thomas M. Devlin and S. Tsuyoshi Ohnishi, Dept. of Biological Chemistry and Dept. of Anesthesiology, Hahnemann Medical College, Philadelphia, PA

PGBx, a water-soluble polymeric derivative of prostaglandin B_1 was found to protect oxidative phosphorylation in rat liver mitochondria from deterioration under certain adverse conditions (Polis et al. (1979) PNAS 76, 1598). This compound seems to have various interesting effect on the membrane. For example, we have demonstrated that PGBx has calcium ionophoretic activity (Ohnishi and Devlin, BBRC (1979) 89, 240).

We have found that this compound also demonstrates a membrane-linked anti-sickling effect. In the absence of calcium, 11 μg/ml of PGBx (4.6 μM) was able to inhibit *in vitro* sickling by about 30 - 40%. This effect was antagonized by 1 mM calcium. An analog of PGBx, designated as PGBx-L, was found to protect oxidative phosphorylation but does not demonstrate calcium ionophoretic activity. PGBx-L showed anti-sickling activity similar to that of PGBx, but both in the presence and absence of calcium. The mechanism of the anti-sickling effect of these compounds will be discussed in reference to the role of cellular calcium.

(Supported by a contract from the Office of Naval Research (N 00014-77-C-0340.)

M-PM-F1 STATIC STRAIN DOES NOT ALTER THE ANGLE OF THE ACTIN-MYOSIN BOND IN RIGOR MUSCLE FIBERS. Aron Yoffe & Roger Cooke. Dept of Biochemistry & Biophysics and the CVRI, University of California, San Francisco, California 94143

We have used EPR spectra to measure the angular distribution of spin label probes bound specifically to sulfhydryl groups on myosin heads of glycerinated rigor rabbit muscle fibers. Most EPR cavities do not allow the experimenter to easily exert tension on fibers whose long axis is parallel to the magnetic field. This fiber orientation provides the most informative spectra and we have drilled holes in the side faces of a Varian 231 cavity to allow tension to be applied to a fiber oriented along the magnetic field while spectra are recorded. This modification does not significantly alter the Q of the cavity. As has been shown previously, in the unstressed rigor fiber at a sarcomere length of 2.4 μ, the angular distribution of the specifically bound probes is described by a Gaussian curve centered at 68°, with a full width at half-maximum of 15° (Thomas & Cooke, Biophys. J. Dec., 1980). When a tension of approximately 1 kg/cm^2 was exerted on these rigor fibers, no detectable change in the spectrum occurred. Since the spectrum would be sensitive to a 2° difference in the average angle or in the width of the angular distribution, these results demonstrate that forces which significantly lengthen the series elastic element in rigor muscle do not alter the angular distribution of probes specifically bound to the myosin head. Hence we conclude that the actin-myosin bond is stiffened and does not measurably contribute to the elasticity of rigor striated muscle. (Supported by NIH grant HL16683 to R.C. and an NSF Graduate Fellowship to A.Y.)

M-PM-F2 ORIENTATION AND ROTATIONAL DYNAMICS OF SPIN-LABELED MYOSIN HEADS IN VERTEBRATE STRIATED MUSCLE FIBERS: DEPENDENCE ON SARCOMERE LENGTH. David D. Thomas and Vincent A. Barnett, Department of Biochemistry, University of Minneosta Medical School, Minneapolis, MN 55455.

Current models of the molecular mechanism of muscle contraction involve specific predictions about the orientation and rotational motion of myosin heads (crossbridges). With the goal of obtaining direct information about these orientations and motions, we have attached spin labels selectively to myosin heads in glycerinated rabbit psoas muscle fibers. Conventional electron paramagnetic resonance (EPR) experiments are used to determine the orientation distribution of the probes relative to the fiber axis, and saturation tranfer (ST-EPR) experiments are used to detect sub-millisecond rotational motion (Thomas and Cooke, Fed. Proc. 39: 1962 [1980]). In previous fiber studies, we performed only conventional EPR experiments; in the present study, we report the results of both conventional and saturation transfer EPR experiments on the same preparation. When fibers are at rest length (2.4 μm/sarcomere), we observe a high degree of order in spin-labeled heads. The probes are in a single, narrow orientation distribution (full width 15°), and they exhibit no detectable sub-millisecond rotational motion. When fibers are stretched (sarcomere length ↑), either before or after labeling, so that a large fraction of the myosin heads are no longer in the overlap zone between thick and thin filaments, the order decreases. Some of the probes, roughly proportional to the fraction of heads in the overlap zone, remain oriented and immobile, while the rest are highly disordered (angular spread ≥ 90°) and mobile (rotational correlation time about 10 μsec). Thus, it appears that myosin heads are rigidly immobilized by actin, but they rotate through large angles in the microsecond time scale when detached from actin, even in the absence of ATP. Supported by grants from NSF, NIH, and MDA.

M-PM-F3 THREE-DIMENSIONAL DISORDER OF DIPOLAR PROBES IN HELICAL SYSTEMS : APPLICATION TO FLUORESCENT AND E.S.R. LABELS ON MUSCLE CROSS-BRIDGES. Robert A. Mendelson and Michael G.A. Wilson, Dept. Biochem. & Biophys. and Cardiovascular Research Institute, Univ. of Calif., San Francisco, CA 94143. In helical systems, fluorescence polarization and e.s.r. spectra can give information about physiologically-induced changes in declination (θ) of the dipole axis or axes of probe molecules relative to the helix axis. To date, theories relating fluorescence polarization [Tregear & Mendelson (1975) Biophys.J. 15,455; Mendelson & Morales (1977) Biochim.Biophys.Acta 459,590] and e.s.r. spectra [McCalley et al.(1972) Chem.Phys.Lett. 13,115; Thomas & Cooke (1980) Biophys.J.,in press] have been derived for systems possessing a high degree of orientation in θ, or involving a spread of θ which is either uniform in a sector or a one-dimensional Gaussian. However, if the probe is bound to a moiety which itself exhibits orientational disorder, the disordering of a rigidly-attached dipole may be rather complex. We have derived transformation equations for this problem and applied the method, as an example, to the e.s.r. data from relaxed muscle fibers [Thomas & Cooke, op.cit.]. We have numerically calculated many spectra and compared them with the available data, assuming the following sources of stationary 3-D cross-bridge disorder : (1) Torsional freedom of the myosin S-1 , (2) S-1 uniformly dispersed within a cone, (3) combinations of (1) & (2), and (4) cases (1) or (2) with a two-dimensional Gaussian distribution about the median θ, to simulate Hookean restoring forces. In certain cases we have obtained closed analytical expressions for fluorescence polarization values. (Supported by USPHS grant # HL-16683 and NSF grant # PCM 75-22698. We thank Dr. R. Cooke for supplying data prior to publication. M.W. is a Career Investigator Fellow of the American Heart Association.)

M-PM-F4 CROSS-BRIDGE TURNOVER DURING Ca-FREE, NON-RIGOR, CONTRACTION IN SKINNED MUSCLE FIBERS. Jagdish Gulati, Albert Einstein College of Medicine, Bronx, NY 10461

Contraction kinetics of frog skeletal fibers were examined in low ionic strength in absence of Ca. The fibers developed reversible isometric tension in relaxing solution (pCa $\geq$ 8) of low ionic strength (composition mM: 5 EGTA; 5 ATP; 1 $MgCl_2$, ionic [Mg] ~20 μM; 10 Imidazole, no added KCl) at room temperature; the level of this tension equals the Ca-activated (pCa = 5) tension in physiological ionic strength (190 mM) as first shown by Gordon et al. (1973, J Gen Physiol V62). Ca-free tension was dependent upon: (a) temperature; tension was negligible at 0°C and was maximal at 22-25°C. (b) ionic Mg; tension with 20 μM [Mg] was reversed when [Mg] was raised to near 0.5-1 mM, with Mg ATP or free ATP held constant at 1 mM. This effect was present whether or not 5 mM CP and 1 mg/ml CPK were included. (c) sarcomere length; the Ca-free tension was lower when the filament overlap was reduced. The sarcomere uniformity was confirmed separately, with laser diffraction and direct microscopic techniques.

In quick release experiments, the isotonic shortening in the Ca-free (0 KCl) solution was similar to the response in pCa = 5 (140 KCl). However, the displacement trace following a load step was curved in Ca-free solution and the speed decreased continuously (for 350 msecs) with shortening. This shows that the cross-bridge properties are under additional influence in Ca-fre condition than in pCa = 5 or in rigor (low ATP). Our findings, indicating cross-bridge turnover in Ca-free solution, suggest that (a) operation of the steric blocking model (e.g. HE Huxley, 1972, Cold Spr H Symp V37), and/or (b) conformation change in the actin monomer affecting cross-bridge turnover (e.g. Adelstein & Eisenberg, 1980, A Rev Biochem) are controlled by Ca-independent mechanism under these conditions. (Supported by NIH Grant AM 26632 and Muscular Dystrophy Assoc).

M-PM-F5 A MODEL FOR THE ARRANGEMENT OF MYOSIN CROSS-BRIDGES IN VERTEBRATE SKELETAL MUSCLE. R. Smith* and P. Dreizen, Biophysics Program and Dept. of Medicine, State University of New York Downstate Medical Center, Brooklyn, N.Y. 11203.

The arrangement of myosin cross-bridges in the thick filament of relaxed vertebrate skeletal muscle has been controversial, in that the 6/2 helical model, as originally proposed by Huxley and Brown (1967), has been disputed by Squire and associates, who noted that the X-ray diffraction data could also be attributed to a 9/3 or 12/4 helix, with the intensity of distribution along layer lines somewhat more suggestive of a 9/3 helix. We have reinvestigated this question by the method of optical transforms, using masks prepared from computer-simulated models of cross-bridge arrangement, with systematic examination of effects related to cross-bridge shape and orientation, and to the myofilament lattice. There are no striking differences among the optical transforms of regular 6/2, 9/3, and 12/4 helices, as previously reported. However, a modified 12/4 helix with asymmetric placement of the helical strands generates optical transforms with similar helical features as in the regular helices, and also generates certain meridional reflections which have been observed experimentally on X-ray diffraction patterns of relaxed muscle, but have not been accounted for by earlier helical models of cross-bridge arrangement. Variations in cross-bridge shape affect the intensity distribution along layer lines, but the differences in shape do not greatly alter the overall pattern of meridional reflections as obtained for the different helical models. The existence of a myofilament lattice results in sampling of the layer lines generated by a single myofilament, but does not in general introduce significant new reflections on the optical transforms. The modified 12/4 helical model, as here proposed, is consistent with biochemical evidence of four myosin molecules per 143 Å repeat in vertebrate skeletal muscle.

M-PM-F6 THREE-DIMENSIONAL RECONSTRUCTION OF ARROWHEADS FORMED BY SCALLOP MYOSIN S-1s. Peter Vibert & Roger Craig, Rosenstiel Center, Brandeis University, Waltham, MA 02254.

Three-dimensional reconstructions have been calculated from images of negatively stained thin filaments or F-actin decorated with two kinds of scallop S-1. S-1s containing regulatory light chains (Ca-Mg S-1) are about 50 Å longer than those lacking regulatory light chains (EDTA S-1). The extra mass is located at the "neck" end of S-1, andprobably represents a combination of part of the light chain and a region of the myosin heavy chain. Superposition of these extra regions gives the characteristic "barbed" appearance to the arrowheads (Craig et al., J. Mol. Biol., 140, 35-55 (1980)). Vertebrate skeletal S-1s also form barbed arrowheads in the presence of the DTNB light chain, suggesting that this chain may contribute to the neck region. Since the "essential" light chain probably also extends into the neck region of scallop myosin (Flicker et al., this volume), this part of the myosin head may consist of parts of three extended polypeptide chains. This region is more than 120 Å away from the actin-binding site; therefore the regulatory light chain itself probably does not extend into the binding region, and could not block attachment sterically.

Polar actin monomers and a continuous strand of tropomyosin can also be recognized in the reconstructions. The tropomyosin is located on the opposite side of actin to that assumed until recently (cf. Seymour & O'Brien, Nature 283, 680-682 (1980)) for the "steric blocking model," but makes extensive contact with the inner concave surface of S-1. Thus a new "steric" model is plausible (cf. Taylor & Amos, J. Mol. Biol., in press).

Supported by grants (to C. Cohen) from NIH, NSF and MDA. P.V. is an Established Investigator of AHA; R.C. held a Fellowship from MDA.

M-PM-F7 A NEW MODEL FOR THE GEOMETRY OF THE BINDING OF MYOSIN CROSS-BRIDGES TO MUSCLE THIN FILAMENTS

K. A. Taylor and L. A. Amos. Intr. by Harold P. Erickson.
MRC Laboratory of Molecular Biology, Cambridge, England.

We have used the method of three-dimensional image reconstruction of electron micrographs to analyze the binding of myosin subfragment 1 to muscle thin filaments and purified actin filaments. To help improve on the earlier work of Moore, Huxley and DeRosier (1970), we have obtained all our data using minimal electron dose procedures to reduce radiation damage. Modifications in the specimen preparation have enabled us to process stretches of filament twice as long as any used in the earlier work, resulting in a corresponding improvement in the signal-to-noise ratio and the resolution. The results of two independent averaged sets of decorated thin filament reconstructions and three independent averaged sets of decorated pure actin filaments show significant changes in the density distribution in the region near the axis of the structure. Compared with the model of Moore et al., the reconstructions show the presence of extra density close to the axis of the particle. We present a case for identifying actin with the density in this region, rather than with the density at higher radius designated as actin by Moore et al. Our new assignment for the position of actin within the decorated filament structure leads to a radical change in the structural model for S-1 actin interaction. Furthermore, by comparing the feature which we identify as actin with the reconstructed images of Wakabayashi et al. (1975), we conclude that the polarity of the thin filament previously assumed is wrong. By reversing the polarity, we find that a new steric blocking model can be constructed.

Moore, P.B., Huxley, H.E., & DeRosier, D.J. (1970). J. Mol.Biol. 50, 279-295.
Wakabayashi,T., Huxley, H.E., Amos,L.A. & Klug,A. (1975). J. Mol.Biol. 93, 477-497.

M-PM-F8 THE EFFECT OF MgATP ON THREE EXPONENTIAL PROCESSES --- A POSSIBLE PRESENCE OF ALTERNATE HYDROLYSIS ROUTES.

M. Kawai and R.N. Cox*. Columbia University, N.Y., N.Y. 10032

Three exponential processes were studied as a function of a wide range of MgATP concentration (3μM-5mM) in Ca-activated, chemically skinned rabbit psoas fibers by use of the sinusoidal analysis technique. Activating conditions were (Na salts in mM): 0-5 MgATP, 2.38 CaATP, 0.47 Ca^{++}, 1 free ATP, 7.5 phosphate, 15 CP, 74 unit/ml CPK, 26-21 sulfate, 37 propionate, 6 imidazole (pH 7.00), and 20°C. As fibers were transfered (from an EDTA-rigor solution) to solutions of increasing MgATP concentration, the 3 exponential processes appeared sequentially, each with a unique K_M. The order of appearance is process (A), process (C), and process (B); the K_M's are approximately 10μM, 0.2mM, and 0.8mM, respectively. The single phase advance (process (A)) remaining at very low MgATP concentrations was found to be better described by a distributed rate constant ("constant phase angle" of Cole & Cole, 1941) than by a discrete rate constant. These observations are interpreted in terms of (i) distributed strain in the rigor cross-bridges, (ii) unidirectional shortening, which requires attachment and detachment cycles, and (iii) oscillatory work, which may not require myosin head dissociation. (ii) and (iii) further imply the presence of two parallel hydrolysis routes in active muscle. Below: Nyquist plots of complex stiffness data (frequency range 0.125-167Hz); pS=-log[MgATP]. Averaged data from 3 experiments.

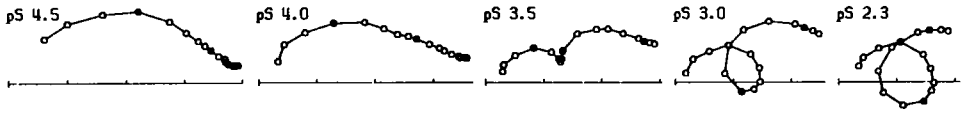

M-PM-F9 TROPONIN PHOSPHORYLATION REGULATES THIN FILAMENT DISASSEMBLY.

GEORGE MCCLELLAN, ANDREA WEISBERG, MARIANNE TUCKER AND SAUL WINEGRAD
DEPT. OF PHYSIOLOGY, SCHOOL OF MEDICINE, UNIVERSITY OF PA., PHILA., PA.

In rat right ventricular trabeculae that have been made highly permeable to ions and small molecules (hyperpermeable cells) exposure to a combination of 1μM or greater Ca^{++} and 50μM or less ATP produces an irreversible decrease in the maximum Ca-activated tension. This decrease is associated with fragmentation of the thin filaments and the gradual disappearance of the 41,000 and 28,000 bands from SDS Polyacrylamide gels that are associated with the tropomyosin and the inhibitory subunits of troponin (TNT + TNI). These data are consistent with an activation of the Ca-dependent neutral protease. The decline in tension, disappearance of troponin subunits and fragmentation of thin filaments are all prevented by phosphorylation of TNI and TNT. These phosphorylations and their effects on tension and troponin are stimulated by cAMP and inhibited by cGMP. Substitution of CTP, a poor phosphate donor, for ATP also inhibits the phosphorylations and promotes the decline in tension. In the absence of membrane adenylate cyclase or in the presence of μmolar concentrations of cGMP, the decline in tension and loss of troponin may occur in concentrations of ATP as high as 1-2mM. These data suggest that disassembly of thin filaments and ultimately the relative mass of contractile material in a cardiac cell may be regulated by neuroendocrine activity operating through cyclic nucleotides.

M-PM-F10 CHOLINERGIC REGULATION OF TROPONIN PHOSPHORYLATION IN CARDIAC MUSCLE. ROBERT HOROWITS AND SAUL WINEGRAD, DEPT. OF PHYSIOLOGY, UNIVERSITY OF PA., PHILA., PA.

In isolated cardiac contractile proteins and in cardiac cells made hyperpermeable by 10mM EGTA so that their contractile proteins can be directly probed with a Ca-EGTA buffer in the superfusion solution, the pCa necessary for 50% activation of the contractile proteins (Ca sensitivity) is decreased by catecholamine stimulated phosphorylation of TNI. The level of endogenous catecholamines in ventricular trabeculae can be reduced by repeated washing of tissues in well-oxygenated, modified Krebs solution immediately following dissection before any exposure to EGTA. Although the washing decreases the positive intropic response to GTP, the response to epinephrine remains, indicating the integrity of the adrenergic system after repeated washing. In both washed and unwashed preparations exposure to 10 μM methacholine results in a change in Ca sensitivity that is inversely and linearly related to the initial Ca sensitivity of the fibers (correlation coefficient 0.92). Ca sensitivity was increased in all fibers that initially required 3.3 μM Ca or greater for 50% activation. The effect of methacholine on Ca sensitivity was not reversed by a 30 min wash in relaxing solution. These results are consistent with the hypothesis that cholinergic agents act by inhibiting catecholamine stimulated adenylate cyclase and they may be involved along with adrenergic agents in regulating the properties of cardiac contractile proteins.

M-PM-F11 TROPOMYOSIN REGULATION OF THE MYOSIN BINDING SITE OF ACTIN: AN ELECTRIC FIELD MODULATION HYPOTHESIS. N.B. Ingels, Jr., Palo Alto Medical Research Foundation, Palo Alto, CA 94301.

Recently, Seymour and O'Brien (Nature 283:680, 1980) and Lin and Dowben (Fed. Proc. 39: 1621, 1980) have placed tropomyosin on the opposite side of the actin molecule from the myosin binding site, a finding difficult to reconcile at present with a steric blocking model for tropomyosin regulation. One alternative model suggests that tropomyosin movement changes the conformation of actin subunits. Another model, proposed and investigated in the present study, suggests that the azimuthal movement of tropomyosin results in a modulation of the electric field in the vicinity of the myosin binding site. By assuming a 2.5 nm radius spherical G-actin monomer with a 2.6 nm ion exclusion radius, a 5:1 unbalanced internal actin dipole oriented along a line from the actin center to the myosin binding site, a transverse tropomyosin dipole associated with each actin monomer and rolling 36° toward the actin filament groove with activation, an external dielectric constant of 80, actin dielectric constant of 4, and Debye length of 1 nm, a model based on a solution of the Poisson-Boltzmann equation given by Kirkwood (J. Chem. Phys. 2:351, 1934) suggests that the electric field within 10 nm of the myosin binding site can be modulated in such a manner as to attract or repel a negatively charged myosin head appropriately with tropomyosin position. With this model of regulation, prior to activation the myosin heads execute Brownian motion, constrained in an electric potential well between the actin and myosin filaments. On activation, local actin fields become attractive and the phosphorylated myosin heads migrate electrophoretically, on a submillisecond time scale, to the myosin binding sites. With this scheme, the far field due to actin is essentially unchanged with activation, thereby maintaining muscle filament lattice stability during both contraction and relaxation.

M-PM-F12 LIMULUS AND PARASTICHOPUS SKINNED FIBERS: IS REGULATION OF CONTRACTION VIA A Ca^{2+} SENSITIVE LIGHT CHAIN KINASE/PHOSPHATASE SYSTEM? W.G.L. Kerrick and L.L. Bolles. Dept. of Physiology and Biophysics, University of Washington, Seattle, WA 98195.

Recent developments allowed us to distinguish between regulation of muscle contraction by a Ca^{2+}-sensitive light chain kinase (MLCK)/phosphatase (P) system and other Ca^{2+} control systems in skinned muscle fibers (Kerrick et al., Fed. Proc. 39:1558, 1980). We made use of the correlation between the myosin light chain phosphorylation and irreversible thiophosphorylation vs. activation of tension. In these studies we used two different invertebrates from divergent lines of evolution. Limulus (horseshoe crab, a protostome) was chosen since in vitro studies (Sellers, Fed. Proc. 39:2041, 1980) suggest the presence of a MLCK/P system being involved in the regulation. Parastichopus californicus (sea cucumber) was chosen since it belongs to the phylum echinodermata, one of the earliest of the phyla called deuterstomes. The phylum chordata is included in the deuterstomes. Parastichopus body wall muscle showed a good correlation between Ca^{2+}-activated tension and phosphorylation of the myosin light chains Irreversible thiophosphorylation of the myosin light chains using the ATP analog ATPγS resulted in Ca^{2+}-insensitive irreversible activation of tension. However, known affectors of the MLCK (trifluoperazine (TFP), catalytic subunit of cAMP-dependent protein kinase, and calmodulin) had no effect upon Ca^{2+}-activated tension. These results suggest contraction is regulated by a Ca^{2+}-sensitive MLCK which may not be controlled by calmodulin. Limulus tail and leg muscle showed no incorporation of phosphate into myosin light chains during Ca^{2+} activation of tension nor was the Ca^{2+} activation altered by treatment with TFP, calmodulin, C-subunit, or pretreatment with ATPγS. Skinned limulus muscle fibers did not appear to be regulated by a Ca^{2+}-sensitive MLCK. (Supported by grants from the American Heart Assn. (79-664) and the Muscular Dystrophy Assn.)

M-PM-G1 THE ORDER OF CALCIUM AND ADP RELEASE FROM THE CALCIUM PUMP OF SARCOPLASMIC RETICULUM. J.J. Feher and F.N. Briggs, Medical College of Virginia, Richmond VA

The order of calcium and ADP release from the calcium pump of cardiac sarcoplasmic reticulum was studied by comparing the unidirectional calcium and nucleotide fluxes during steady-state calcium uptake. Unidirectional calcium influx, Jf, was determined by adding ^{45}Ca after steady-state calcium uptake was reached. Because net calcium flux is zero at steady-state, this was equal to calcium efflux. Total calcium efflux was divided into a passive flux, Jp, and a pump-mediated efflux, Jr, by separately determining Jp by quenching the pump and calculating Jr as Jf - Jp. Unidirectional nucleotide fluxes were estimated from the net ATPase activity, JNET, and the reverse nucleotide flux, JR, measured by adding ^{3}H-ADP during steady-state calcium uptake. The forward nucleotide flux is JF = JNET - JR. All of these unidirectional fluxes were determined under conditions in which steady-state calcium uptake was varied by including varying concentrations of EGTA. The plot of unidirectional calcium influx *vs* forward nucleotide flux was linear and described by Jf = 2.41 JF. The plot of Jr *vs* JR was also linear and described by Jr = 5.36 JR. Thus, the apparent stoichiometry in the forward direction is different from that in the reverse direction. Since it is difficult to believe a stoichiometry of 5 moles of calcium transported per mole of nucleotide, we propose that at least some calcium is released from the enzyme before ADP. In this case unidirectional calcium flux can occur without nucleotide flux. Our data is consistent with an order of release of Ca-ADP-Ca or Ca-Ca-ADP but not with ADP-Ca-Ca. (Supported in part by NIH grants HL19485 and HL23142 and a grant-in-aid from the American Heart Association, Virginia Affiliate)

M-PM-G2 CHANGE IN THE CONFORMATION OF THE SARCOPLASMIC RETICULUM ATPase ASSOCIATED WITH THE PHOSPHORYLATION REACTION K. Miki and N. Ikemoto, Dept. of Muscle Res., Boston Biomed. Res. Institute, and Dept. of Neurology, Harvard Med. School, Boston MA 02114

The thiol-directed fluorescent reagent N-(1-aminonaphthyl-4) maleimide (ANM) reacts with the Ca^{2+}-ATPase of fragmented sarcoplasmic reticulum in two phases, rapid and slow, as determined by the increase of fluorescence intensity and OD_{350}. In the rapid phase, about 1 mol SH per 10^5 g ATPase (SH1) is blocked. There is no inhibition of phosphoenzyme (EP) formation nor of Ca^{2+}-uptake until the second most reactive SH (SH2) has been blocked. Upon addition of Mg.ATP in the μM range there is a 10-15% increase in the fluorescence intensity of ANM attached to SH2 at $[Ca^{2+}] \geq 1$ μM, while the ANM attached to SH1 does not respond to Mg.ATP. In the absence of Mg^{2+}, on addition of ADP prior to Mg.ATP, or on substitution for ATP of the noncleavable analog AMPPNP, there is no increase in the fluorescence intensity even if activating $[Ca^{2+}]$ is present. Under none of the preceding conditions is there formation of EP. Furthermore, as the enhancement of ANM fluorescence produced by Mg.ATP is reversed by the addition of ADP, the EP breaks down to form ATP. Thus, it appears that the Mg.ATP-induced fluorescence increase reflects changes of enzyme conformation produced by EP formation. Studies of accessibility of ANM to the nonpermeable fluorescence quenching reagent acrylamide indicate that SH1 and SH2 are located in distinct domains of the ATPase molecule. For ANM attached to SH2 becomes nonquenchable upon EP formation, while ANM attached to SH1 is not affected by EP formation. (Supported by grants from NIH, NSF, MDA, and AHA)

M-PM-G3 EPR STUDIES OF SPIN-LABELLED PHOSPHOLIPID INCORPORATED INTO FUNCTIONAL RECONSTITUTED SARCOPLASMIC RETICULUM MEMBRANE VESICLES (RSR). J. Oliver McIntyre, Philip Samson, Lauraine A. Dalton and Sidney Fleischer. Department of Molecular Biology, Vanderbilt University, Nashville, TN 37235

Spin-labelled lecithin analogues were synthesized with the oxazolidinyloxyl moiety located at either carbon 5 (SL-I) or carbon 16 (SL-II) of the sn-2 acyl chain. R-SR were prepared containing either SL-I or SL-II (1.7% of the total phospholipid). R-SR membranes consist mainly of one protein component (>90%), the calcium pump protein (CPP). The lipid to protein ratio (L/P) of RSR was varied from 60-108 moles phospholipid per mole CPP, i.e., in the range of the normal SR membrane, L/P=110. The EPR spectra of SL-I in RSR (L/P=61) are similar to that of SL-I in SR phospholipid vesicles (SR-PL) alone, but exhibit a slight increase in hyperfine splitting from 61.0 G (SR-PL) to 62.4 G at 2°C, reflecting a small decrease in the average motion and/or disorder of the phospholipid in the presence of CPP in R-SR. With SL-I, there is no evidence for a signal referable to very slow motion in the presence of CPP. In contrast, SL-II exhibits a slight decrease in hyperfine splitting from 35.6 G (SR-PL) to 34.7 G (RSR, L/P=60) at 2°C reflecting a small increase in the motion and/or disorder of the bulk phospholipid in the presence of CPP. In addition, SL-II exhibits a spectral component referable to immobilized phospholipid. Approximately 8 moles of phospholipid/mole CPP are constrained. We conclude that: 1) the lipid in the membrane containing CPP is motionally similar to that of bilayer phospholipid; and 2) a small amount of constrained phospholipid in the presence of CPP can be detected which appears to be insufficient to constitute a boundary or annulus of immobilized phospholipid surrounding the CPP. [Supported by NIH AM 21987]

M-PM-G4 INHIBITION OF DIFFERENT ELEMENTARY STEPS OF THE CA-ATPASE REACTION IN SARCOPLASMIC RETICULUM AFTER MODIFICATION OF LYSINE RESIDUES WITH FLUORESCAMINE. C. Hidalgo and D.A. Petrucci (Intr. by T.L. Scott), Department of Muscle Research, Boston Biomedical Research Institute, 20 Staniford Street, Boston, MA 02114.

Labeling with fluorescamine of fragmented sarcoplasmic reticulum vesicles or of a purified enzyme preparation devoid of amino phospholipids and containing only dioleoylphosphatidylcholine results in inhibition of phosphoenzyme formation and of phosphoenzyme decomposition. Complete inhibition of phosphoenzyme formation is observed after seven lysine residues per mol of purified enzyme have reacted with fluorescamine; total inhibition of phosphoenzyme decomposition is observed after only six lysine residues have reacted with the label. The presence of ATP during labeling prevents the inhibition of both phosphoenzyme formation and phosphoenzyme decomposition, while the presence of a non-hydrolyzable ATP analog during labeling only prevents the inhibition of phosphoenzyme formation but not of phosphoenzyme decomposition. These results are compatible with a model in which labeling of one out of seven equally reactive lysine residues per mol of enzyme results in inhibition of phosphoenzyme formation and labeling of another lysine residue, in inhibition of phosphoenzyme decomposition. (This work was supported by NIH grant HL-23007 and by a grant from the American Heart Association.)

M-PM-G5 ROTATIONAL MOBILITY OF PROTEIN AND BOUNDARY LIPID IN SARCOPLASMIC RETICULUM MEMBRANES. David D. Thomas, †Cecilia Hidalgo, Diana J. Bigelow, and Thomas C. Squier. Dept. of Biochemistry, University of Minnesota Medical School, Minneapolis, MN 55455; †Dept. of Muscle Research, Boston Biomedical Research Institute, 20 Stanford St., Boston, MA 02114. Intr. by Russell K. Hobbie.

We have used spin labels and electron paramagnetic resonance (EPR) to study the correlation between lipid fluidity and protein mobility in sarcoplasmic reticulum (SR) membranes. A short-chain maleimide spin label was used to monitor the sub-millisecond rotational mobility of the calcium pump enzyme (using saturation transfer EPR), a long-chain fatty acid spin label was used to monitor the sub-microsecond fluidity of the bulk hydrocarbon phase (using conventional EPR), and a long-chain maleimide spin label (a gift from P. Devaux) attached to the protein was used to monitor the fluidity of the hydrocarbon phase adjacent to the protein (i.e., the "boundary lipid"). In the native SR membranes, the protein was highly mobile (effective correlation time 50-100 μsec, as we have previously reported) and the bulk lipid phase was quite fluid. But the boundary lipid probe revealed two roughly equal components: one in which the probe environment was as fluid as the bulk lipid, and one in which it was strongly immobilized. Immobilization of the boundary lipid could be caused by rigid binding of the hydrocarbon chain to the surface of the protein, or by protein-protein interactions that trap the chains. Reducing the lipid-to-protein ratio by a factor of two greatly increased the immobile portion of the boundary lipid while also decreasing the protein mobility. This change, which was reversed by adding back lipid, was almost certainly due to increased protein-protein interactions, not to changes in lipid binding sites at the protein's surface. Supported by grants from N.I.H. and A.H.A.

M-PM-G6 TEMPERATURE INDUCED CHANGES IN THE SECONDARY STRUCTURE OF THE CA^{2+}-ATPase FROM SARCOPLASMIC RETICULUM. Javier Navarro, Ta-Lee Hsiao, and Kenneth J. Rothschild. Departments of Physics and Physiology, Boston University, Boston, MA 02118.

The enzymatic activity and the secondary structure of the purified Ca^{2+}-ATPase from rabbit sarcoplasmic reticulum has been examined as a function of the temperature. Arrhenius plots of Ca^{2+} dependent ATPase activity demonstrated a discontinuity at about 20°C. This break was observed in both Ca^{2+}-ATPase containing endogenous phospholipids (NAT-ATPase) and Ca^{2+}-ATPase whose lipids have been replaced by dioleoyllecithin (DOL-ATPase). The activation energies above and below the transition temperature were 18 Kcal mol^{-1} and 33 Kcal mol^{-1} respectively. Circular dichroism spectra of the NAT-ATPase and DOL-ATPase at various temperatures indicated a marked change in the ellipticity at 223 nm between 20°C to 30°C (17%). Light scattering measurements were carried out in order to rule out possible artifacts. These results strongly suggest that the observed discontinuity of the Arrhenius plots of the Ca^{2+} dependent ATPase activity is independent of the bulk lipid composition of the membrane and instead reflects a change in the secondary structure of the Ca^{2+}-ATPase. Supported by grants from the NEI-NIH and NSF. KJR is an Established Investigator of the American Heart Association.

M-PM-G7 REGULATION OF THE Ca^{2+} ATPase IN SKELETAL SARCOPLASMIC RETICULUM BY PROTEIN KINASE(S). E.G. Kranias, F.J. Samaha and A. Schwartz. Departments of Pharmacology and Cell Biophysics, and Neurology. University of Cincinnati College of Medicine, Cincinnati, Ohio 45267.

Sarcoplasmic reticulum from rabbit fast skeletal muscle contains an intrinsic cyclic AMP-(cAMP)-independent protein kinase activity and a substrate for this activity. Phosphorylation of skeletal SR by either endogenous cAMP-independent protein kinase or exogenous cAMP-dependent protein kinase occurs on a 100,000 dalton protein and both enzyme activities result in enhanced calcium uptake and Ca^{2+}-dependent ATPase. To study the molecular mechanism by which phosphorylation regulates Ca^{2+} ATPase activity, the time course of formation (5-200 msec) and decomposition (0-73 msec) of the acid stable phosphorylated enzyme intermediate of the Ca^{2+} ATPase (E∿P) was measured with a quench flow apparatus under transient state conditions. Phosphorylation of skeletal sarcoplasmic reticulum resulted in: a) stimulation of initial rates and levels of E∿P formed, and b) stimulation of initial rate of E∿P decomposition which was more pronounced in the presence of oxalate.

These data indicate that regulation of the Ca^{2+} ATPase in skeletal sarcoplasmic reticulum may be mediated by phosphorylation of a 100,000 dalton component of these membranes. (Supported by the Muscular Dystrophy Association and by NIH grant HL 00775).

M-PM-G8 Ca MOVEMENTS ACROSS THE SR MEMBRANE DURING TETANUS AND RECOVERY. A.V. SOMLYO, H. GONZALEZ-SERRATOS, H. SHUMAN, G. McCLELLAN and A.P. SOMLYO. Pennsylvania Muscle Institute University of Pennsylvania.

Electron probe analysis (EPA) of ten paired flash-frozen frog muscles has shown that ~60% of the Ca is released from the terminal cisternae (TC) during a 1.2 sec tetanus. The accompanying uptake of K + Mg (76meq/Kg dry wt) into the TC, while significant, does not balance the amount of Ca released (-138meq). The movement of protons or organic ions not measured by EPA, may compensate the apparent charge deficit. The Na and Cl content of the TC is not significantly altered during the tetanus; cytoplasmic Ca is increased (by ~3.5mmole/Kg dry wt), and Mg is decreased (by~7mmole/Kg, $P < .001$) from paired resting values (n=451). Analysis of longitudinal SR and the adjacent cytoplasm indicates that the released Ca is distributed in the cytoplasm and not sequestered in the longitudinal SR. The amount of Ca released into the cytoplasm (~0.8mmol/l cell H_2O) can be accounted for by the Ca binding sites on troponin and on parvalbumin. Experiments in progress are designed to measure the rate of return of Ca to the TC in muscles frozen at 1.0 and 2.1 sec after a 1.2 sec tetanus, and to test the hypothesis based on preliminary results, that the time course of Ca return is rate limited by the "off rate" of Ca from parvalbumin. (Supported by HL15835 to the Pennsylvania Muscle Institute)

M-PM-G9 THE Ca^{2+}-Mg^{2+}-ATPase PUMP SARCOPLASMIC RETICULUM OPERATES NON-ELECTROGENICALLY: DEMONSTRATION USING THE ELECTRICALLY-SILENT IONOPHORE NIGERICIN. Duncan H. Haynes, Dept. of Pharmacology, Univ. Miami Medical School, Miami, Fla. 33133

The ionophore nigericin increases active Ca^{2+} uptake by skeletal sarcoplasmic reticulum (SR) as much as 50%. Analysis of the intrinsic permeabilities of the SR and consideration of the ionophore's mechanism of action show that the effect can be explained by a non-electrogenic model of pump function and cannot be explained by an electrogenic model. Ca^{2+} uptake was monitored using the fluorescence of 1-anilino-8-naphthalenesulfonate (ANS^-) or chlorotetracycline (CTC). The study was carried out on an ATPase-rich fraction with buoyant density equivalent to 29% sucrose. Previous studies (McKinley, D. & Meissner, G., J. Membrane Biol. 44:159 (1978), and Chiu, V.C.K. & Haynes, D.H., J. Membrane Biol. 56:_ _ (1980)) have shown that 2/3 of the vesicles (Type I) contain an electrically-active monovalent cation (M^+) permeability while the remaining 1/3 (Type II) do not. We have given evidence (above reference) that the Ca^{2+} uptake activity of Type II vesicles is inhibited by depletion of the internal K^+ concentration by the $Ca^{2+}/2K^+$ exchange activity of the pump. The presentation will demonstrate that in the presence of 30 mM Tris buffer, pH 7.0, the 50% increase in Ca^{2+} uptake is the result of unmasking the pump activity in Type II vesicles. A series of experiments testing the permeability of all ions in the system shows that the nigericin effect is explained by the non-electrogenic mechanism given in the insert. The result is not readily explained by electrogenic mechanisms. Supported by GM 23990 and HL 23392.

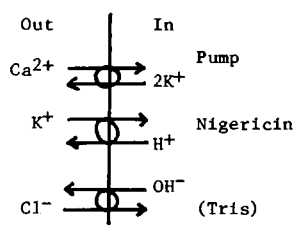

M-PM-G10 PURIFICATION OF PHOSPHOLAMBAN AND ANOTHER PROTEOLIPID FRACTION FROM CARDIAC SARCOPLASMIC RETICULUM. J.H.Collins, E.Kranias, A.S.Reeves, L.M.Bilezikjian and A.Schwartz. Dept. Pharmacology and Cell Biophysics, Univ. Cincinnati Coll. Med., Cincinnati, OH 45267.

We have isolated two proteolipid fractions from canine cardiac sarcoplasmic reticulum by chromatography on Sepharose CL-6B and Sephadex LH-60. One of these is phospholamban, the phosphorylatable activator protein. Our phospholamban preparation has an amino acid composition similar to that of a small, phosphorylated protein isolated from cardiac Na,K-ATPase by Dowd, et al.(Arch. Biochem. Biophys. 175, 321, 1976), but distinctly different from the phospholamban composition reported by LePeuch, et al.(Biochemistry 19, 3368,1980). The other fraction we obtained is not phosphorylated and appears to contain a Mr~11,000 species as its main component. The amino acid composition of this fraction is similar to the phospholamban composition reported by LePeuch, et al., and also to those of proteolipids that we recently isolated from lamb kidney Na,K-ATPase (Reeves, et al., BBRC 95, 1591, 1980). It thus appears that Na,K-ATPase and the Ca-ATPase of sarcoplasmic reticulum are associated with structurally similar proteolipids.
(Supported by the Muscular Dystrophy Association, the American Heart Association and its Southwestern Ohio Chapter and by NIH grants AM-20875, HL-22619, HL-07382, HL-00555 and HL-00775.)

M-PM-G11 CARDIAC SARCOLEMMAL (SL) AND SARCOPLASMIC RETICULUM (SR) MEMBRANE VESICLES EXHIBIT DIFFERENT Ca-Mg-ATPase SUBSTRATE SPECIFICITIES. W.R. Trumble, J.L. Sutko and J.P. Reeves Departments of Physiology, Internal Medicine, and Pharmacology, The University of Texas Health Science Center at Dallas, Dallas, Texas.

The Ca-Mg-ATPase activity of cardiac SL preparations show striking differences in nucleoside 5' triphosphate (NTP) specificity from that of cardiac SR. In the SL vesicles, only ATP and dATP were capable of driving Ca transport, with dATP less than 60% as effective as ATP; ITP, GTP, CTP and UTP were totally ineffective in supporting transport of Ca. All of the NTPs tested functioned to drive Ca transport into SR vesicles; dATP was at least as effective as ATP while ITP, GTP, CTP and UTP range from 20-35% of the activity of ATP. The SR vesicles also exhibited Ca-stimulated, Mg-dependent hydrolysis of all tested NTPs to an extent which correlated well with the abilities of the respective NTPs to drive Ca transport. For the SL membranes, Ca-activated dATP hydrolysis occurred at 60% of the rate for ATP; ITP, GTP, CTP and UTP were hydrolyzed by the SL preparation at only 7-9% of the activity produced by ATP. The hydrolysis of the latter NTPs by the SL membranes may reflect contamination by "leaky" SR membranes, which contribute to NTPase activity but not to Ca transport activity. Based on this assumption, we calculate that our SL preparations contain 5-10% SR on a per mg protein basis. In summary, the results indicate that SL and SR membranes contain markedly different ATP-dependent Ca transport systems. They also illustrate a relatively simple procedure for estimating the extent of SR contamination in SL membrane preparations.

M-PM-G12 A RELATION BETWEEN THE CALCIUM UPTAKE PROPERTIES OF SARCOPLASMIC RETICULUM AND THE ATPase OF MYOFIBRILS IN HEARTS OF EXERCISING RATS. Edward D. Pagani* and R. John Solaro. University of Cincinnati, College of Medicine, Cincinnati, Ohio 45267.

We developed methods for measuring myofibrillar and sarcoplasmic reticulum (SR) function in individual hearts from sedentary rats and rats that had been swimming 75 min twice daily for eight weeks. We measured actomyosin and myosin ATPase in isolated myofibrils, and in the same heart, measured oxalate supported calcium uptake of SR vesicles in ventricular homogenates. Analysis of the pooled data showed that the Vmax of myofibrillar ATPase and the relation between free Ca^{2+} and normalized myofibrillar ATPase was the same in hearts from controls and swimmers. The Ca^{2+}-stimulated myosin ATPase was higher in preparations from swimmers while the K-EDTA myosin ATPase was the same. Analysis of the pooled data from our studies of SR function showed that the velocity of Ca^{2+} uptake and the steady state uptake (capacity) of SR vesicles of controls and swimmers were not different. The rate constant (velocity/capacity) for calcium transport was .751±.05/min for control and .747±.01/min for swimmers. Although our results agree with existing data that swimming induces an increase in myosin Ca^{2+}-ATPase, our studies with individual hearts do not show the reported increases in myofibrillar ATPase and SR Ca^{2+} transport. We have found the measurements of both controls and swimmers vary from heart to heart, and we feel this reflects a real heterogeneity among hearts. In view of this we asked if SR and myofibrillar function change from heart to heart in a related way. While we found that there was a positive correlation between myofibrillar ATPase and SR Ca^{2+} uptake in the controls (r=0.74), there was a strong negative correlation (r=-0.94) in the swimmers. Our data suggest that with chronic swimming, a new relation evolves between the Ca^{2+} uptake properties of the SR and actomyosin ATPase which does not appear to exist in the sedentary animal. Supported by NIH-BRSG & Pol-HL 22619(3B).

M-PM-H1 MULTIPLE SITE OPTICAL RECORDING OF MEMBRANE POTENTIAL FROM AN ELECTRICAL SYNCITIUM: MONITORING THE SPREAD OF EXCITATION IN A SALIVARY GLAND. B.M. Salzberg, D.M. Senseman, and G. Salama. University of Pennsylvania and Monell Chemical Senses Center, Philadelphia, PA.

In a number of electrically coupled tissues, it would be instructive to be able to follow the spatial spread of activity along normal and anomalous conduction pathways, and to analyse the changes that occur during normal development and in pathological states. To this end, and as a model for other systems, we have been using potentiometric dyes to monitor the spread of excitation in the salivary gland of the fresh water snail Helisoma trivolvis. In these experiments, the gland is mounted on the stage of a modified Reichert Zetopan microscope and illuminated quasi-monochromatically, after having been incubated for 20 minutes in a Ringer's solution containing 20 mM Ca^{++} (5X normal), 10 mM $NaVO_3$, and 200 µgm/ml NK 2367, a dye that behaves as a linear potentiometric probe. The high Ca^{++} appears to protect the gland from the pharmacological effects that normally attend such high dye concentrations (25 µgm/ml may be used safely without Ca^{++} protection) and the sodium meta-vanadate blocks the beating of the cilia that line the acini of the gland and contribute a major component of the optical noise. A 10X water immersion objective forms a real image of the gland in the objective image plane, first on a diffusion screen carrying the outline of a 5X5 silicon photodiode array; then, after positioning, onto the array itself. The photocurrent outputs, representing the transmitted intensities reaching the central 16 elements of the array, are passed, in parallel, to a 16 channel I-V converter and high gain amplifier, then multiplexed into digital memory. The salivary gland can be stimulated, either through the salivary nerve, or directly, with a focal suction electrode. If desired, a single acinar cell can be impaled with a microelectrode to monitor local activity electrically.

Supported by NSF grant BNS 7705025 and USPHS grants NS 16824 and DE 05536

M-PM-H2 "M" AND "F" CURRENTS IN VOLTAGE-CLAMPED HIPPOCAMPAL PYRAMIDAL CELLS. J.V. Halliwell, P.R. Adams and D.A. Brown. (Intr. by M. Brodwick.) Dept. of Physiology & Biophysics, University of Texas Medical Branch, Galveston, TX 77550.

Guinea pig hippocampal slices were studied at 22°-30°C using KCl or K-acetate electrodes and continuous superfusion. A single intrasomatic electrode was used to voltage clamp CA3 or (mostly) CA1 cells using the Wilson-Goldner switching method. Cells were clamped at various holding potentials and subjected to long ($\gtrsim$ 1 sec) hyperpolarizing commands. In healthy cells (resting potentials < -65 mV; action potentials > 100 mV) the resulting inward currents depended critically on the holding potential. Cells held at about -55 showed ohmic behavior for small hyperpolarizing clamps, whereas cells held more negative showed additional slow inward currents which grew with further hyperpolarization. Cells held at -40 showed slow inward currents that diminished to zero with steps to -80 mV. These data are consistent with there being 2 sets of voltage dependent channels operating in the subthreshold and hyperpolarized range of potentials: an inward current that is turned on by hyperpolarization beyond about -80 mV, that by analogy to heart can be called $I_{F(unny)}$, and an outward current that is turned off by hyperpolarization (with a reversal potential close to E_K). The latter current appears analogous to I_M of sympathetic ganglia (Nature, 283, 673). In support of this, in 2 experiments perfusion of carbachol selectively eliminated this current.

I_F may explain "anomalous rectification" in these cells since its time course is similar to the sag in the hyperpolarizing electronic potential. It may or may not reflect current in an inwardly rectifying K channel. Suppression of I_M would tend to accentuate anomalous rectification. Supported by NS-14986.

M-PM-H3 ; AN OPTICAL DETERMINATION OF THE SERIES RESISTANCE IN GIANT AXONS OF Loligo pealei. B.M. Salzberg, F. Bezanilla, and H.V. Davila. Marine Biological Laboratory, Woods Hole, Mass.

The membrane capacitance in squid giant axons has, in series with it, a small resistance, arising primarily in the narrow Schwann cell clefts. The true membrane potential, therefore, differs from that recorded between voltage electrodes in a voltage clamp by an amount that is proportional to the membrane current, and, if this resistance is not properly compensated, serious errors are introduced into membrane conductance and AC impedance measurements.

We have measured the series resistance optically by exploiting the potential dependent changes in light absorption exhibited by an axon stained with a merocyanine-oxazolone dye, NK 2367. This molecule behaves as a linear potentiometric probe with a microsecond time constant. The transmission at 720 nm of a perfused voltage clamped giant axon was recorded during hyperpolarizing and depolarizing potential steps ($\mp$ 70 mV from -70 mV). The optical record during the hyperpolarization closely resembled the voltage clamp step, since no ionic current crossed the series resistance. The feedback compensation was then varied until the optical signal assumed a square shape during both potential steps. The value of the series resistance could then be read from the calibrated potentiometer in the feedback circuit.

In natural seawater, the value of the series resistance obtained in this manner was $2.8 \pm 0.6\ \Omega\,cm^2$. The method described here employs a 15 Å molecular voltage probe to afford an essentially independent determination of the series resistance. Because the probe is located between the axolemma and the external series resistance, it is capable of distinguishing between the effects of the series resistance itself, and the anomalous dispersion of the dielectric.

This work is dedicated to Kacy Cole on the occasion of his 80th birthday, and was supported by NSF grant NS 77 05025 and USPHS grants AM 25201 and NS 12253.

M-PM-H4 MEMBRANE POTENTIAL CHANGES DURING STRETCH IN SQUID GIANT AXONS. Jay B. Wells and David E. Goldman, Lab. of Biophysics, NINCDS, NIH, MBL, Woods Hole, MA 02543.

Axons were prepared and maintained in artificial seawater (ASW) for transmembrane potential recording with conventional internal axial electrodes. A voice coil applied brief stretches, up to five percent of axon segment length, to one end at rates of 0.8 and 1.5 m/sec. Longitudinal tension in the axon was monitored at the other end. The characteristic response to sudden stretch was an initial depolarization which slightly lagged stretch, decayed within two msec of termination of lengthening, and usually ended in a brief wave of hyperpolarization. Stretches applied to axons in ASW compared to ASW containing TTX revealed two components of the initial depolarization. The primary rapid component was correlated with rate and amplitude of stretch and was not abolished by TTX. The slower secondary component was abolished by TTX and ASW solutions in which choline replaced Na^+. The rapid repolarization seen at the end of lengthening could not be delayed or avoided by maintaining the stretch. The period of hyperpolarization was increased in amplitude and duration by increasing stretch amplitude. Some axons showed sequentially increasing electrical responses to each of several identical stretches applied at five minute intervals. This ultimately led to action potential generation. The mechanically evoked action potentials showed time course, amplitude and threshold membrane potential similar to those evoked by current pulses. These results suggest that the primary depolarizing response to sudden membrane strain activates the conventional ionic channels involved in regenerative discharge phenomena.

M-PM-H5 EFFECTS OF $(K^+)_o$ ON INTRA-AND POST-TETANIC ENHANCEMENT OF QUANTAL RELEASE. S. Misler and W. P. Hurlbut, Rockefeller Univ. N.Y. (Intro by A. Mauro).

Increases in the rate of quantal release of transmitter occur under several conditions of presumed Na^+ accumulation within nerve terminals and are usually attributed to resultant increases in free $(Ca^{2+})_i$, though the source(s) of the latter is uncertain. Since tetanization of the frog nerve trunk in varying $(K^+)_o$ is a convenient way of altering axonal Na^+ content, we examined the effects of $(K^+)_o$ present during the tetanus on intra and post-tetanic enhancement of quantal release at the frog neuromuscular junction. When tetani were performed for 5 - 20 min. at 5 - 20 Hz in low $(Ca^{2+})_o$ and high $(Mg^{2+})_o$, we observed intra-tetanic rises in both e.p.p. quantal content, m, and m.e.p.p. frequency, F, as well as post-tetanic enhancement (PTE) of m and F lasting many minutes. All three effects were inversely related to $(K^+)_o$ during the tetanus, $(K^+)_o$ ranging from 0 - 8 mM. When similar tetani were performed in Ringer containing high $(Mg^{2+})_o$, no added Ca^{2+} and 1 mM EGTA, we observed an intratetanic rise in F as well as PTE of m and F which developed on restoration of $(Ca^{2+})_o$ at the end of the tetanus. These effects were also inversely related to intratetanic $(K^+)_o$ and the decay of the PTE of m and F closely paralleled that seen after tetani in Ca^{2+} containing solutions. In the latter experiments we attribute that intratetanic rise in F in part to the displacement of bound Ca_i by accumulating Na_i; we attribute the PTE of m and F to activation of a plasmalemmal Ca_o-Na_i exchange when Ca_o is readmitted after accumulation of Na_i. We suggest that both mechanisms may contribute to the intra and post-tetanic enhancement of m and F seen in Ca Ringer.

M-PM-H6 ETHYLENEDIAMINE TETRAACETIC ACID (EDTA) TRIETHYLENETETRAMINE (TRIEN) AND D-PENICILLAMINE HCL CONTERACT THE EFFECTS OF COPPER ON AN ISOLATED NEURON. K-S Tan, J.H. Van de Sande and S.H. Roth. Divisions of Pharmacology and Therapeutics and Biochemistry, Faculty of Medicine, University of Calgary, Calgary, Alberta, Canada. T2N 1N4

The effects of cuprous (CuI) and cupric (CuII) chloride and sulphate salts were examined on the firing output of a single isolated neuron - the tonic muscle receptor organ of the crayfish Procambarus Clarkii (MRO). The MRO was maintained at 10°C in a tissue chamber under constant tension and continuously perfused with Van Harreveld's physiological solution (Van H). Van H solutions containing 10^{-5} M or less CuII salts produced a characteristic effect which consisted of a concentration dependent initial phase of depression of firing frequency which lasted approximately 1-2 min followed by a secondary enhancement phase (5-10 min duration), and then a third and final phase of a sharp decrease in firing rate leading to complete depression. CuI produced only depression and appeared less active than CuII. Exchange of copper Van H (Cu-Van H) with fresh (wash) Van H during the initial depression phase produced a gradual reversal to less than control values. Washing during the latter part of the enhancement phase or final depression phase did not reverse the effects. At copper concentrations of $2x10^{-5}$ M or greater the effects could not be reversed. However, Cu-Van H solutions containing EDTA, Trien or D-penicillamine could quickly and completely restore the firing frequency to control levels. All three agents were also capable of protecting the neurons from all the effects of copper when applied in combination with Cu-Van H solutions. On a molar basis, Trien appears to be the most effective, which agrees with its therapeutic efficacy as a treatment for Wilson's Disease.

Supported by Canadian Medical Research Council (S.H.R.).

M-PM-H7 THE EFFECTS OF ACUTE DEMYELINATION ON THE IONIC CURRENTS IN FROG INTERNODE. S.Y.Chiu, (Intr. by R.Aldrich), Dept. of Pharmac., Yale Univ. School of Medicine, New Haven, Connecticut 06510.

Voltage-clamp studies were performed on a narrow segment(40-60 um) on single frog internodes with the two neighboring nodes of Ranvier cut away. The axoplasm was equilibrated in isotonic KCl and the segment was exposed to a Ringer solution containing 0.2% lysolecithin, a detergent known to cause demyelination. During the first 10-30 minutes of treatment the capacity and leakage current showed a parallel increase followed by a period when the leakage started to stabilize whereas the capacity continued to increase. The capacity transient at this stage showed a prominent slow phase following the initial fast phase. Concomitantly,a test pulse to +70 mV revealed a delayed outward current which increased roughly linearly with the increasing fast capacity component. At 40-50 minutes the preparation stabilized momentarily and ionic currents measured with depolarizations from -80 to +70 mV showed only outward and no inward current. The outward current was markedly reduced by TEA applied externally(4-12 mM) or internally(20 mM) and by internal Cs ions. The changes in the capacity and leakage currents during treatment is consistent with a gradual disruption of the myelin leading to exposure of the internodal axon. These observations suggest that potassium channels are normally present in the frog internode covered by the myelin.

Supported by a Grant RG1162 from the National Multiple Sclerosis Society and by grants NS 08304 and NS 12327 from the USPHS.

M-PM-H8 USE OF H^3 NSP TO STUDY RETROGRADE AXONAL TRANSPORT IN XENOPUS OPTIC NERVE. Szaro, B.G., *Loh, Y.P., Hunt, R.K. Dept. of Biophysics, Johns Hopkins University, Baltimore, Md.21218. *Lab. Develop. Neurobiol., NICHD, Bethesda, Md. 20205.

H^3 N-succinimidyl propionate (H^3NSP)-- an amino acylating agent which reacts covalently with the N-terminal amine of proteins, and the ϵ-amine of their lysine residues -- can be used to (i) label proteins in a local region of nerve axons and then (ii) track the retrograde transport of these proteins to the nerve cell bodies (Fink & Gainer, J. Cell Biol. 85, 175). Rapid diffusion and high permeability, however, produce background labelling over a 6-8 mm area. Nevertheless, with some analysis, the major components of retrograde transport can be demonstrated in short nerves, like the 6-10 mm optic nerve of Xenopus laevis frogs. We pressure injected .5-1 µl of frog Ringers containing about 70 µCi of H^3 NSP directly into the tectum of juvenile frogs. At timepoints thereafter (.25 hr, 2.5 hr, 5,8,12, and 16 hr), we dissected the tecta, nerves and eyes and analyzed each on 11% SDS polyacrylamide gels. After the gels were fixed, stained, sliced and counted in scintillation cocktail, we generated accumulation/decay curves for each peak over time, plotting label/peak as a percentage of total label over 13000 MW on the gel. We reasoned that transported proteins would transiently increase in the nerve and later accumulate in the eye; non-transported proteins would remain constant or monotonically increase or decrease. We found one peak of approximately 68K MW which fit these 'transport' criteria: its maximal radioactivity in the nerve occurred between 5 and 8 hr, and it began to accumulate in the eye thereafter. No such accumulation accurred in controls in which H^3NSP was injected directly into the eye. Fink and Gainer found a similar peak in rat sciatic nerve. Whether this transported protein is made in the neuron (e.g.,a neurofilament component) or taken up by endings for transport (e.g., albumin) remains to be investigated (We thank NIH NS-14807 for support).

M-PM-H9 CHARACTERIZATION OF PERIODIC STRUCTURE IN SUBCELLULAR MACROMOLECULAR ARRAYS BY FOURIER PROCESSING OF STEM VIDEO SIGNALS. William J. Adelman, Jr., Alan J. Hodge and Richard B. Waltz, Lab. of Biophysics, NINCDS, NIH, Woods Hole, MA.

Application of Fourier analytical methods to the video line signals comprising the picture raster in scanning transmission electron microscopy (STEM) represents a convenient and objective method for characterization of the periodic structure inherent in many subcellular macromolecular arrays. Among the model systems we have chosen to explore are the network structure in thin sections of embedded tropomyosin crystals, cross sections of myelin sheath and longitudinal sections of squid mantle muscle fibers. In the simplest method, a prominent specimen axis is aligned along or across the line scanning direction in single line mode and the image focused using y-mode presentation. This single line video signal is recorded repetitively (typically 128 or 256 lines) on a digital signal processor to reduce inherent noise and transferred to a computer for analysis. In most instances, the periodicity visible in the full STEM picture can be observed and directly plotted using a cursor on the single line y-mode signal. Examination of the forward Fourier transform of this trace (visualized as a power spectrum) shows a frequency peak corresponding to this spacing together with extraneous lower and higher frequency peaks arising from specimen background and other noise. Often, several orders of the fundamental are seen, depending on the nature of the specimen. Background noise arising from specimen irregularities caused by sectioning or staining inhomogeneities can be eliminated by removing the lower and/or higher frequency components before carrying out a reverse Fourier transformation. This Fourier filtering can be applied to whole image data as well. The results of these methods as applied to the neuroplasmic lattice of axons are described in another paper.

M-PM-H10 NEUROPLASMIC LATTICE ORDER IN VERTEBRATE AND INVERTEBRATE AXONS: DEMONSTRATION BY STEREOSCOPIC AND AUTOCORRELATION ELECTRON MICROSCOPY AND FOURIER ANALYTICAL TECHNIQUES IN STEM. Alan J. Hodge and William J. Adelman, Jr., Lab. of Biophysics, NINCDS, Woods Hole, MA.

Evidence for an ordered neuroplasmic lattice or network in Loligo and Hermissenda axons using stereoscopic and optical autocorrelative techniques in TEM of relatively thick (0.1-0.5 μm) sections has been extended in scanning transmission electron microscopy (STEM), and by taking advantage of the low chromatic aberration TEM characteristics of the Philips EM400. The neuroplasmic lattice consists primarily of neurofilaments together with their periodically arrayed side projections (40-45 nm apart) which appear to act as cross-bridges. The lattice often includes neurotubules and other filamentous elements. This lattice structure spatial continuity appears to account for the gel-like character of axoplasm and its anomalously low optical anisotropy. An essentially identical neuroplasmic lattice structure and cross-bridge spacing is observed in Bufo peripheral axons both in internodal regions and in constricted zones associated with nodes of Ranvier and Schmidt-Lanterman clefts. In zones of the latter type, the neurofilament packing density often exceeds $1000/\mu m^2$, a value approaching that $(1283/\mu m^2)$ for hexagonal close packing of elements with a lateral spacing of 30 nm. This closer packing of neurofilaments appears to allow better preservation of lattice order during specimen preparation. Imaging of the neuroplasmic lattice in longitudinal sections by STEM has allowed preliminary characterization in terms of cross-bridge spacing by using Fourier analytical methods as described in another paper. In all cases examined, the neuroplasmic lattice showed an apparent longitudinal spacing of 40-45 nm, in good agreement with TEM stereo and autocorrelative findings. The STEM and TEM results both suggest that the cross-bridges might be related to a larger unit cell by screw axis symmetry.

M-PM-H11 PRIMARY NEURONAL CHANGES ARE RETAINED AFTER ASSOCIATIVE LEARNING. A. West*, E. Barnes*, and D. L. Alkon. Section on Neural Systems, LB, IRP, NINCDS, NIH at the Marine Biol. Lab., Woods Hole, MA 02543

Associative training of the mollusc Hermissenda crassicornis produces a persistent(≥3 days) behavioral change which has many features of vertebrate associative learning(Alkon, 1974, J. Gen. Physiol. 64:70-84; Crow and Alkon, 1978, Science 201:1239-1241). Type B photoreceptors within the eye are more depolarized and show increased input resistance following acquisition of this behavioral change (Crow and Alkon, 1980, Science 209:412-414). Here we examine Type B cells with synapses and impulses eliminated by axotomy during the retention period for the behavioral change, i.e. 1-2 days after 3 days of 1 hr training periods with paired light and rotation stimuli ("Paired" animals), with randomized stimuli ("Random") or no training ("Control"). Input resistance was greater for "Paired" as compared to "Random" and "Control" animals ($p<.01$ for positive current pulses; $p<.02$ for negative pulses, Mann-Whitney U-test). Long-lasting depolarization (LLD) following a 30 sec light step (10^4ergs/cm^2-sec) was also greater for the "Paired" group ($p<.001$, 30 sec after the step). This LLD difference was small after the third of 14 light steps (presented at 2.5 min intervals), was enhanced at more positive holding potentials (∿ +15 mV), and eliminated at more negative potentials (∿ -25 mV) with respect to the resting level. The LLD difference was greatly increased ($p<.001$) by injection of EGTA. The increased input resistance of "Paired" cells can be explained by a long-lasting decrease of voltage-dependent K^+ conductance(s) within the Type B soma membrane (Shoukimas and Alkon, 1980, Soc. for Neurosci.) and in turn explains the enhanced LLD (also voltage-dependent,cf. Alkon,1979, Science 205:810-816) for the "Paired" animals. This membrane change, since it is intrinsic to a cell presynaptic to interneurons and motorneurons, can play a primary role in retention of the associative behavioral change.

M-PM-H12 CORRELATION BETWEEN SPINAL CORD LESION VOLUME AND IMPACT PARAMETERS. Noyes, D.H. and Bresnahan, J. (Intr. by Jack Rall) Department of Physiology, Ohio State University, Columbus, OH 43210.

A mechanical impact to the exposed dorsal surface of the mammalian spinal cord produces a lesion which is centrally located. There is rarely evidence of damaged tissue at the surface point of impact or in the immediately underlying dorsal tracts. The central, caustic-shaped lesion location may be due to reflected compression waves and internally generated shear waves or it may be caused by axial flow of neural tissue.

In order to understand better the basis for the lesion location, a study was done to relate the lesion volume with the parameters of the mechanical impact. The spinal cords of 9 rats were exposed by laminectomy and the cords were impacted with an electromechanical transducer. Force applied to the cord and the displacement of the cord surface were recorded with an impedance head and oscilloscope. The animals were sacrificed after one week and the lesion volume was determined by planimetry of serial sections. Impact data were used to determine: (1) impulse-momentum (2) force pulse duration (3) average force (4) maximum work on cord (5) peak force (6) peak displacement of the cord surface (7) peak power into the cord (8) average power (9) peak velocity of the surface.

The correlation between these impact descriptors and lesion volume was best for impulse-momentum ($r = 0.85$) and decreasing in the order given. There was no statistically significant correlation for the last three. Presumably the pressure wave amplitudes are proportional to the impactor velocity. Since the velocity and power descriptors are proportional to the impactor velocity, the axial flow hypothesis seems more likely than the shear wave idea. We acknowledge the assistance of the O.S.U. Spinal Cord Injury Research Center.

M-PM-Po1 RESONANCE RAMAN SPECTROSCOPY OF COMPOUND C, AN OXYGEN INTERMEDIATE OF THE MIXED VALENCE CYTOCHROME OXIDASE E.K. Yang, F.Adar, J. Leigh and B. Chance, Johnson Foundation, Univ. of Penna., PA 19104, G. Ching, Bell Laboratories, Murrey Hill, NJ 07974

Low temperature resonance Raman (RR) effect has been studied on Compound C, an oxygen intermediate prepared from the mixed valence cytochrome oxidase (1), in an attempt to assign the electronic configuration of the intermediate. The variable temperature dewar is adapted to spin the sample and to control temperature by flow of cold nitrogen gas. RR measurements of various liganded (formate, N_3^- and CN^-) and valence states of cytochrome oxidase between 21°C and -120°C by excitation in the Soret region using 406.7 and 413.1 nm Krypton laser lines show no band shift or narrowing of linewidth by temperature although there is variation in the relative intensities. Photoreduction process can be avoided by spinning the sample but it is more prominant in frozen samples most probably due to slow relaxation mechanism. At low temperature, the RR spectrum of photoreduced enzyme is nearly identical to the fully reduced spectrum except that no 1665 cm^{-1} band characteristic of a_3^{+2} is present and only a very weak band at 1670 cm^{-1} is evident. A new band at 1713 cm^{-1} also appears which may arise from combination of two symmetric modes or shifted formyl vibration. Preliminary results on the RR effect of Compound C at -70°C clearly show a doublet in the oxidation state marker band region(1360-1370 cm^{-1}). Since the RR modes associated with a^{+3}(S=1/2) can be identified, the 1358-1369 cm^{-1} doublet is taken to indicate $a^{+3}a_3^{+2}$. The presence of 1612-1620 cm^{-1} doublet is interpreted as being due to a_3^{+2}(S=0) which support the original configuration of Compound C: $Cu_a^{+2}a^{+2}Cu_{a3}^{+2}a_3^{+2}\cdot O_2^-$ (1).

1. Chance, B. et al., Biochem. J. 177, 931 (1979).

(Supported by NSF grant # PCM 78-07954)

M-PM-Po2 A UBISEMIQUINONE RADICAL FROM THE b-c_1 COMPLEX OF THE MITOCHONDRIAL ELECTRON TRANSPORT CHAIN. Y. H. Wei, Tsoo E. King, R. LoBrutto,* and C. P. Scholes, Laboratory of Bioenergetics and Dept. of Physics, SUNY at Albany, Albany, NY 12222.

A stable ubisemiquinone radical has been observed in bovine heart b-c_1-II complex following reduction by succinate in the presence of catalytic amounts of succinate dehydrogenase. The radical was further stabilized by addition of fumarate. The maximal radical formation was observed as the fumarate to succinate ratio approached 4. The midpoint potential of the radical was thus estimated at 50 mV. The formation of the ubisemiquinone radical occurred concomitantly with the reduction of cytochrome b but after the reduction of cytochrome c_1. Addition of antimycin A to the system caused the disappearance of the radical; however, thenoyltrifluoroacetone (TTFA) showed incomplete inhibition.

EPR spectra were taken both at 9 and 35 GHz. At 9 GHz the $d\chi''/dH$ signal has a g-value of 2.0046 ± .0003, has a symmetric line shape centered at the zero-crossing with no resolved hyperfine structure, and has a line width between derivative extrema that changes only slightly from 8.1 ± .5 Gauss at T>0°C to 8.4 ± .5 Gauss at 77°K. 35 GHz work done at both temperatures shows very similar, well-resolved g-anisotropy. The room temperature 35 GHz spectra taken from a liquid sample have a field separation between derivative extrema of 26 ± 1 Gauss, and they bear a striking resemblance to spectra of ubisemiquinone radical in bacterial reactions centers, which were obtained at 1.3°K by Feher et al. [BBA 267 (1972) 222]. Since a freely tumbling ubisemiquinone radical would not show g-anisotropy, would show resolved hyperfine structure, and would show substantial lineshape differences between liquid and frozen solutions, our EPR work clearly shows that the radical is immobilized--presumably by protein interactions. (Work supported by NIH Grants AM-17884, HL-12576, and GM-16767.)

M-PM-Po3 DEOXYCHOLATE BINDING TO THE HYDROPHOBIC SURFACE OF PURIFIED CYTOCHROME c_1. Neal C. Robinson, The University of Texas Health Science Center, San Antonio, Texas 78284.

Cytochrome c_1 was isolated as a single non-denatured subunit from the bovine heart cytochrome bc_1 electron transport complex by: 1) disruption of the reduced complex with 1.5 M guanidinium choloride and 1.2% cholate; 2) partial purification of cytochrome c_1 (A_{417}/A_{278} = 1.2-1.5) using $(NH_4)_2SO_4$ fractionation of the protein from a cholate solution; and 3) final purification of cytochrome c_1 using a G3000SW HPLC gel permeation column (Toyo Soda Co.) that had been equilibrated with 10 mM deoxycholate (DOC). The purified subunit had: the expected visible spectrum of the non-denatured cytochrome c_1; a ratio of A_{417}/A_{278} = 2.95-3.15; a heme content of 25-32 nmole heme c_1/mg protein; and a MW_{app} = 31,000 as judged by polyacrylamide gel electrophoresis in dodecyl sulfate (95% of the Coomassie blue staining protein was in this single band). A maximum of 100 moles of DOC/heme bound cooperatively to purified cytochrome c_1 near the CMC of this detergent (measured by equilibrim dialysis) indicating that this protein has a fairly large hydrophobic surface. The effective size of the DOC-protein comples was found to be 35Å using a calibrated HPLC gel permeation column. This means the complex has a ratio of R_e/R_{min} = 1.25. These data suggest that cytochrome c_1 is a globular, slightly asymmetric protein, one end of which is hydrophobically associated with the cytochrome bc_1 complex, the other end of which is capable of ionically interacting with cytochrome c. (Supported by USPHS NIH grant GM 24795)

M-PM-Po4 A STRUCTURE-BASED REACTION MECHANISM FOR THE CYTOCHROME OXIDASE-OXYGEN REACTION. B.Chance# and L.Powers+. #Johnson Research Foundation, University of Pennsylvania, Philadelphia, PA; +Bell Telephone Laboratories, Murray Hill, New Jersey.

The enigmatic structure of the antiferromagnetically coupled iron-copper complex in the redox center of cytochrome oxidase has been determined by EXAFS distance measurements(1). These structures function in oxygen reduction intermediates(2,3)as follows: Reduction of the sulphur-bridged resting state $[a_3^{3+}\!>\!S\!<\!Cu_{a_3}^{2+}]^{+5}$ is initiated by the donation of an electron pair(not by oxygen)from $[a^{2+}\ Cu_a^{1+}]^{3+}$ by tunneling to heme a_3 and electron transfer from heme a_3 to oxidized copper (probably by the sulphur-bridge) to give $[a_3^{2+}\ Cu_{a_3}^{1+}]^{3+}$ which can now accept CO or O_2 as a ligand. At -130° light-activated CO/O_2 ligand replacement forms oxycytochrome oxidase $[a_3^{2+}-O_2\ Cu_{a_3}^{1+}]^{3+}$ which is identical to oxy-(or carboxy)hemoglobin(1). At -100° electrons are transferred nearly simultaneously from copper and iron to reduce oxygen to a bridged intermediate, compound B $[a_3^{3+}\text{-}O\text{-}O\text{-}Cu_{a_3}^{2+}]^{3+}$ analagous to oxyhemocyanin $[Cu^{2+}\text{-}O\text{-}O\text{-}Cu^{2+}]^{2+}$ where the copper-copper distance is 3.74Å(4), compared with 3.75±0.05Å determined for the sulphur-bridged resting oxidase(1). At -60° two more electrons are transferred from $[a_3^{2+}\ Cu^{1+}]^{3+}$ to afford a sequence of as yet unidentified intermediates involving peroxide-bond rupture, higher valence states of iron(ferryl ion, π-cation radicals, etc) concomitant with protonation of the intermediates and reformation of the oxidized state. The proximal structure of copper and iron, stabilized by the peroxide bridge in compound B, may recycle in rapid catalytic function ($300sec^{-1}$) without the reformation of the sulphur bridge of the resting state(5). The close coupling of iron and copper in the binuclear complex of the active site affords a key to cyclic function of cytochrome oxidase in biological oxidations.(1)Powers, et al., this vol.,(2)Chance, et al.,Biophys.J.25,44a,1979,(3)Chance,B.,in "Oxygen and Electron Transport"(Chien Ho,ed.)Elsevier,inpress,(4)Brown, et al. J.Am.Chem. Soc.102:124-210,1980,(5)Antonini, et al.PNAS 74:3128,1977. HL-18708,GM-27308,GM-27476,423B.

M-PM-Po5 STRUCTURE OF THE REDOX CENTERS OF CYTOCHROME c OXIDASE;EDGE AND EXAFS STUDIES. L.Powers+,B.Chance#,Y.Ching+,P.Angiolillo#. +Bell Telephone Laboratories, Murray Hill, New Jersey; #Johnson Research Foundation, University of Pennsylvania, Philadelphia, PA.

X-ray edge absorption of copper and extended fine structure studies of both copper and iron centers have been made of cytochrome oxidase from beef heart, Paracoccus denitrificans, and HB-8 thermophilic bacteria(1-2.5mM in heme). The desired redox state(fully oxidized, reduced + CO, mixed valence formate and CO) in the X-ray beam was controlled by low temperature (-140°C) and was monitored by simultaneous optical spectroscopy and by epr every 30 min (1). The structure of the active site, cytochrome a_3-copper pair in fully oxidized and mixed-valence formate states where they are spin-coupled, contains a sulphur bridge having three ligands 2.60±0.05Å from iron(a_3) and 2.17±0.05Å from copper. The distance between iron and copper is 3.75±0.05Å, making the sulphur bond angle 103°, typical for sp sulphur bonding. The iron(a_3) first shell has four typical heme nitrogens with a proximal nitrogen at 2.14± 0.03Å. The sixth ligand is the bridging sulphur. The copper first shell is identical to stellacyanin in both oxidized and reduced states as we reported earlier(2), containing the bridge-forming sulphur. Upon reduction with CO the iron first shell is identical to oxyhemoglobin but has CO instead of O_2. The other redox centers, cytochrome a and the other, "epr detectable" copper, are not observed from one another or from the active site.
Iron has six equidistant nitrogens which do not change on reduction. Copper has two(or one) nitrogens and two(or three)sulphurs with typical distances. These structures afford the basis for the mechanisms in the accompanying abstract(3). (1)Chance, et al.,FEBS Lett. 112:2,178 1980, (2)Powers, et al. BBA 546,520, 1979, (3) Chance, et al., This Vol. HL-18708, GM-27308, GM-27476, SSRL Project 423B.

M-PM-Po6 **RESONANCE RAMAN OF BLUE COPPER PROTEINS.** **David F. Blair, Gary W. Campbell, Vanessa R. Lum, Bo G. Malmström,[1] Harry B. Gray, and Sunney I. Chan. (Intr. by David F. Bocian) Caltech, Pasadena, CA 91125 and [1]University of Göteborg and Chalmers Institute of Technology, S-412 96 Göteborg, Sweden.**

Resonance Raman (RR) spectra in the 200 cm^{-1}-1000 cm^{-1} region have been obtained by excitation at λ_{max} of the $\sigma S(cys) \rightarrow Cu(II)$ charge transfer band of the blue copper in azurin, plastocyanin, stellacyanin, Rhus vernicifera laccase, type II copper-depleted Rhus vernicifera laccase, Polyporus versicolor laccase, ceruloplasmin, and ascorbate oxidase. Several new peaks have been observed in the 400 cm^{-1} region, suggesting that a simple assignment scheme based on only four metal-ligand stretching vibrations may be an oversimplification. All of the spectra display a broad envelope of overtones in the 750 cm^{-1} region. A relatively sharp, intense peak, varying in energy between 744 cm^{-1} and 763 cm^{-1}, is also observed. Some of the proteins exhibits a sharp feature close to 655 cm^{-1} as well. Removal of type II copper from Rhus vernicifera laccase results in a RR-detectable perturbation of the type I site; in contrast, binding F^- to the type II copper induces no RR-detectable changes at this site.

Stellacyanin was also examined by excitation into the $\pi N(his) \rightarrow Cu(II)$ charge transfer band. Excitation of stellacyanin at 454.5 nm results in a new pattern of resonance enhancement and the appearance of several new peaks at energies consistent with assignment to histidyl ring vibrations. **(Supported in part by a National Research Service Award 1 T32 GM07616 from the National Institute of General Medical Sciences and by USPHS NIH Grant GM22432.)**

M-PM-Po7 THE CONFORMATIONS OF OXIDIZED CYTOCHROME c OXIDASE. Randall H. Morse, Gary W. Brudvig, Tom H. Stevens, and Sunney I. Chan. Caltech, Pasadena, CA 91125.

When reduced cytochrome c oxidase is reoxidized with air, it first is found in a transient "g5" conformation characterized by EPR resonances at g=5, 1.8, and 1.7 (R. W. Shaw, R. E. Hansen, and H. Beinert (1978) J. Biol. Chem. 253 6637-6640). The enzyme then quickly relaxes into the well known 'oxygenated' conformation, which is characterized by its optical Soret maximum at 428 nm. We have found that this conformation may also be identified by EPR spectroscopy, by the appearance of a unique fluorocytochrome a_3-Cu_{a_3} EPR signal in the presence of fluoride. EPR studies also show that the 'oxygenated' conformation slowly relaxes into a conformation exhibiting an EPR absorption at g=12 at X-band (9 GHz), which we have called the "g12" conformation. This slow decay is incomplete, however, as a fraction of the enzyme molecules is found to remain in the 'oxygenated' conformation. These observations underscore the importance of recognizing conformational heterogeneity in studies of oxidized cytochrome c oxidase. In fact, the oxidized enzyme, as isolated from beef heart, is comprised of these two conformations (the "g12" and 'oxygenated' conformations), and often a third, which we have called the "resting" conformation. The "resting" conformation is characterized by the induction by NO of a high-spin, rhombic cytochrome a_3 EPR signal, and, interestingly enough, is always lost after turnover, emphasizing the importance of turnover on the enzyme's conformation. On the basis of the EPR spectral results, models for the structure of the cytochrome a_3-Cu_{a_3} site can be proposed at various stages during reoxidation of reduced cytochrome c oxidase. (Supported by USPHS NIH Grant GM 22432)

M-PM-Po8 REACTIONS OF NITRIC OXIDE WITH LACCASES. **Craig T. Martin, Randall H. Morse, Robert M. Kanne, H. B. Gray, B. G. Malmström,[1] and S. I. Chan. Caltech, Pasadena, CA 91125 and [1] University of Göteborg and Chalmers Institute of Technology, S-412 96 Göteborg, Sweden.**

The reactions of nitric oxide with laccases from the fungus Polyporus versicolor and from the lacquer tree Rhus vernicifera have been studied by EPR and optical spectroscopy. In Polyporus laccase, NO rapidly reduces the type 1 and the type 3 coppers. The reaction follows first order kinetics with $t_{1/2}$ = 100 sec. Reduction of the type 2 copper occurs more slowly. Concomitant with the reduction of the metals is the appearance of two new EPR signals which we attribute to NO bound to Cu(I) centers. These new EPR signals resemble matrix-bound NO except that they are detectable at temperatures as high as 60K and show NO-nitrogen hyperfine structure. Similar studies with Rhus laccase show that NO both oxidizes and reduces this enzyme. These different observations are consistent with the lower redox potentials of the Rhus enzyme as compared with the Polyporus enzyme. (Supported in part by a National Research Service Award 1 T32 GM07616 from the National Institute of General Medical Sciences and by USPHS NIH Grant GM22432.)

M-PM-Po9 IMMUNOCHEMICAL CHARACTERIZATION AND PURIFICATION BY IMMUNOEXCLUSION CHROMATOGRAPHY OF BOVINE HEART MITOCHONDRIAL TRANSHYDROGENASE. W. Marshall Anderson, William T. Fowler, Robin M. Pennington, and Ronald R. Fisher, Northwest Center for Medical Education, Indiana University School of Medicine, Gary, Indiana 46408 and Department of Chemistry University of S.C., Columbia, S.C. 29208

Antibodies raised to homogeneous bovine heart mitochondrial transhydrogenase selectively immunoprecipitated the enzyme from detergent extracts of submitochondrial particles. Anti-transhydrogenase inhibited NADH→$NADP^+$ and NADPH→NAD^+ transhydrogenation of submitochondrial particles as well as that catalyzed by the purified soluble and reconstituted enzyme. Energy-linked forward transhydrogenation and reduction of $NADP^+$ by NADPH catalyzed by submitochondrial particles were inhibited to a significantly greater extent than non-energy linked reactions. The following submitochondrial particle catalyzed reactions were not inhibited by the antibody: NADH and NADPH oxidases, NADH and NADPH dehydrogenase, NADH-ferricyanide reductase, and ATP dependent reduction of NAD^+ by succinate. A simplified immunochemical procedure for the purification of bovine heart transhydrogenase has been developed. A transhydrogenase-free Triton extract of bovine heart submitochondrial particles was used to produce antibodies to several extract proteins. These antibodies, coupled to Sepharose, in conjunction with NAD affinity chromatography, provide a rapid three step purification of transhydrogenase. The enzyme, functionally incorporated into phosphatidylcholine liposomes, couples the inward translocation of protons to the reduction of 3-acetyl pyridine adenine dinucleotide by NADPH. Supported by USPHS GM 22070.

M-PM-Po10 KINETICS OF REVERSE ELECTRON TRANSFER AND HEME-HEME SPECTRAL INTERACTION IN CYTOCHROME OXIDASE: THE ELECTRONIC CONFIGURATION OF COMPOUND C. Kamal de Fonseka and Britton Chance (Intr. by B.Masters) Johnson Research Foundation, U. of Pa., Phila., PA 19104

The above phenomena were studied using the mixed-valence state of carboxy-cytochrome oxidase (MV.CO) $[a^{3+}Cu_a^{2+}]^{+5}$ $[a_3^{2+}.CO\ Cu_{a_3}^{+}]^{+3}$ prepared by the addition of ferricyanide (excess,at 20°) to reduced CO-bound mitochondria. Continuous illumination of this species in the absence of O_2 in the 2° to -40° range results in the oxidation of cytochrome a_3 by a first order process ($k=9.1\times10^{-3}$/s at -25°, E_a=15.2 kcal/mol) which is not affected by freezing the sample. This oxidation is attributed to the transfer of electrons to heme a. The high E_a indicates no significant electron transfer at temperatures below -40°. The MV.CO compound is also formed using chloroiridate (at -20°) rather than ferricyanide; these samples have optical and epr properties that give no artifacts in the 430 nm and g=3 regions respectively. They extend previous results on the lack of heme-heme spectral interaction in cytochrome aa_3 and also the lack of heme a^{3+} reduction in the formation of intermediate Compound C[1] in the O_2 reaction of mixed-valence oxidase at -80°, a result that is consistent with the large E_a value shown above. Better resolution of the i.r. absorbance changes in the formation of Compound C, confirms the broad increase at 748 nm (ε= 4/mM.cm; half-width=170 nm). The peaks at 608 and 748 nm in the difference spectrum of Compound C minus MV.CO which are characteristic of a type-I blue copper are attributed to Cu_{a_3}, and Compound C is assigned : $[a^{3+}Cu_a^{2+}]^{+5}$ $[a_3^{2+}\ O_2^{-}\ Cu_{a_3}^{2+}]^{+3}$. The primary electron donor in the reduction of O_2 in the reactions of both the fully-reduced and mixed-valence states of cytochrome aa_3 is identified as Cu_{a_3}. (Supported by NIH grant # GM 27308)

1. Chance, B. et al., Biochem. J. 177, 931 (1979).

M-PM-Po11 CORRELATION OF UNCOUPLER-INDUCED K^+ RELEASE AND NADP OXIDATION IN BEEF HEART MITOCHONDRIA. D.W. Jung and G.P. Brierley, Dept. Physiological Chem., Ohio State Univ., Columbus, Ohio 43210.

Uncouplers (CCP) induce efflux of $^{42}K^+$ from labeled heart mitochondria when (1) CCP is added after one min of respiration-dependent Pi uptake or (2) CCP is present initially with low concentrations of chelator (EDTA or EGTA). Efflux of $^{42}K^+$ occurs in either KCl or K^+-free media and results in loss of 60-70% of matrix label within one min of CCP addition. CCP induced efflux occurs with NAD-linked substrates, but not with succinate in the presence of rotenone. In the former case, both NAD and NADP are completely oxidized following addition of uncoupler, whereas in the latter, >90% of NAD and NADP are reduced. Acetoacetate which oxidizes 70% of NADH but has no effect on NADPH, does not affect uncoupler-induced $^{42}K^+$ efflux in the presence of rotenone. Reaction (1) is stimulated by Ca^{2+} (0.1mM) and inhibited by ADP, ATP, and oligomycin. In contrast, reaction (2) is inhibited by Ca^{2+}, only slightly inhibited by ATP and not affected by ADP, Mg^{2+}, or oligomycin. The uncoupler-induced efflux of K^+ seems best explained by the opening of one or more cation uniport pathway(s) which are controlled by NADPH, by extramitochondrial Ca^{2+}, and by adenine nucleotides. The loss of matrix $^{42}K^+$ induced by CCP is clearly distinct from the respiration- dependent, uncoupler-sensitive $^{42}K^+/K^+$ exchange which results from interplay between electrophoretic K^+ influx and electroneutral K^+ extrusion in coupled mitochondria (Jung et al, JBC 255, 408, 1980). The correlation between K^+ efflux and NADPH oxidation closely resembles that reported for Ca^{2+} efflux in glucagon-treated rat liver mitochondria (Prpic and Bygrave, JBC 255, 6193, 1980).
Supported in part by USPHS Grant HL09364.

M-PM-Po12 EFFECT OF DIBUTYLCHLOROMETHYLTIN CHLORIDE ON MITOCHONDRIAL K^+ FLUX. Joyce J. Diwan. Biology Department, Rensselaer Polytechnic Institute, Troy, New York 12181.

Dibutylchloromethyltin chloride (DBCT) is a covalent inhibitor of the mitochondrial ATP synthase complex (Cain, Partis, & Griffiths, Biochem. J. 166:593, 1977). It has been suggested that DBCT may react with a dithiol group on Coupling Factor B (Stiggall, Galante, & Hatefi, Arch. Biochem. Biophys. 196:638, 1979). Mercurials, which also react with Factor B (Shankaran, Sani, & Sanadi, Arch. Biochem. Biophys. 168:394, 1975), stimulate K^+ flux into mitochondria (Diwan et al., Indian J. Biochem. Biophys. 14:342, 1977). In these studies unidirectional K^+ flux into and out of isolated rat liver mitochondria was measured by means of ^{42}K, with succinate present as energy source. DBCT, at approx. 5-10 nmoles per mg protein, is found to stimulate unidirectional K^+ influx and efflux rates. With higher concentrations of DBCT (e.g. 15 nmoles/mg protein) there is a substantial net loss of endogenous K^+, and the stimulation of K^+ influx is not seen. The stimulated K^+ influx in the presence of DBCT remains sensitive to the respiratory inhibitor AntimycinA. The effect of DBCT does not depend on the Cl^- concentration of the medium. The combined presence of the mercurial mersalyl (150 μM) and DBCT (5-7 nmoles/mg protein) results in a higher rate of K^+ influx than is observed with either stimulatory reagent alone. It remains unclear whether the effects of DBCT and mersalyl on mitochondrial K^+ transport result from interaction of these reagents with Coupling Factor B. (This work was supported by USPHS Grant GM-20726. DBCT was supplied by D. E. Griffiths)

M-PM-Po13 RECONSTITUTION OF COLICIN E1 AND A PROTEOLYTIC FRAGMENT OF THE COLICIN INTO DIMYRISTOYLPHOSPHATIDYLCHOLINE MEMBRANE VESICLES. Y. Uratani, C. Grabau, J.R.Dankert, and W.A. Cramer, Dept. of Biological Sciences, Purdue Univ., W. Lafayette, IN. 47907.

Colicin E1 has been incorporated (∿ 10 molecules/vesicle) into large unilamellar DMPC membrane vesicles that retain inulin and sucrose. The ability of colicin E1 to conduct ion flow across the vesicle membrane was measured above (32°C) and below (12°C) the measured phase transition (T_m=23.5-24°C) of the vesicles by dissipation of an ionophore-induced potassium diffusion potential. The diffusion potential which can be generated by the addition to K^+-loaded vesicles, of valinomycin or gramicidin at 32°C, and of gramicidin at 12°C, was dissipated at both temperatures by colicin E1 but not by heat-denatured colicin or BSA. Conduction of transmembrane ion flow by colicin was also measured by fluorescence changes of encapsulated ANS. Salt added to the vesicle suspension at 12°C did not affect the fluorescence of trapped ANS in the absence of colicin, or in the presence of BSA or heated colicin. However, addition of salt to vesicles containing active colicin caused an increase in fluorescence of the entrapped ANS. No selectivity was found for the colicin-mediated ion flow for a series of salts, of which tetrapropylammonium bromide was the largest. A channel-like function of colicin E1, with a size discrimination against sucrose, but not several salts of smaller molecular weight, can thus be defined for colicin E1 incorporated into membrane vesicles made of a single lipid. Trypsin digestion of colicin E1 results in the formation of a proteolytic fragment of MW=18K daltons which does not inhibit cellular transport. Incorporation of the fragment into DMPC vesicles shows, however, that the fragment conducts different solutes across the vesicle membrane, above and below the phase transition of the DMPC vesicles. The 18K dalton fragment may be a membrane active portion of colicin E1, deficient in the receptor binding domain. (Supported by NIH grant GM-18457).

M-PM-Po14 EVIDENCE THAT MG++, NOT CA++, REGULATES THE K/H EXCHANGER IN RAT LIVER MITOCHONDRIA. Richard Nakashima, Robert S. Dordick, and Keith D. Garlid, Dept. of Pharmacology, Medical College of Ohio, Toledo, Ohio 43699.

Previous reports from our laboratory have shown that the mitochondrial K/H exchanger is released by swelling in hypotonic sucrose, by respiration in tetraethylammonium salts and by treatment with ionophore A23187. Studies of these processes, reported in detail elsewhere, have lead to the conclusion that the K/H exchanger is inhibited by divalent cations. The physiological role of this carrier brake mechanism is to provide volume homeostasis with minimal energy expenditure and this role is best filled by a cation whose amount in the matrix remains relatively stable. On this basis, we have postulated that Mg++, rather than Ca++, regulates the K/H exchanger. We have examined this question using two experimental protocols: (1) Addition of Ca++ to respiring mitochondria resulted in a rapid K+ loss into low-K+ media, and this ejection was reversed by valinomycin. Therefore Ca++ is an inducer, rather than an inhibitor, of K/H exchange under these conditions. (2) Mitochondria were loaded with Ca++ (20μmol/g), exposed for 1 min to different doses of ionomycin or A23187, then separated by rapid centrifugation and analyzed for their cation contents. Comparison of the dose response curves for the two ionophores demonstrates that K+ efflux follows Mg++ loss and is independent of matrix Ca++ content. From the doses giving 50% cation efflux, we report the following apparent cation "affinity" ratios for A23187 and ionomycin, respectively: 3 and 35 for Ca++/Mg++, 5 and 135 for Ca++/K+, and 2 and 3 for Mg++/K+. The results of these two series of experiments may be summarized as follows: In the presence of matrix Mg++, Ca++ uptake induces K+ efflux, while Ca++ loss has no effect on K+ efflux. These findings support the contention that the divalent cation responsible for regulating K/H exchange is Mg++, not Ca++. (Research supported by USPHS Grant GM 24297)

M-PM-Po15 K^+ TRANSPORT IN MITOPLASTS. Hsiao-Sheng Chang* and Joyce J. Diwan (Introduced by J.L. Katz), Biology Department, Rensselaer Polytechnic Institute, Troy, N.Y. 12181.

It has been proposed that voltage-dependent channels in the outer mitochondrial membrane may provide variable control of diffusion of small molecules into mitochondria (Colombini, Nature, 279:643, 1979). Mitoplasts, which lack the outer mitochondrial membrane, were prepared by the procedure of Pedersen et al (Meth. in Cell Biol. 20:411, 1978) involving treatment of isolated rat liver mitochondria with digitonin. The mitoplasts were found to have an acceptor control ratio in the absence of added Mg^{2+} of about 2 to 2.5 with succinate as the substrate. In the presence of succinate the rate of unidirectional K^+ flux into rat liver mitoplasts measured by means of ^{42}K depends on the K^+ concentration in the medium. Lineweaver-Burk plots of 1/(K^+ influx) vs. the reciprocal of the external K^+ concentration are linear. Apparent kinetic constants have been determined at pH 7.5. The Km for K^+ influx is 6.4 to 6.9 mM and the measured Vmax is 5.0 to 5.2 µmoles/gm. protein/min. The K^+ influx rate increases as the pH of the medium is increased from 6.8 to 8.0. The pH-dependence of the K^+ influx and the dependence on external K^+ concentration are similar to results obtained with intact mitochondria (Diwan and Lehrer, Membr. Biochem. 1:43,1977). The succinate-supported K^+ influx is inhibited by antimycin A and by the oxidative phosphorylation inhibitor dicyclohexylcarbodiimide. In contrast, oligomycin has no effect on the rate of K^+ influx. This inhibitor sensitivity is similar to that observed with intact mitochondria (Gauthier and Diwan, BBRC. 87:1072, 1979). Supported by NIH Grant GM-20726.

M-PM-Po16 SUBMITOCHONDRIAL PARTICLES ARE NOT "HYBRIDIZED" OR "SCRAMBLED" H. James Harmon and J. M. Kunkel, Dept. of Physics and School of Biological Science, Oklahoma State Univ., Stillwater, OK 74078.

Electron transport particles (ETP) isolated by alkaline treatment of beef heart mitochondria characteristically show a homogeneous orientation (>94% of the vesicles are "inside-out"). Previous work indicates that succinate oxidase activity is not affected by washing with 0.15 M KCl or the addition of either cyt c or protamine sulfate. Further, ATPase activity is inhibited more than 90% upon addition of isolated ATPase inhibitor protein to ETP. Mild sonication of intact beef heart mitochondria yields submitochondrial particles (SMP) that, like alkaline ETP, are predominately inverted. KCl-washed mitochondria lose 90-95% of their endogenous cyt c. KCl-washed SMP, however, exhibit less than 6-10% increase in succinate oxidase activity upon addition of cyt c and a similar extent of inhibition upon addition of protamine sulfate in the presence of cyt c. The extent of inhibition of ATPase in SMP by addition of ATPase inhibitor protein corresponds to the homogeneity of the vesicles as determined by cytochrome c, e.g., 90% inverted particles show 90% inhibition of ATPase activity. This indicates that SMP are almost completely inverted. Membranes that can react with cyt c are apparently those that cannot react with the impermeant inhibitor protein to ATPase; they are intact mitochondria. Because of the lack of effect with cyt c and the inhibition of ATPase, SMP isolated by sonication are not extensively "scrambled" or "hybridized". Homogeneously-oriented SMP (>94%) can be isolated. The remainder of the membranes are intact mitochondria.

This work was supported by a Grant-in-Aid from the American Heart Association and with funds contributed in part by the Oklahoma Affiliate.

M-PM-Po17 PARAMAGNETIC CENTERS IN METHANOBACTERIUM BRYANTII. Jack R. Lancaster, Jr., Thomas Kirby, and Irwin Fridovich. Department of Chemistry and Biochemistry, Utah State University, and Department of Biochemistry, Duke University.

The methanogens are the major representative of the Archaebacteria, which are proposed to be only distantly related to prokaryotes and eukaryotes. All methanogens are capable of reducing CO_2 to CH_4 using molecular hydrogen as reductant. Recent evidence suggests the production of transmembrane ion gradients during this reduction. We report here the presence of paramagnetic centers in M. bryantii. The oxidized soluble fraction contains an EPR signal typical of an oxidized iron-sulfur center (axial symmetry, $g \approx 2.02$). There also is an active iron-containing superoxide dismutase. The purified enzyme shows an EPR signal very similar to that of other iron SOD's ($g_z = 4.78$, $g_x = 4.1$, $g_y = 3.73$), indicative of high-spin iron in an asymmetric environment. The value for D is 2.39 cm^{-1} and for E is 0.6 cm^{-1}. The presence of this enzyme may suggest that the extreme oxygen toxicity of these organisms is not due to superoxide formation. The oxidized membrane fraction contains a very unusual rhombic high-temperature signal with all three g-values significantly above 2.0 (2.3, 2.23, 2.02). This signal may be of a new type of iron cluster, but the more likely explanation is that it is of a transition metal other than iron, probably low-spin nickel III in an environment of octahedral symmetry (possibly factor F_{430}). Double integration of the signal yields a value for concentration of this species in the membrane fraction approximately 0.2 nmole per mg protein. Upon reduction there is the appearance of at least two "g = 1.94"-type iron-sulfur centers. These membrane-bound centers are excellent candidates for energy transduction by hydrogen reduction of CO_2. (We are indebted to R.S. Wolfe, Univ. Illinois for providing samples of the bacterium.)

M-PM-Po18 PROTON NMR STUDIES OF METABOLITES IN YEAST USING ^{13}C DECOUPLING L.O. Sillerud, J.R. Alger, and intro by Peter B. Moore. Yale University, Dept. of MB&B P.O. Box 6666, New Haven, CT 06511.

In order to increase the sensitivity, simplicity and specificity of proton spectroscopy applied to the study of intracellular metabolites in yeast we have utilized a novel method. We have used ^{13}C labeled acetate, $^{13}CH_3COO^-$, as the substrate for respiration in an aerobic suspension of Saccaromyces cerevisiae. We looked at the ^1H difference spectra obtained by subtracting the ^{13}C -^1H coupled spectra from the ^{13}C decoupled spectra where ^1H is observed in the presence of broad-band ^{13}C decoupling. Thus signals remain in the difference spectra only from protons that are coupled to the ^{13}C label. Time courses of a yeast suspension after ^{13}C acetate feeding show the disappearance of label from the acetate pool and the subsequent appearance of ^{13}C in glutamate C_3 and C_4 and in aspartate C_3. These results are in accord with the known fluxes of metabolites through the Krebs cycle. Selective single frequency ^{13}C decoupling was used to provide assignments for the difference signals. This technique shows a potential for application in a wide variety of systems where the resolution of the ^{13}C spectrum may be combined with the sensitivity for proton detection to observe metabolites that have been previously unobservable.

M-PM-Po19 HYPOTHESIS: ENERGETIC PROTONS IN REVERSIBLE HYDRATION OF MgATP. Reuven Tirosh, Dept. of Anesth. and Bioeng., (RN-10), University of Wash., Seattle. WA 98195.

(1) A reversible conversion of mass into kinetic energy is considered to be an elementary mechanochemical transformation. (2) The proton is the best candidate for efficient gain of the kinetic energy and its vectorial transfer to the surrounding fluid by electrical interaction. (3) To generate molecular streaming in water, a quantum of energy is needed to overcome the cohesive forces; therefore it is equal to the latent heat of evaporation, namely $\Delta E \approx 46$ kJ/mole. (4) Hydronium ions, at pH 7 and 0° C, can be the source of such energetic protons, according to the Boltzmann equation: $[H_2O\text{-}H^+]/[H_2O] = \exp(-\Delta E/kT)$. (5) MgATP is hypothesized to catalyze the release or association of energetic protons and water molecules, as described by the exothermic reaction: $MgATP^{-2} + HOH\text{-}H^+ \rightleftharpoons MgADPH\text{-}OHP + H^+ + 46$ kJ/mole.

(6) Specific interaction of the enzymatic system with MgATP can impose favorable orientation of the high energy complex, so as to generate (or absorb) vectorial fluxes.
(7) In the soluble actomyosin system, such a volume flux can account quantitatively for the phenomena of cell motility and muscle contraction, where the fluid phase is actively involved rather than the so-called "contractile proteins."
(8) In the membrane-associated F_0-F_1 system, such a vectorial flux across the non-dissipative phase of the membrane, may form a "proton pump" that can maintain a backward "proton-motive force" of up to 0.5 Volt. In the reverse process, protons moving down the potential difference across the membrane, can gain enough kinetic energy to reform hydronium ions and synthesize MgATP, through dehydration of the MgADPH-OHP complex. This molecular mechanism may thus form the physical basis for the chemiosmotic hypothesis.

M-PM-Po20 SATURATION TRANSFER NMR STUDIES OF IN VIVO ATPASE KINETICS IN E. COLI AND S. CEREVISIAE

J.R. Alger, J.A. den Hollander and R.G. Shulman. Department of MB&B, Yale University; P.O. Box 6666, New Haven, CT 06511.

The saturation transfer ^{31}P NMR technique[1] has been used to measure the dependence of the unidirectional ATP synthesis rate, catalyzed by the proton translocating ATPase, in E. coli upon cellular energetics. The rate is constant as the external pH is changed from 7.3 to 6.25. Thus, the ATPase activity does not depend on the external pH; nor does it depend on the transmembrane pH gradient (ΔpH) since the internal pH remained constant when the external pH changes. We have performed measurements after incubation with compounds which reduce the proton-motive force, including the uncoupler CCCP. Under conditions when $\Delta pH = 0$, addition of CCCP severely reduces the ATP synthesis rate, corresponding to the presumed decrease in $\Delta\psi$.

The yeast, S. cerevisiae, has mitochondrial as well as plasma membrane ATPase activity. We have measured the sum of these activities by saturation transfer under respiratory conditions. The relative proportion of the two activities have been distinguished by compounds such as DCCD which inhibit the mitochondrial ATPase. Incubation in 20μM DCCD results in loss at least 70% of the total activity indicating the majority of the activity resides in the mitochondrial protein.

(1) Brown, T.R., Ugurbil, R. and Shulman, R.G. P.N.A.S. 74, 5551 (1977)

M-PM-Po21 STOICHIOMETRY OF THE MITOCHONDRIAL REDOX CENTERS AND HETEROGENEITY OF THE UBIQUINONE POOL. David F. Wilson, David Nelson and Maria Erecinska, Department of Biochemistry and Biophysics, Medical School, University of Pennsylvania, Philadelphia, PA 19104.

A small volume ($\approx$ 1.7 ml) stirred spectrophotometer cuvette (0.8 cm light path) has been constructed which allows injection or withdrawal of electrons under strictly anaerobic conditions. An electrical circuit controls the rate of electron injection and measures the charge to 1×10^{-5} coulombs or better even when suspensions of submitochondrial membranes from pigeon breast mitochondria are being titrated. Coulometric titrations establish that all of the redox components in the respiratory chain with half-reduction potentials (E_m) values more positive than +150 mV at pH 7.0 are accounted for. The components with E_m values between -60 mV and + 150 mV are dominated by ubiquinone 10 which is present at high concentrations (10 moles/mole c_1). The ubiquinone pool is heterogeneous; with approximately 81% titrating with an E_m of 60 mV, n = 2.0 while the remainder behaves as a single electron donor/acceptor with an E_m of 0 mV. The latter suggests the presence of multiple high affinity quinone binding sites which preferentially bind oxidized ubiquinone and which exchange very slowly with the main quinone pool. The total number of equivalents accepted or donated in this potential region is also equal within experimental error to the content of known redox components. Supported by NIH Grant GM12202.

M-PM-Po22 THE CONTROL OF HEART MITOCHONDRIAL RESPIRATION BY THE FUNCTIONAL COUPLING OF CREATINE KINASE (CK_m) AND ADENINE NUCLEOTIDE TRANSLOCASE. R.W. Moreadith and W.E. Jacobus, Medicine/Physiological Chemistry, Johns Hopkins School of Medicine, Baltimore, MD 21205

Different enzyme systems were used to control respiratory rates in rat heart or liver mitochondria. Measured phosphate potentials (ATP/ADPxPi) were correlated to rates of O_2 consumption. Rat liver mitochondria, in the presence of rabbit creatine kinase (CK) or hexokinase and varying amounts of ATP, reached maximum rates of respiration at equivalent phosphate potentials. However, when rat heart mitochondria were incubated in 20 mM creatine and ATP, respiration occurred at a significantly higher phosphate potential. This difference in the phosphate potentials associated with maximal rates of respiration can be explained by the microcompartmentation of CK_m and adenine nucleotide translocase. Atractyloside (ATR) inhibition curves in both heart and liver mitochondria under the above conditions demonstrated that: (1) Liver mitochondrial respiration, induced by ADP, CK or HK, was reduced in a linear manner and fully inhibited by 1.2 - 1.8 nmoles ATR/mg protein. When respiration was rate-limited by either low HK or CK, respiratory rates were not altered by initial addition of ATR until the translocase again demonstrated its rate-limiting character. (2) Heart mitochondrial respiration induced by an ADP pulse was biphasic when ATR was added and completely inhibited by 2.5 - 3.0 nmoles/mg, suggesting at least two translocase sites with varying affinity for ATR. (3) When heart mitochondria were incubated in 20 mM creatine + 1 mM ATP (Vmax for CK_m), respiration was less sensitive to ATR addition, and up to 20 nmoles ATR/mg were required for full inhibition, indicating effective competition between ATR and ADP from CK_m. Together, these and previous data show that the adenine nucleotide translocase directly couples both the supply of ATP to, and the removal of ADP from, heart mitochondrial creatine kinase. (Supported by HL 20658).

M-PM-Po23 PARTIAL PURIFICATION OF CYTOSOLIC PROTEINS ESSENTIAL FOR OPTIMAL YEAST MITOCHONDRIAL PROTEIN SYNTHESIS. ERIC FINZI (INTR. by DIANA BEATTIE) MT. SINAI SCH. MED. NEW YORK, N.Y. 10029

Protein synthesis in isolated yeast mitochondria can be stimulated 6-8 fold by addition of dialyzed postpolysomal supernatant at the start of the incubation. The stimulatory proteins have been partially purified by incubating the postpolysomal supernatants with 0.5M salt prior to chromatography on Sephacryl S-200. Stimulatory activity was eluted in two peaks, one in the 40-80,000 molecular weight range and a broad peak with a molecular weight of 10,000 or less containing half of the initial activity. Stimulation of mitochondrial protein synthesis by the low molecular weight activator fraction was sensitive to chloramphenicol, insensitive to cycloheximide and proportional to the protein concentration of activator added. The rate of mitochondrial protein synthesis with the activator was 20 times greater than achieved by mitochondria alone and represented a 40-fold purification of the stimulatory activity in the postpolysomal supernatant. Analysis of the products of the stimulated mitochondrial protein synthesis by gel electrophoresis revealed that the activator increased equally the labelling of all the products. Addition of GTP to the medium stimulated protein synthesis 3 to 4 fold, but the reaction was linear only for 20 minutes. Dialyzed postpolysomal supernatants from either yeast or rat liver as well as purified activator stimulated protein synthesis at least 2-fold above the GTP stimulation. In the presence of activator protein synthesis continued at a linear rate for 40 minutes suggesting that activator and GTP work by different mechanisms. Furthermore, these results indicate that low molecular weight protein(s) present in the cytosol are necessary for optimal rates of mitochondrial protein synthesis. (Supported by NIH HD 04007; EF trainee on GM-07280)

M-PM-Po24 FLUORESCENCE LIFETIME AND POLARIZATION BEHAVIOR OF POTENTIAL-SENSITIVE OXONOL DYES IN BEEF HEART SUBMITOCHONDRIAL PARTICLES. J. C. Smith[1], L. Hallidy[2], and M. R. Topp[2], Dept. Chem., Georgia State U., Atlanta, Ga.[1], Dept. Chem., U. Penn., Philadelphia, Pa.[2].

To further elucidate the mechanisms by which the potential-dependent dye fluorescence quenching occurs in beef heart submitochondrial particle (SMP) suspensions, the behavior of the dye fluorescence lifetime and polarization has been investigated. In the presence of the membrane, the oxonol V and VI fluorescence decay curve becomes biphasic and can be fitted to a double exponential function. The lifetime of the shorter lived component is, within the fitting error, the same as that of the free dye in aqueous medium. The longer lived species suffers a lifetime decrease in the presence of ATP but can be restored to the control level by CCCP addition. Under the same experimental conditions, the dye fluorescence undergoes a massive uncoupler-sensitive, ATP-dependent depolarization. These observations cannot be explained by Perrin type behavior and suggest that concentration depolarization is occurs via energy transfer in the membrane bound dye fraction, the lifetime decrease resulting from radiationless processes competing with energy transfer. Concentration depolarization could be detected for oxonols free in aqueous solution at concentrations above 20 μM. The fluorescence lifetime of oxonol V in ethanol exhibited Stern-Volmer behavior suggesting that at high concentration the dye emission is self quenched. These observations are consistent with a redistribution mechanism in which additional dye occupies membrane binding sites in the presence of substrate thereby incrementing the membrane bound dye concentration. Compared to that of the free dye, the rotational relaxation time increases by over an order of magnitude when the dye binds to the SMP membrane and suggests that the fluorophore is strongly immobilized in the membrane. Supported by USPHS GM-122202-15, NS-10939-06, RR-09201-01, and NSF grant CHE-76-10336.

M-PM-Po25 SINGLE TURNOVER KINETICS IN MITOCHONDRIAL ELECTRON TRANSFER: THE RECOGNITION OF A QUINONE FUNCTIONALLY CENTRAL TO THE MITOCHONDRIAL UBIQUINONE-CYTOCHROME c OXIDOREDUCTASE. K. Matsuura, N. Packham, M. Tiede, P. Mueller and L. Dutton, U. of Penn., Phila., PA 19104

Single turnover electron transfer through isolated ubiquinone-cytochrome c (Q-c) oxidoreductase from beef heart mitochondria was studied in combination with isolated photoactivatable reaction center (RC) of Rps. sphaeroides and horse heart cyt. c (1). The redox state of the system before the flash activation was controlled potentiometrically. After rapid cyt. b reduction and cyt. c oxidation by the photoactivated RC, antimycin sensitive ferrocyt. b oxidation and ferricyt. c reduction occurred simultaneously. The rate of electron transfer from cyt. b to cyt. c was dependent on the redox state of a component of E_m (pH 7.0) 115 mV, n=2; E_m/pH -60 mV from 6.3 to 8.5. When reduced, the redox component promoted electron transfer from cyt. b to cyt. c; when oxidized this reaction was ∿25 x slower. The character of the component is similar to Q_z, a special quinone found in the Q-c_2 oxidoreductase of Rps. sphaeroides (2) and an EPR detected semiquinone in the mitochondrial Q-c oxidoreductase (3); it may also be the component which in the reduced form stabilizes the mitochondrial Q-c oxidoreductase (4). In Rps. sphaeroides Q_z is vital not only for electron transfer from cyt. b to cyt. c but also for an electrogenic reaction and H^+ transport. Figure 1. proposes a simple general model that is consistent with the above. One electron moves from cyt. b to cyt. c (via FeS and c_1) using the Q_zH_2/Q_z^- couple (3) which effects the electrogenic movement of $2H^+$ through a proposed channel (?) aided by coupled conformational changes (4). 1. PNAS Nov. 1980 2. JBC 254 11307 1979 3. JBC 255 3278 1980 4. JBC 242 4854 1967. Supported by NIH GM-27309.

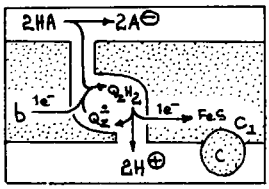

M-PM-Po26 KINETICS OF HYDROGEN ION DIFFUSION ACROSS PHOSPHOLIPID VESICLE MEMBRANES. Constance M. Biegel and J. Michael Gould, Department of Chemistry, University of Notre Dame, Notre Dame, Indiana 46556.

The membrane-impermeant, pH-sensitive fluorescence probe 8-hydroxy-1,3,6-pyrenetrisulfonate can be entrapped within the internal aqueous compartment of unilamellar phospholipid vesicles, where it serves as a reliable indicator of internal aqueous hydrogen ion concentration (Clement, N. R. and Gould, J. M., Biochemistry, in press). When the external (medium) pH of a suspension of soybean phospholipid vesicles was rapidly changed from 8.2 to 6.65, the rate of subsequent H^+ influx into the vesicles, measured as the change in pyranine fluorescence, was limited (in KCl media) by the rate of charge compensating counterion redistributions. The half-time for the pyranine fluorescence change (corresponding to an internal pH change from 8.2 to 7.4), which was several minutes in the absence of valinomycin, could be decreased to about 300 msec, but not further, by the K^+ ionophore valinomycin. Proton ionophores such as gramicidin or bis-(hexafluoroacetonyl)-acetone (1799), on the other hand, decreased the time required for transmembrane H^+ equilibration to < 1 msec. Similar results were also obtained using vesicles comprised of either egg phosphatidylcholine or synthetic dimyristoylphosphatidylcholine. These findings indicate that the intrinsic permeability of unilamellar vesicle membranes to hydrogen ions is unexpectedly high, and is much greater than the observed permeabilities of other small ions. (Supported by grants from the USDA, the Indiana Kidney Foundation, and Miles Laboratories.)

M-PM-Po27 DIRECT, CONTINUOUS OBSERVATION OF LIGHT DEPENDENT CHANGES IN THE INTRAVESICULAR pH OF BACTERIORHODOPSIN PROTEOLIPOSOMES. Duncan H. Bell, Nancy R. Clement, L. K. Patterson, and J. Michael Gould, Radiation Laboratory and Department of Chemistry, University of Notre Dame, Notre Dame, Indiana 46556.

Anionic soybean phospholipid vesicles incorporating the light-driven proton pump bacteriorhodopsin have been formed by a sonication procedure with the pH sensitive membrane-impermeant fluorescence probe 8-hydroxy-1,3,6-pyrenetrisulfonate (pyranine) entrapped within the intravesicular aqueous compartment. Illumination of the reconstituted proteoliposomes caused changes in the fluorescence intensity of entrapped pyranine indicative of an increase in hydrogen ion concentration within the proteoliposomes. The fluoroescence change had a half-time of 15-30 seconds. The maximum extent was linearly proportional to the actinic light intensity, the amount of bacteriorhodopsin present during sonication, and the duration of the sonication period. The rate of the light-dependent fluorescence change was enhanced by the K^+ ionophore valinomycin, and was abolished by the uncoupler gramicidin. It is concluded that the fluorescence intensity of vesicle-entrapped pyranine can be employed as a useful probe for continuous, real-time measurements of hydrogen ion concentration within reconstituted proteoliposomes. (Supported by the U. S. Department of Energy, the U. S. Department of Agriculture, and the Indiana Kidney Foundation).

M-PM-Po28 ANALYSIS OF THE SPECTROSCOPIC PROPERTIES OF BACTERIORHODOPSIN IN THE PURPLE MEMBRANE BY A CRYSTALLINE EXCITON MODEL. Donald D. Muccio and Joseph Y. Cassim. Dept. of Chemistry, Case Western Reserve University, Cleveland, Ohio and Dept. of Microbiology and Div. of Sensory Biophysics, The Ohio State University, Columbus, Ohio.

The p3 symmetry of bacteriorhodopsin in the purple membrane results in a perturbation of the electronic transitions and, consequently, the spectroscopic properties of the retinylidene chromophore of monomeric bacteriorhodopsin. This perturbation may play an important role in determining primary photoevents in the energy transducing process of this membrane. In view of this, an exciton model has been employed to calculate transition energies, dipole and rotational strengths of the all-trans and 13-cis isomers of bacteriorhodopsin in the membrane. This calculation utilizes the recently determined positions of the retinylidene chromophore in the membrane(1). The signs and magnitudes of these parameters are consistent with those found experimentally in the absorption and circular dichroic (CD) spectra. This method has been extended by symmetry considerations to the calculation of the dipole and rotational strength tensorial elements. For light incident normal to the membrane plane, the absorption spectra contains only the in-plane excitonic transition while the CD spectra vanishes. The perturbation energy has been calculated by a weak-coupling interaction of vibronic transitions. This results in an increase and splitting of each monomeric vibrational energy due to interactions among translationally and nontranslationally equivalent chromophores, respectively. An 150 cm^{-1} upper limit of these interaction energies has been determined; however, more realistic values are probably an order of magnitude smaller. Based on this value, picosecond energy transfer lifetimes are expected to occur. A possible role for excitonic energy transfer in the phototransduction process will be presented.

(1) King, G.I. et al. 1980. Proc. Natl. Acad. Sci. U.S.A. 77, 4726.

M-PM-Po29 EFFECTS OF ETHYLENE GLYCOL ON THE SPECTRA OF PURPLE MEMBRANE. James E. Draheim and Joseph Y. Cassim, Department of Microbiology and Division of Sensory Biophysics, The Ohio State University, Columbus, Ohio 43210.

The addition of 30% (v/v) ethylene glycol to light-adapted purple membrane solutions results in a small red shift of the 568-nm absorption band with a large increase in band width and a small decrease in band intensity. Difference absorption spectrum reveals extrema at 560 and 640 nm. The characteristic bilobed circular dichroic band associated with this absorption band is transformed into two distinct bands with no crossover point and a region of about 15 nm of zero ellipticity separating them. This results in a positive and a negative band displaced slightly and greatly to the red, respectively, of the positive and negative lobes of the original band. Also the 317-nm circular dichroic band is drastically reduced in intensity and slightly red shifted. Furthermore, the near and the far ultraviolet spectra remain essentially invariant indicating that the structure of the bacteriorhodopsin or the purple membrane are not significantly altered by glycol. Additional glycol accentuates the observed spectral alterations. The main finding is that glycol addition results in formation of a 640-nm optical species in equilibrium with the 568-nm species. The circular dichroic behavior of the 640-nm species which is similar to that of the 568-nm one indicates excitonic interaction. It is noteworthy that this long wavelength species has been observed in low pH solutions of the purple membrane but not in glycerol solutions. Possible molecular mechanisms will be discussed.

Ref: Muccio, D.D. and J.Y. Cassim. J. Mol. Biol. (1979) 135, 595-609.
Hsiao, T.L., G.K. Papadopoulos and J.Y. Cassim. Biophys. J. (1978) 18, 182a (Abstr.).

M-PM-Po30 SOLID STATE NMR STUDIES OF PURPLE MEMBRANE. David M. Rice, Judith Herzfeld and Robert G. Griffin, Francis Bitter National Magnet Laboratory, Massachusetts Institute of Technology, Cambridge, MA 02139 and Biophysical Laboratory, Harvard Medical School, Boston, MA 02115.

Bacteriorhodopsin is a protein in which internal motion and structure can be conveniently studied with solid state NMR techniques. We have isotopically enriched purple membrane by biosynthetic incorporation of several specifically labeled amino acids and we demonstrate the manner in which solid state NMR spectroscopy can be used to extract information about the rate and mechanism of motion at the labeled sites. The motion of the aromatic ring in Phe-d_5 is typical of the type of motion amenable to investigation by NMR methods. For 180° flips about the C_β–C_γ bond axis, a distinctive axially asymmetric ^2H spectrum results which is easily distinguishable from spectra due to continuous rotation about this bond or from rigid lattice spectra. Flipping rates near 10^5 Hz result in an intermediate exchange ^2H spectrum and the rates may be determined from the lineshape. This is illustrated by spectra of polycrystalline Phe-d_5 and by spectra of Phe-d_5 labeled bacteriorhodopsin.

Since isotopic enrichment of bacteriorhodopsin generally occurs at several sites, we have investigated methods for separating multiple contributions to the NMR spectra. Using ^{31}P chemical shift powder spectra, we demonstrate that, under appropriate conditions, strong magnetic fields acting on the diamagnetic anisotropy of the purple membrane sheets can be used to prepare oriented samples. The technique is of interest because it potentially allows resolution of overlapped powder spectra. Another approach to the same problem is magic angle sample spinning and we demonstrate the utility of this technique for the resolution of overlapped chemical shift powder patterns. (Supported by NIH grants GM23316, GM23289, RR05381, RR00995, and a Faculty Research Award to JH from the American Cancer Society.)

M-PM-Po31 IN VIVO ^{31}P NMR MEASUREMENTS OF UNCOUPLING EFFECTS OF SATURATED FATTY ACIDS ON BACTERIA. R. V. Mustacich, D. S. Lucas,* and F. S. Ezra, Miami Valley Laboratories, Procter and Gamble Company, Cincinnati, OH 45247.

Saturated, mid-chain fatty acids are chemiosmotic uncouplers of oxidative phosphorylation in bacteria. The protonophore activity of these acids has been inferred from their inhibition of active transport of certain amino acids, and by the established mitochondrial uncoupling activity of long-chain unsaturated fatty acids. In our studies, ^{31}P nmr was used to measure in vivo phosphate metabolism and transmembrane proton gradients (Δ pH). These studies directly demonstrate protonophore activity of octanoic acid with E. coli and S. aureus. The concentration dependences of the collapse of Δ pH with the fatty acid are substantially different with the two organisms. Differential respirometry data with both organisms also shows a concentration dependent response to octanoic acid. In addition, the ^{31}P nmr results show uncoupling at low octanoic acid concentrations which was not detectable by manometry with S. aureus. The concentration dependence of the collapse of Δ pH in these two organisms is not directly related to the concentrations required by standard tests for microbial growth inhibition.

M-PM-Po32 AN ESTIMATE OF THE CONDUCTANCE OF A SINGLE CONNEXON IN RAT LIVER. David J. Meyer, S. Barbara Yancey, and Jean-Paul Revel, Division of Biology, California Institute of Technology, Pasadena, California 91125.

In view of the evidence that gap junctions are aggregates of intercellular channels, it is desirable to estimate the conductance of a single channel or connexon. Such an estimate affords a test of the identification of the connexon as the intercellular channel and is of particular interest in view of extensive structural and biochemical data available for liver gap junctions. A cable analysis of the spatial dependence of electrotonic potentials in rat liver yielded an estimate of 2500 Ω cm. As cytoplasmic resistance is ~100 Ω cm, this value primarily reflects the resistance of intercellular junctions. Scanning electron microscopy of rat liver reveals that hepatocytes are flattened hexagonal prisms about 15 μ across. Each of six facets that form the perimeter of a hepatocyte is roughly 100 μ in area. Freeze fracture of rat liver demonstrates that gap junctions occupy $3\ \Omega^2$ of each facet. The electrical resistance of a hepatocyte to radial current injected into a single cell elsewhere in the network is Ri(l/a) where l is the length of the pathway and a is the area through which current flows. If current traverses hepatocytes by way of gap junctions, then l is 15 μ and a is 100 μ^2. The resistance of a hepatocyte is then $3.8 \times 10^6 \Omega$. In glutaraldehyde fixed material there are 11,000 connexons/μ^2 of gap junction. Hence the resistance of a hepatocyte may be attributed to 3.3×10^4 connexons. The resistance of a single connexon is then calculated to be about $10^{11} \Omega$. Use of a cubic model for the structure of a hepatocyte yields an estimate of $3 \times 10^{10} \Omega$ for the resistance of a connexon. These estimates are consistent with the hypothesis that connexons are intercellular channels.

Supported by NIH grants RR07003, GM0695 and fellowships NS06240 and AM05700.

M-PM-Po33 CO_2 DOES NOT UNCOUPLE HEPATOCYTES IN RAT LIVER. David J. Meyer and Jean-Paul Revel, Division of Biology, California Institute of Technology, Pasadena, California 91125.

We have examined the effect of CO_2 on intercellular communication in rat liver. Pieces dissected from the edge of the liver were superfused with a constant flow of warmed saline (Graf and Petersen, J. Physiol. 284:105) gassed with either 95% O_2/5% CO_2 or with 100% CO_2. Electrical coupling was monitored by measuring the size of electrotonic potentials produced by intracellular injection of 50 nA current pulses. CO_2 produced a rapid and reversible depolarization of about 10 mv, but did not produce uncoupling even after exposure for 1 hour. Analysis of the spatial dependence of electrotonic potentials also failed to reveal an increase in intercellular resistance. The failure of liver cells to uncouple following treatment expected to decrease intracellular pH stands in contrast to the responses of Xenopus blastomeres (Turin and Warner, Nature 270:56) and pancreatic acinar cells (Iwatsuki and Petersen, J. Physiol. 291:317). The depolarization of hepatocytes exposed to CO_2 saline demonstrates that the saline reaches the cells. The failure of hepatocytes to uncouple may indicate differences in the structure of the intercellular channels. Alternatively, it may reflect differences in the metabolic responses of cells to CO_2.

Supported by NIH grants RR07003, GM0695 and fellowship NS06240.

M-PM-Po34 A MODEL FOR EXOCYTOSIS: FUSION AND AGGREGATION OF UNILAMELLAR VESICLES WITH PLANAR BILAYER MEMBRANES. F.S. Cohen*, M.Akabas*, A. Finkelstein*. Depts. of Physiology, Rush University, Chicago, Il. 60612 and Albert Einstein College of Medicine, Bronx, N.Y. 10461. (Intr. by C. A. Lewis).

In order to understand the mechanisms of fusion of intracellular vesicles to plasma membranes, we are studying the fusion of phospholipid vesicles to planar bilayer membranes (BLM). Porin, a channel from the outer membrane of E. Coli, is reconstituted in egg phosphatidylcholine vesicles by cholate dialysis, and these vesicles are then added to one side (cis) of a BLM separating symmetrical solutions. Discrete current jumps (in a voltage clamped membrane) occur following the addition of several mM $CaCl_2$ to the cis side and the establishment of an osmotic gradient across the BLM (cis side hyperosmotic). The jumps continue for 30-60 minutes after which time the current no longer rises. These jumps of current are consistent with the fusion of vesicles to the BLM rather than transfer of porin from vesicles to BLM because (1) porin is an integral membrane protein that spans the bilayer and is unlikely, a priori, to transfer, (2) several porin molecules are observed to simultaneously incorporate into the BLM, and (3) the necessity for an osmotic gradient and divalent cation are the same conditions that lead to fusion of multilamellar vesicles to BLMs (J. Gen. Physiol. 75:241 & 251 (1980)). We will present evidence that the cessation of current jumps is not due to Ca^{2+} induced changes in either the vesicles or the planar membrane. It results from vesicles aggregating to, but not fusing with, the BLM, thereby reducing the exposed area of BLM available for contact with new vesicles,. Supported by NIH grants GM27367-01, NS14246-03, and 5T32GM7288.

M-PM-Po35 ELECTRICAL PROPERTIES OF OAT COLEOPTILE CELLS. G.W. Bates, M.H. Goldsmith, T.H. Goldsmith, Dept. of Biology, Yale University, New Haven, CT 06511.

Resolving the contributions of the plasmalemma and vacuolar membrane (tonoplast) to the electrical properties of higher plant cells is made difficult by the thinness of the cytoplasmic compartment. Microelectrodes penetrate the vacuole, with both membranes in series between the probe and the external environment. Work in this laboratory has suggested that the specific resistance of the tonoplast is higher than that of the plasmalemma, and that much of the variation in recorded input resistance (1-100MΩ) is caused by leakage shunts of variable size across the tonoplast. Membrane voltage and input resistance have been measured with both a single electrode and a bridge circuit as well as with double penetrations using a pair of micropipettes. Low resistance (<10MΩ) impalements exhibit membrane potentials about 40-50 mV more negative than high resistance (>20 MΩ).

Our interpretation is that low resistance impalements are those in which the electrode is seated in the vacuole, but because of leakage shunts across the tonoplast the electrode more nearly measures the electrical properites of the plasmalemma. Impalements with high resistance are those in which the tonoplast forms a good seal around the electrode, and the electrode therefore measures the properties of both membranes in series. It is possible to convert high-R/low-V impalements into low-R/high-V types by passing excess current through the electrode or by disturbing the electrode tip by over-compensating the capacitance neutralization circuit until it rings.

M-PM-Po36 EFFECTS OF THE SPATIAL PATTERN OF CELLULAR INTERCONNECTION ON A PROPAGATED CARDIAC ACTION POTENTIAL. R. W. Joyner, Dept. of Physiology, U. of Iowa, Iowa City, IA, 52242.

Numerical techniques were used to simulate the propagation of a cardiac action potential model (Beeler and Reuter, 1977) along one dimensional strands of cells coupled with electrical junctions. We used a fixed cell length (Δx, 25μ) to examine how the shape and velocity of the propagating action potential was altered as we decreased the resting length constant, L, by increasing the longitudinal resistance either a) homogeneously, by increasing all cell-cell resistance or b) introducing a periodic spacing of high resistance junctions. For the homogeneous case, the shape of the AP was modified (when $\Delta x/L > 0.2$) by increased maximal dV/dt but a decrease in peak inward current. Achieving the same value of high longitudinal resistance by periodically spaced "barriers" produced even greater effects on the AP shape and greater slowing of conduction velocity. Even with a constant membrane model and cell size, variations in the spatial pattern of cellular interconnections produce significant changes in action potential shape and velocity, with some patterns producing decremental conduction or propagation failure. Supported by NIH grant HL22562.

M-PM-Po37 JUNCTIONAL MEMBRANE RESISTANCE OF Chironomus CELL PAIRS DEPENDS ON (NONJUNCTIONAL) MEMBRANE POTENTIAL. Ana Lia Obaid and Birgit Rose. Dept. Physiol. & Biophys. Univ. Miami Sch. Medicine, Miami, FL 33101.

The effect of membrane potential on junctional membrane resistance (r_j) of 2-cell preparations isolated from Chironomus salivary glands was determined with the use of a voltage clamp. Depolarization of cells by outward current or by exposure to high K-medium increased junctional resistance; r_j increased in direct relationship with depolarization. With both methods of depolarization, r_j returned to control levels upon restoration of the resting potential -- in the case of K-exposure this ensued both by inward current and by return to control medium. r_j did not depend on transjunctional potential per se. These results confirm earlier findings in the whole, multicellular gland where, however, only electrical coupling was measured (1,2). To explain these phenomena, a membrane potential-dependent binding of Ca^{2+} to the inner surface of nonjunctional membrane has been proposed: depolarization would release Ca^{2+} that could then interact with and close the junctional channels, and repolarization would reverse this reaction (2). Thus the effectiveness of nonjunctional membrane repolarization in restoring r_j should depend on the level of $(Ca^{2+})_i$. We find, in agreement with this hypothesis, that r_j recovers only partially upon repolarization of cells subjected to treatments known to raise $(Ca^{2+})_i$ such as exposure to NaCN or Nigericin (3).

(1) Socolar, S. J. and Politoff, A. L. 1971, Science 172: 492.
(2) Rose, B. and Loewenstein, W. R. 1971, J. Membrane Biol. 50: 20
(3) Rose, B. and Rick, R. 1978, J. Membrane Biol. 44: 377.

This work was supported by DHE grant CA 14464.

M-PM-Po38 AN ELECTRIC FIELD MODEL FOR INTERACTION BETWEEN EXCITABLE CELLS NOT CONNECTED BY LOW-RESISTANCE PATHWAYS. Nick Sperelakis and James E. Mann, Jr. Departments of Physiology and Applied Mathematics, University of Virginia, Charlottesville, VA 22908.

We recently developed a model for electrical transmission between contiguous excitable cells, e.g., myocardial cells, without the requirement of low-resistance connections between cells. The model was analyzed by means of circuit analogs and computer simulation. The major requirements are that the junctional membranes (JM) be excitable, that the junctional cleft (JC) be narrow (e.g., 200 Å), and that the pre-JM fire an action potential (AP) a short time (e.g., 0.1 msec) before the adjacent surface membrane (SM). Transmission occurs by means of the electric field that develops in the narrow JC during the course of the AP in one cell. When the pre-JM fires, the JC becomes negative with respect to ground (interstitial fluid), and this negative cleft potential depolarizes the post-JM by the same amount, thus bringing it to threshold. The inner surface of the post-JM remains at nearly constant potential, since virtually no local-circuit current flows through the post-cell. Excitation of the post-JM causes the SM of the post-cell to discharge. Transmission is facilitated by narrowing the JC (increasing radial cleft resistance), by decreasing the capacitance (or τ_m) of the JMs, and by lowering the JM threshold (e.g., by increasing $\bar{g}_{Na}$) or increasing the kinetics of activation of the fast Na^+ channels. The model can account for bidirectional propagation at about 0.3 m/sec for cardiac muscle, and for block of transmission when the JC is widened under pathological conditions. The model works when the lumped membrane units follow Hodgkin-Huxley dynamics. It is proposed that this mechanism might apply to those situations in which low-resistance connections between excitable cells either do not exist or have been altered, and to synchronization of oscillators (e.g., heart SA nodal pacemaker cells).

M-PM-Po39 CHANGES IN THE ELECTRICAL PROPERTIES OF UTERINE SMOOTH MUSCLE DURING PARTURITION. Sims, S.M., R.E. Garfield and E.E. Daniel. Dept. of Neurosciences, McMaster University Medical Center, Hamilton, Ontario. Canada. L8N 3Z5.

Morphological studies have shown that gap junctions are rarely if ever present between uterine smooth muscle cells except at the time of parturition. We have asked, how might the appearance of gap junctions affect the electrical properties of uterine smooth muscle? The proposal that gap junction formation leads to closer coupling between cells has been supported by our experiments that showed the longitudinal impedance of a strip of muscle to be lower when gap junctions were present (Fed. Proc. 39:1786, 1980). From this observation we would predict that the length constant (λ) would be greater when gap junctions were present. We have measured λ in tissue strips with and without gap junctions to test this prediction.

Microelectrodes were used to measure the membrane response of individual cells at various distances from a point of stimulation using the partitioned bath technique of Abe and Tomita (J. Physiol. 196:87, 1968). The λ of tissues taken from animals before term was 2.14 mm ± 0.58 (SD). Tissues from animals actually delivering, in which gap junctions are known to exist, had λ of 2.70 mm ± .76 (SD). This increase of 1.3 times from before term to delivering tissues is of the same magnitude that we would expect from the changes in the longitudinal internal impedance of the muscle.

While we are unable to attribute the changes in λ solely to formation of gap junctions the results are consistent with the theory that gap junction formation leads to closer electrical communication between cells. This would support the hypothesis that gap junction development may be the basis for the coordinated contractile activity that occurs at the time of parturition. Supported by MRC Canada.

M-PM-Po40 THE EFFECT OF D_2O ON NEXAL MEMBRANE PERMEABILITY. P. R. Brink, S. Young-Gaylinn* and M. M. Dewey. Anatomical Sciences, SUNY at Stony Brook.

Nerve cords of the earthworm Lumbricus terrestris were dissected in saline. The cords were then placed in a D_2O saline for 18-24 hrs. Sypropolis and Ezzy (A.J.P. 197:808, 1959) showed that for a myelinated fiber (d=20 μ) complete exchange of D_2O for cellular H_2O occurred in 30 min. For the partially myelinated earthworm axon (d=100 μ) exchange would occur within 1-2 hrs. The septate axons were iontophoretically injected with dichlorofluorescein. The diffusion of the dye across the septal membrane and within the cytoplasm were monitored via microscopic photomultiplier in conjunction with a motorized stage on a fluorescence microscope. Similar experiments were carried out in H_2O saline for comparison. All experiments were done at 21°C. In H_2O saline, only small decreases in conduction velocity were seen but the action potential was increased in duration by 30-50%. Nexal membrane permeability was decreased from 3.8×10^{-5} cm/sec to 1.6×10^{-5} cm/sec indicating a reduction of 57% which was statistically significant to the 0.01 level. The axoplasmic diffusion coefficient was reduced from 5×10^{-7} to 3.5×10^{-7} cm^2/sec, a reduction of only 30%. From studies like that of Tedgold and Jones, (BBA 550:543, 1979) it has been shown that D_2O decreases channel conductions of gramicidin by 20% at 20°C and ionic conductances in solution are reduced by a similar value. The decrease in junctional permeability beyond the predicted levels most likely represents an effect of D_2O on the hydration radius of the dye molecule as well as junctional transport mechanism. Further experiments are planned with varied temperature to analyze the effect of hydration on junctional permeability.
This work was supported by NIH Grant GM 24905.

M-PM-Po41 DISTRIBUTION OF NEXUSES AND THE STRUCTURE OF THE TIGHT JUNCTION IN FROG EPIDERMIS. D. Colflesh*, M. M. Dewey and P. Brink. Anatomical Sciences, SUNY at Stony Brook, New York

Frog skin was fixed (1.5% gluteraldehyde), treated with 20% glycerol and fractured at -118°C. Replicas revealed particles 9.5 mm ± 1.5 nm SD in diameter in the PF face of cell membranes in all epidermal layers except that facing the basement membrane and that of the outer surface of the penultimate cell layer. These particles occurred in small plaques, rings, strands or single particles similar to those described in frog cardiac muscle (Kensler *et al.*, J. Cell Biol.: 73:763, 1977). Corresponding pits in plaques, rings, strands and single pits were observed in the EF face of membrane replicas. Area measurements reveal that these particles constitute 23% of the membrane surface area. This represents a particle density of ~ 1200 particles per square micron. To our knowledge this is the highest percentage of nexal to plasma membrane demonstrated.

Tight junctions were revealed in the penultimate cell layer. Three to five strands occurred in the PF face of the membrane. Peroxidase diffused from the basement membrane to the apical surface of penultimate cells. Peroxidase applied to the outer surface of the epidermis diffused to the apical surface of this cell layer.

This work was supported by NIH Grant GM24905.

M-PM-Po42 GLUTARALDEHYDE DIFFERENTIALLY AFFECTS GAP JUNCTIONAL CONDUCTANCE AND ITS pH AND VOLTAGE DEPENDENCE. D.C. Spray, A.L. Harris and M.V.L. Bennett, Div. Cellular Neurobiology, Dept. Neurosci., Albert Einstein College of Medicine, Bronx, N.Y. 10461.

Gap junctions are comprised of channel macromolecules which provide a pathway of ionic conductance between electrically coupled cells. To probe the structure of the channel molecule we examined the effects of glutaraldehyde (glutal) on the conductance of gap junctions and on gating of junctional conductance by cytoplasmic pH and transjunctional voltage. Each cell of isolated pairs from early embryos of either *Fundulus* or *Ambystoma* was impaled with two microelectrodes; junctional conductance (g_j) was measured under voltage clamp or junctional and nonjunctional conductances were calculated from input and transfer resistances. Cytoplasmic pH (pH_i) was measured in one cell of the pair using a Thomas-type recessed tip electrode. Glutal irreversibly reduced junctional conductance in a dose-dependent manner with a 50% reduction below 50μM. With concentrations as low as 1-10μM, g_j was very slightly affected whereas the normally pronounced voltage dependence of g_j on pH_i over the range of 6.8-7.8 was eliminated. With concentrations of glutaraldehyde as high as 1 mM, which reduce g_j by more than 90%, the voltage dependence of *Ambystoma* junctions (J. Gen. Physiol., Jan. '81) was not markedly altered. Fixative concentrations of glutal (above 10 mM) abolished g_j without reducing pH_i below 7.4. We conclude that this reagent has two separate effects on junctional conductance: a) modifying the molecular channel so that its conductance is reduced and b) modifying the site at which protons act to gate channel conductance. The sensitivity of the pH dependence and insensitivity of the voltage dependence to glutaraldehyde provide additional evidence for multiple gating mechanisms of the gap junctional channel.